KONINKLIJKE AKADEMIE VAN WETENSCHAPPEN
TE AMSTERDAM

PROCEEDINGS

VOLUME XXXV

No. 7

President: J. VAN DER HOEVE
Secretary: B. BROUWER

CONTENTS

Chemistry. — *On the Law of Additive Atomic Heats in Intermetallic Compounds.* IX. *The Compounds of Tin and Gold, and of Gold and Antimony.* By J. A. BOTTEMA and F. M. JAEGER.

(Communicated at the meeting of September 24, 1932.)

§ 1. In just the same way as in the case of the compound *PtSn*[1]), the question of the validity of the rule of additive atomic heats in compounds was studied in that of the compounds *AuSn* and $AuSb_2$. The alloy *AuSn* was prepared by carefully melting together the components, mixed in the theoretical proportion, in an atmosphere of pure hydrogen; the melting was repeated until a microscopically homogeneous mass was finally obtained. That the compound *AuSn* was really present, was controlled by means of *X*-ray-analysis[2]). Table I contains the data collected in this way. They prove, that the *hexagonal* compound *AuSn*, formerly studied by OWEN and PRESTON[3]), is really present here. No superstructure-lines were observed; the chemical analysis, moreover, yielded: 62.40 % *Au* and 37.58 % *Sn*, while the calculated values are: 62.42 % *Au* and 37.58 % *Sn*; so that the preparation may be considered as being chemically pure.

The structure of the compound *AuSn* is evidently quite analogous to that of *PtSn*: the dimensions of the elementary cell: $a_0 = 4.307$ Å and $c_0 = 5.496$ Å are somewhat greater than in the case of the *platinum*-compound. If 2 molecules are present within the elementary cell, the specific gravity of *AuSn* is calculated to be: 11.807 at 0° C.; the specific volume of the compound is about 12 % *smaller* than the sum of the specific volumes of its components.

---

1) F. M. JAEGER and J. A. BOTTEMA, Proceed. R. Acad. Sciences Amsterdam, **35**, (1932), 352.

2) Spectogram by J. BEINTEMA.

3) E. A. OWEN and G. D. PRESTON, Phil. Mag., **4**, (1927), 133.

TABLE I. Powder-Spectogram of *AuSn*.

No. of Line:	$2l$ in m.M.:	Estim. Intens.:	Wave-length λ:	Angle Θ:	$Sin^2\Theta$ (observed):	$Sin^2\Theta$ (calculated):	Indices (hkl) or ($hkil$):
1	42.36	1	β	10° 35′	0.0337	0.0347	(100) = (10$\bar{1}$0)
2	47.58	4	α	11 54	0.0425	0.0426	(100) = (10$\bar{1}$0)
3	52.16	1	β	13 2	0.0509	0.0506	(101) = (10$\bar{1}$1)
4	57.80	4	α	14 27	0.0623	0.0622	(101) = (10$\bar{1}$1)
5	73.30	3	β	18 19	0.0988	0.0985	(102) = (10$\bar{1}$2)
6	75.38	3	β	18 51	0.1044	0.1040	(110) = (11$\bar{2}$0)
7	81.56	10	α	20 23	0.1213	0.1210	(102) = (10$\bar{1}$2)
8	83.98	8	α	21 0	0.1284	0.1277	(110) = (11$\bar{2}$0)
9	97.44	2	α	24 22	0.1702	0.1702	(200) = (20$\bar{2}$0)
10	99.92	1	β	24 59	0.1784	0.1783	(103) = (10$\bar{1}$3)
11	103.24	2	α	25 49	0.1897	0.1898	(201) = (20$\bar{2}$1)
12	107.22	2	β	26 48	0.2033	0.2025	(202) = (20$\bar{2}$2)
13	111.76	2	α	27 56	0.2194	0.2190	(103) = (10$\bar{1}$3)
14	119.92	5	α	29 59	0.2497	0.2486	(202) = (20$\bar{2}$2)
15	132.46	1	α	33 7	0.2985	0.2979	(210) = (21$\bar{3}$0)
16	134.54	1	β	33 38	0.3068	0.3066	(212) = (21$\bar{2}$2)
17	136.22	2	α	34 3	0.3135	0.3136	(004) = (0004)
18	137.58	1	α	34 24	0.3192	0.3175	(211) = (21$\bar{3}$1)
19	144.16	1	α	36 2	0.3460	0.3466	(203) = (20$\bar{2}$3)
20	146.76	2	β α	36 41	0.3577	0.3562 0.3593	(104) = (10$\bar{1}$4) (114) = (11$\bar{2}$4)
21	151.62	5	α	37 54	0.3773	0.3763	(212) = (21$\bar{3}$2)
22	153.50	2	α	38 22	0.3853	0.3830	(300) = (30$\bar{3}$0)
23	166.62	5	α	41 39	0.4417	0.4418	(114) = (11$\bar{2}$4)
24	174.42	1	α	43 36	0.4756	0.4743	(213) = (21$\bar{3}$3)
25	176.58	1	α	44 9	0.4852	0.4838	(204) = (20$\bar{2}$4)
26	182.84	1⁻	α	45 43	0.5125	0.5107	(220) = (22$\bar{4}$0)
27	187.38	1⁻	α	46 51	0.5323	0.5303	(221) = (22$\bar{4}$1)
28	196.74	1⁻	α	49 11	0.5727	0.5729	(311) = (31$\bar{4}$1)
29	205.64	2	α	51 25	0.6111	0.6115	(214) = (21$\bar{3}$4)
30	210.42	3	α	52 36	0.6311	0.6317	(312) = (31$\bar{4}$2)
31	226.18	4	α	56 33	0.6962	0.6966	(304) = (30$\bar{3}$4)
32	238.96	4	α	59 44	0.7460	0.7482	(106) = (10$\bar{1}$6)
33	242.60	1	α	60 39	0.7598	0.7594	(402) = (40$\bar{4}$2)

Radius of Camera: 57.2 m.M. Exposure: 100 m. Amp. hours.

Wave-Length: $\lambda_{Cu_\alpha} = 1.539$ Å.: $\lambda_{Cu_\beta} = 1.389$ Å.

Quadratic Equation: $sin^2\Theta = 0.04256\,(h^2 + hk + k^2) + 0.01960\,.\,l^2$. . . . ($\alpha$)

$sin^2\Theta = 0.03466\,(h^2 + hk + k^2) + 0.01596\,.\,l^2$. . . . ($\beta$)

Parameter of Lattice: $a_0 = 4.307$ Å.: $c_0 = 5.496$ Å. Hexagonal.

§ 2. The quantities of heat developed by 1 gramme of *AuSn* were determined in a series of measurements which proved to be reproducible within 0.1 %. The results obtained were the following:

TABLE II.

Temperature t in °C.:	Final temp. t' of the Calorimeter:	Quantities of heat Q developed between t and t':	Quantities of heat Q_0 developed between t and 0° C.:
100°	20°.3	3.1680	3.9730
190	20.7	6.7652	7.5862
219.5	20.7	7.9778	8.7988
307.7	20.7	11.6493	12.4703

At 410° C. indications were obtained of an initial melting of the compound; no measurements at temperatures exceeding 400° C. could, therefore, be made.

The quantities of heat Q_0 mentioned can be very accurately expressed by the formula:

$$Q_0 = 0.039649 \,.\, t - 0.1679.10^{-6} \,.\, t^2 + 0.9779{,}10^{-8} \,.\, t^3.$$

The true specific heats c_p of *AuSn* at each temperature can, therefore, be calculated by means of the equation:

$$c_p = 0.039649 - 0.3358.10^{-6} \,.\, t + 2.9337.10^{-8} \,.\, t^2.$$

Some values of c_p and of the molecular heats C_p of the compounds are thus calculated and, in Table III, compared with the sum Σ of the atomic heats of *gold* and *tin*, as deduced from previous experiments [1]):

TABLE III.

Temperature t in °C.:	c_p:	C_p:		Diff. $(\Sigma - C_p)$ in %:
0°	0.03965	12.525	12.544	+ 0.15 %
100	0.03991	12.607	12.911	2.42
200	0.04075	12.873	13.406	4.25
300	0.04219	13.328	—	—
400	0.04421	13.966	—	—

[1]) F. M. JAEGER and J. A. BOTTEMA, loco cit.; F. M. JAEGER, E. ROSENBOHM and J. A. BOTTEMA, these Proceed., 35 (1932), 772. For *gold* the values for the "molten and solidified" metal are taken, as they are given in the last mentioned paper.

Just as in the case of *Pt Sn*, the sum Σ of the atomic heats of the components here appeared to be *greater* than the molecular heats actually observed: the differences are, also in this case, augmenting with an increase of the temperature. (Fig. 1).

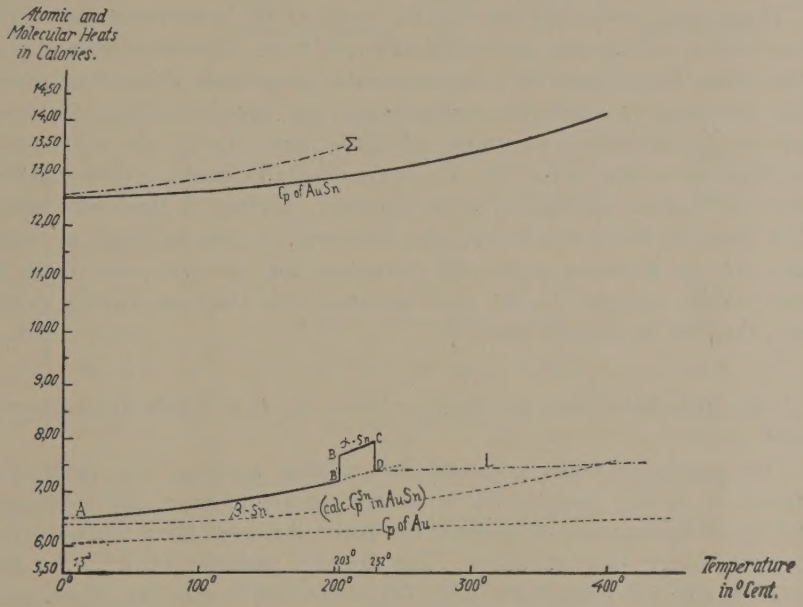

Fig. 1

If however, the values of the atomic heats of *gold* are subtracted from the molecular heats C_p of the compound, the (virtual) values of the atomic heats of *tin*, as present in the compound, no longer show any analogy with those of *grey* tin, — as was emphasized in the case of the *platinum*-compound. These virtual values C_p^{Sn} prove to be much higher than in the previous case, altough much lower than those for tetragonal *tin* at the same temperatures:

t:	C_p^{Sn} (virt.):
0°	6.382
100	6.415
200	6.612
300	6.980
400	7.529

They are represented by a *continuous* curve which starts at 0° with a value of C_p^{Sn}, which is somewhat lower than C_p for tetragonal *tin;* it ends at 400° C. with a value which is about equal to the corresponding value of C_p for liquid *tin* at these temperatures and the curve is convex towards the axis of the temperatures.

These data prove that the specific heats of *tin* in the compound *AuSn* have values which are *completely different* from those in *PtSn* and also, that their dependence on the temperature is quite an other than in the case previously studied. Notwithstanding the perfect analogy between the crystallographical structures of *PtSn* and *AuSn*, the substitution of *Pt*-atoms in the lattice by *Au*-atoms evidently causes a quite different way of thermal oscillation of the *tin*-atoms present in these two cases. The law of NEUMANN-KOPP, etc., however, is here followed no more than in the previous case; the deviations are, as well with *AuSn*, as with *PtSn*, situated in *the same* direction, but they are smaller in the first, than in the second case.

§ 3. The behaviour of $AuSb_2$, however, is a much more complicated one.

This compound was prepared by melting together the theoretical quantities of the components in an atmosphere of pure, dry hydrogen, and by tempering and re-melting the mass obtained, till a homogeneous product finally was produced. The analysis yielded: 44.72 % *Au* and 55.22 % *Sb;* calculated: 44.74 % *Au* and 55.26 % *Sb*. An *X*-ray-analysis gave the results collected in Table IV; the powder-spectrogram appeared to be identical with that obtained by OFTEDAL [1]) and did not show any extra diffraction-lines. The compound possesses a *pyrite*-structure; the simple cubic cell has an edge: $a_0 = 6.636$ Å and contains 4 molecules $AuSb_2$ pro cell. The space-group is evidently T_H^6.

§ 4. A sample weighing 22.5578 grammes was included within a vacuum-crucible of the usual shape; it weighed 30.2202 grammes. For the purpose of controlling the exactness of the indications of the thermo-couple, the sequence of the experiments was taken quite arbitrarily, as is indicated by the numbers of the first column in Table V.

These measurements proved to be reproducible within 0.1 to 0.2 % of the absolute values.

The compound $AuSb_2$ evidently occurs in *three* polymorphous modifications; the transformations prove to be quite reversible. From the data obtained, the first transition-temperature: $\gamma\text{-}AuSb_2 \rightleftarrows \beta\text{-}AuSb_2$ was calculated to be: about 355° C.; the second: $\beta\text{-}AuSb_2 \rightleftarrows \alpha\text{-}AuSb_2$ must be situated in the neighbourhood of 405° C.

---

[1]) I. OFTEDAL, Zeits. f. phys. Chem., **135**, (1928), 291, 296.

TABLE IV.

Powder-Spectogram of the Compound $Au\ Sb_2$.

No. of Line:	$2l$ in m.M.:	Estim. Intens.:	Wave-length λ:	Angle Θ:	$Sin^2\Theta$ (observed):	$Sin^2\Theta$ (calculated):	Indices (hkl):
1	46.46	3	α	11° 37′	0.0405	0.0403	(111)
2	48.64	2	β	12 10	0.0444	0.0438	(200)
3	53.82	6	α	13 27	0.0541	0.0538	(200)
4	60.06	6	α	15 2	0.0673	0.0672	(210)
5	66.10	5	α	16 33	0.0808	0.0807	(211)
6	68.98	2	β	17 15	0.0879	0.0876	(220)
7	76.70	5	α	19 10	0.1078	0.1076	(220)
8	81.36	4	α β	20 20	0.1207	0.1210 0.1205	(300) or (221) (311)
9	90.50	10	α	22 37	0.1476	0.1479	(311)
10	94.80	3	α	23 42	0.1616	0.1614	(222)
11	98.78	4	α	24 42	0.1746	0.1748	(320)
12	102.86	5	α	25 43	0.1883	0.1882	(321)
13	111.54	1	β	27 53	0.2187	0.2190	(420)
14	114.76	1	β	28 41	0.2304	0.2300	(421)
15	121.44	1	α	30 22	0.2556	0.2555	(331)
16	124.94	3	α	31 14	0.2689	0.2689	(420)
17	128.34	2	α	32 5	0.2821	0.2824	(421)
18	131.86	2	α β	32 58	0.2961	0.2958 0.2957	(332) (333) or (511)
19	138.50	2	α	34 37	0.3227	0.3227	(422)
20	145.42	1	α β	36 21	0.3513	0.3496 0.3504	(431) or (510) (440)
21	148.16	8	α	37 2	0.3627	0.3630	(333) or (511)
22	154.32	2	α	38 35	0.3889	0.3899	(432) or (520)
23	157.58	2	α	39 24	0.4029	0.4034	(521)
24	163.82	5	α	40 57	0.4296	0.4303	(440)
25	172.72	2	α β	43 11	0.4683	0.4706 0.4709	(531) (533)

TABLE IV. (*Continued*).

Powder-Spectogram of the Compound $Au\ Sb_2$.

No. of Line:	$2l$ in m.M.:	Estim. Intens.:	Wave length λ:	Angle Θ:	$Sin^2\Theta$ (observed):	$Sin^2\Theta$ (calculated):	Indices (hkl):
26	175.86	2	α	43° 58′	0.4820	0.4841	(442) or (600)
27	182.00	2	α	45 30	0.5087	0.5109	(532) or (611)
28	188.34	2	α	47 5	0.5363	0.5378	(620)
29	197.54	3	α	49 23	0.5762	0.5782	(533)
30	200.80	1	α β	50 12	0.5903	0.5916 0.5914	(622) (552), (633), or (721)
31	203.62	1	α	50 54	0.6023	0.6051	(542) or (630)
32	213.52	2	α β	53 23	0.6442	0.6454 0.6461	(444) (553) or (731)
33	233.50	2	α	58 22	0.7249	0.7261	(552), (633), or (721)
34	240.64	3	α	60 10	0.7525	0.7530	(642)
35	251.38	6	α	62 51	0.7918	0.7933	(553) or (731)

Radius of Camera: 57.2 m.M. Exposure: 100 m. Amp. hours.

Wave-Length: $= 1.539$ Å.; $= 1.389$ Å.

Quadratic Equations:

$$sin^2\,\Theta = 0.013446 \,.\, (h^2 + k^2 + l^2) \quad . \quad . \quad . \quad . \quad . \quad . \quad . \quad (\alpha)$$

$$sin^2\,\Theta = 0.010951 \,.\, (h^2 + h^2 + l^2) \quad . \quad . \quad . \quad . \quad . \quad . \quad . \quad (\beta)$$

Parameter of the Lattice: $a_0 = 6.636$ Å. Simple cubic cell.

Special experiments were made to fix these transition-temperatures more accurately: in a block of ATCHESON-graphite two big holes were bored, parallel and very close to each other; the one was filled with purest *silver*, the other with the compound in a sufficient quantity and two thermocouples were inserted into the two masses. Then the furnace was slowly heated, with a gradient of about 1.1° C. pro minute. The first transition: γ - modification $\rightleftarrows$ β - modification proved to be a rather rapid one; the heat-effect is only small, but the temperature of inversion could be very accurately fixed at 2830 M.V. (corrected), i. e. at 355.2° C. The inversion β - modification $\rightleftarrows$ γ - modification seems to be very sluggish; there is a temperature-interval and it proved impossible accurately to determine the temperature of transition in this way.

The amounts of heat developed in the calorimetric measurements are very well expressed by the following equations:

TABLE V.

No. of the Experim.:	Temperature t in °C:	Final temp. t' of the Calorim.:	Q in calor. between t and t':	Q_0 in calor. between t and 0° C.:	Q_0 (calcul.):
1	190°	20°.6	7.2587	8.1373	γ —
2	250.8	20.63	9.8880	10.7679	γ 10.7788
3	280.8	20.8	11.2219	12.1090	γ —
5	316.8	20.75	12.8518	13.7368	γ —
6	354.14	21.00	14.5350	15.4307	γ 15.4705
9	404.37	21.11	17.3006	18.2009	β —
8	378.73	20.97	16.1741	17.0685	β —
7	365.51	21.20	15.3150	16.2192	β —
4	315.53	20.47	12.8027	13.6758	γ 13.6789
12	439.47	20.86	19.5241	20.4138	α —
10	419.80	20.90	18.1417	19.0331	α —
11	430.51	21.23	18.7737	19.6792	α —

γ-Modification: $Q_0 = 0.043626 \,.\, t - 0.94532 \,.\, 10^{-5} \,.\, t^2 + 0.26521 \,.\, 10^{-7} \,.\, t^3$.

β-Modification: $Q_0 = -0.169785 \,.\, t + 0.11007 \,.\, 10^{-2} \,.\, t^2 - 0.14084 \,.\, 10^{-5} \,.\, t^3$.

α-Modification: $Q_0 = 0.45389 \,.\, t - 0.195633 \;\; 10^{-2} \,.\, t^2 + 0.23419 \,.\, 10^{-5} \,.\, t^3$.

From this, the true specific heats c_p and the molecular heats C_p can be calculated to be:

γ-Modification: $c_p = 0.043626 - 0.189064 \,.\, 10^{-4} \,.\, t + 0.79563 \,.\, 10^{-7} \,.\, t^2$.

β-Modification: $c_p = -0.169785 + 0.22014 \,.\, 10^{-2} \,.\, t - 0.42252 \,.\, 10^{-5} \,.\, t^2$.

α-Modification: $c_p = 0.45389 - 0.39127 \,.\, 10^{-2} \,.\, t + 0.70257 \,.\, 10^{-5} \,.\, t^2$.

The first formula is valid between 150° C. and 355° C.; the second between 360° and 405° C.; the third between 415° C. and 450° C.

In Table VI some values of c_p for the different modifications are collected; (see following page).

The values of c_p for the β-modification appear to *decrease* with the temperature within the interval of 355° — 405° C.

In Table IX a series of the values of C_p for different temperatures t are thus calculated and compared with the sum Σ of the atomic heats of *gold* and *antimony* (2 $\times$), as deduced from the corresponding measurements.

TABLE VI.

Specific Heats c_p of the Compound $Au\ Sb_2$.

Temperature t in °C.:	Specific Heat C_p		
	γ-Modification:	β-Modification:	α- odification:
150°	0.04258	—	—
200	0.04303	—	—
250	0.04388	—	—
300	0.04509	—	—
350	0.04673	—	—
360	—	0.07513	—
370	—	0.06631	—
380	—	0.05663	—
390	—	0.04612	—
400	—	0.03475	—
420	—	—	0.04988
430	—	—	0.07054
440	—	—	0.09244
450	—	—	0.1159

§ 5. *Antimony.* The calorimetrical measurements necessary for the exact determination of the specific heats of *antimony* were executed with a massive, previously stabilized lump of the pure element, brought into the shape of our usual vacuum-crucibles and weighing 59.492 grammes. The data obtained (in the sequence of the experiments as indicated in the first column) are collected in Table VII.

TABLE VII

Specific Heats c_p of Antimony at Different Temperatures.

No. of Experim.	Temperature in °C.:	Final temp. t' of Calorimeter:	Quantity of Heat Q_0 devel. between t and t':	Quantity of Heat Q devel. betw. $t°$ and 0°:	Q'_0 as calculated from the formulae:	
1	233.35°	21.36°	10.822	11.886	—	
2	324.85	21.67	15.632	16.711	—	β
4	386.00	21.57	18.055	19.129	—	
3	411.46	21.95	20.609	21.702	21.699	
8	415.00	21.16	20.633	21.687	—	
7	418.20	21.04	20.771	21.819	21.799	
6	424.8	21.70	20.957	22.037	—	α
5	440.10	22.10	21.932	23.033	—	

The element evidently has a transformation-point [1]) in the neighbourhood of 413° C., although we were not able to fix this temperature more exactly by means of the thermal method.

The quantities of heat Q_0 mentioned can very satisfactorily be expressed by the equations:

β-Modification: $Q_0 = 0.0535656 \,.\, t - 0.233176 \,.\, 10^{-4} \,.\, t^2 + 0.051656 \,.\, 10^{-6} \,.\, t^3$.

α-Modification: $Q_0 = 0.534496 \,.\, t - 0.2261 \,.\, 10^{-2} \,.\, t^2 + 0.2648 \,.\, 10^{-5} \,.\, t^3$.

The first formula is valid between 150° and 411° C., the second above 413° C.

The true specific heats of *antimony*, therefore, can, within the intervals of temperatures indicated, be calculated by means of the formulae:

β-Modification: $c_p = 0.0535656 - 0.46635 \,.\, 10^{-4} \,.\, t + 0.15497 \,.\, 10^{-6} \,.\, t^2$.

α-Modification: $c_p = 0.534496 - 0.4522 \,.\, 10^{-2} \,.\, t + 0.7944 \,.\, 10^{-5} \,.\, t^2$.

In Table VIII a survey is given of a series of values c_p and C_p at different temperatures.

TABLE VIII.

Specific Heats c_p and Atomic Heats C_p of Antimony.

Temperature t in °C.:	c_p of the β-Modification:	C_p of the β-Form.:	Temperature t in °C.:	C_p of the α-Modification:	c_p of the α-Form:
150°	0.05006	6.017	415°	0.02600	3.125
200	0.05044	6.063	420	0.03656	4.394
250	0.05159	6.201	430	0.06217	7.473
300	0.05352	6.433	440	0.08274	9.945
350	0.05623	6.759	450	0.1082	13.005
400	0.05971	7.177	460	0.1354	16.270
411.5	0.06062	7.286			

Most remarkable is the rapid increase of c_p with the temperature above 413° C. The data for C_p are graphically represented in Fig. 2; the same break was also found in the curve representing the dependency of the *mean* specific heats $\bar{c}_p$ on the temperature:

[1]) It may be remarked in this connection, that in the Physical Laboratory of this University recently such a transformation-point was found, by means of *X*-ray-analysis at higher temperatures, in the case of the quite analogously built *bismuthum*. (Private communication by Prof. COSTER).

Between t and t':	Mean Specific Heats $\bar{c}_p$:
233°.35	0.05105
324	0.05156
368	0.05212
411	0.05291
415	0.05239
418	0.05230
424.8	0.05199
440.1	0.05247

In fairly good agreement with this are the values of the mean specific heats $\bar{c}_p$ given in the literature [1]) between 100° and 20° C. ($\bar{c}_p = 0.05037$). In Fig. 2 a curve indicated by *Sch* gives the values of C_p as calculated

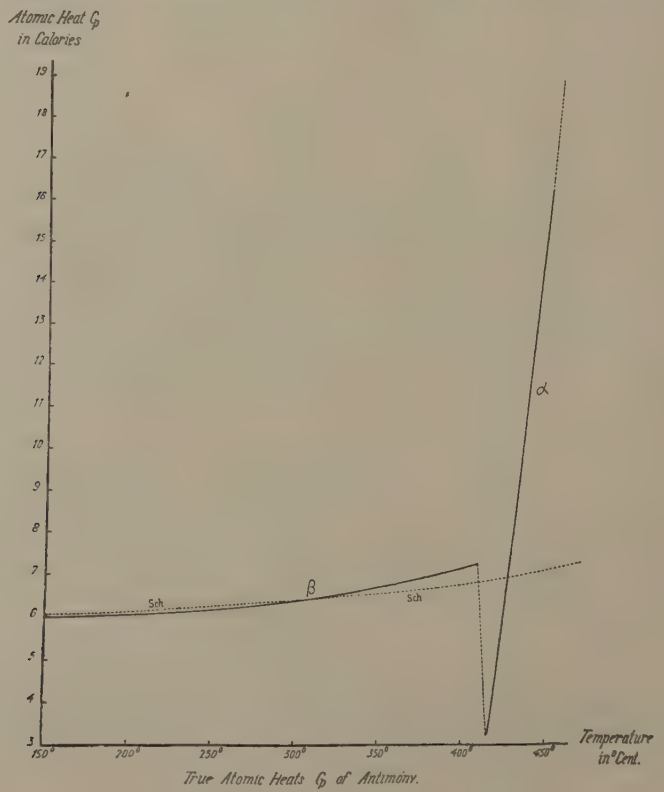

Fig. 2.

[1]) J. A. LINNAVUOP, Soc. Scient. Fenn. Comm. **1**, (10), (1922); P. SCHÜBEL, Zeits. f. anorg. Chem. **87**, (1914), 81; H. SCHIMPFF, Zeits. f. phys Chem., **71**, (1910), 257. The most probable value of c_p between 100° and 20° C. is: 0.0503; between 20° and 0° C.: 0.0498.

by SCHÜBEL (loco cit.). from which it may be seen that the true dependence of C_p on t is rather different from that indicated by this author.

§ 6. With the aid of the values for the atomic heats of *antimony* (and *gold*) thus determined, we are now able to compare the sum Σ of these atomic heats at different temperatures with the molecular heats C_p directly observed. The results are collected in Table IX and in Fig. 3 they are graphically plotted against the temperatures t.

TABLE IX.

Temperature in °C.:	Atomic Heats C_p Gold:	Antimony:	Sum of the Atomic Heats of $Au + 2Sb$:	Observed Molecular Heat C_p of $Au\,Sb_2$:		Difference $(\Sigma - C_p)$ in %:
150°	6.228	6.017	18.262	18.633		— 2.03
200	6.261	6.063	18.387	18.830		— 2.40
250	6.298	6.201	18.700	19.202	γ	— 2.68
300	6.340	6.433	19.206	19.731		— 2.73
350	6.386	6.759	19.904	20.458		— 2.78
360	6.396	6.835	20.066	32.877		— 63.3
370	6.406	6.915	20.236	29.017		— 43.3
380	6.416	6.999	20.414	24.782	β	— 21.4
390	6.426	7.085	20.596	20.182		— 2.0
400	6.437	7.177	20.791	15.206		+ 26.9
415	6.453	3.125	12.703	(20.20)		(— 59.0)
420	6.458	4.394	15.246	21.828		— 43.1
430	6.469	7.473	21.415	30.868	α	— 44.1
440	6.481	9.945	26.371	40.452		— 53.4
450	6.482	13.005	32.492	50.705		— 56.0

Contrary to the previous cases of *PtSn* and *AuSn*, the deviations from the rule of additive atomic heats here are situated in the *opposite* direction: the observed molecular heat of the compound, in all its modifications, proves always to be *greater* than the sum of the atomic heats of its components at the same temperature.

Only for the γ-modification of $AuSb_2$, however, it is still possible really to compare the two sets of values: as well for the β-, as for the α-modifications the two series of numbers prove to be *completely incomparable*, with the exception of a value in the vicinity of 400° and of one in the neighbourhood of 393° C. (β-modification,-which, however, represents a purely accidental coincidence. The behaviour of the β-modification in this respect convincingly illustrates the important fact, that even an approximating validity of the rule of additive atomic heats may completely disappear by the occurrence of a polymorphous transformation; so that evidently a change in the crystalline structure can, in this respect, have a rather catastrophic influence.

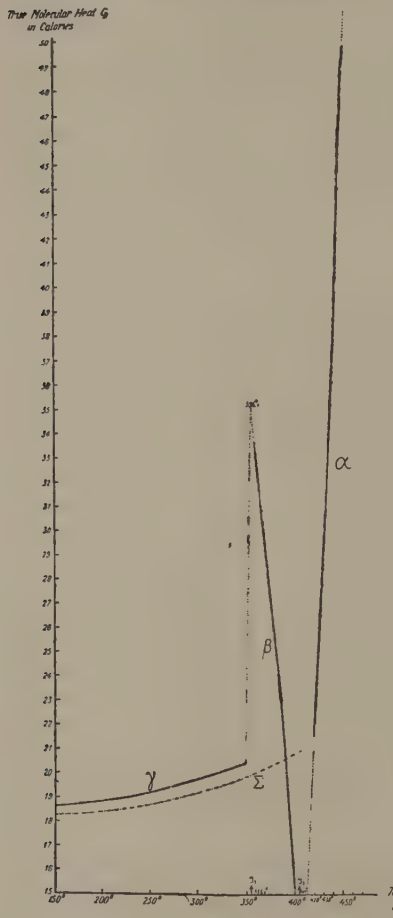

Fig. 3

The facts mentioned are graphically represented in Fig. 3; they show a slow increase of the deviations with the temperature. A definite relationship between an occurring increase or diminution of the specific volume in the formation of the compounds $PtSn$, $AuSn$ and $AuSb_2$, compared with the sum of the atomic volumes of their components on the one hand, and between the algebraic sign of the deviations ($\Sigma - C_p$) from the rule of the additive atomic heats on the other hand, — as suggested by TAMMANN and ROHMANN [1]), — could *not* be stated.

Groningen, Laboratory for Inorganic and Physical Chemistry of the University.

[1]) G. TAMMANN and A. ROHMANN, Zeits. f. anorg. Chem., **190**, (1930), 227.

Chemistry. — *On the Law of Additive Atomic Heats in the Case of Intermetallic Mixed Crystals. X. Silver and Gold.* By J. A. BOTTEMA and F. M. JAEGER.

(Communicated at the meeting of September 24, 1932).

§ 1. After the experience hitherto gathered [1]) in studying the deviations from the so-called law of additive atomic heats in chemical compounds between metals, it appeared of interest to extend these investigations also to mixed crystals. In the present paper an alloy of *gold* and *silver*, consisting of mixed crystals, was investigated by us with the purpose of verifying the presence and the order of magnitude of the deviations from the rule of additive atomic heats in such a case of the formation of mixed crystals between two metallic components. As is well known, *silver* and *gold* yield an uninterrupted series of mixed crystals, ranging from 0—100 % of the two components. The special alloy here studied contained 22.456 grammes of *gold* and 35.766 grammes of *silver*; the total weight of the sample was, therefore, 58.222 grammes. This corresponds to a mixture of 25.56 at. % *Au* and 74.44 at. % *Ag*; the composition of the mixed crystal being, therefore, equivalent to: $Ag_3Au_{1.0387}$, which involves an apparent "molecular weight" of: 531.14.

The quantities of heat Q_0 developed in the different calorimetric experiments are given in Table I.

TABLE I.

N°. of Exp.:	Temperature t in °C.:	Final temp. t' of Calorimeter:	Heat developed Q between t and t':	Heat developed Q_0 between t and 0°:	Q'_0 as calculated from the formula:
6	100°.03	21°.63	3.6135	4.6134	—
1	234.37	20.96	9.9910	10.9599	10.9748
5	310.65	21.72	13.6981	14.7021	14.6905
10	348.28	21.31	15.6586	16.6437	16.5428
2	394.3	21.40	17.9516	18.9408	18.8307
9	431.73	21.89	19.7582	20.7701	20.7079
8	466.43	21.53	21.4975	22.4907	22.4626
7	509.5	22.19	23.6347	24.6605	—
3	629.43	21.63	29.9040	30.9039	30.8890
4	800.77	22.59	39.0255	40.0698	—

[1]) F. M. JAEGER and J. A. BOTTEMA, these Proceedings, **35**, (1932), 352 and the previous paper.

These quantities of heat Q_0 can sufficiently well [1]) be represented by means of the equation:

$$Q_0 = 0.0455677 \,.\, t + 0.05514.10^{-4} \,.\, t^2 + 0.08879.10^{-9} \,.\, t^3$$

and c_p, therefore, by:

$$c_p = 0.0455677 + 0.11028.10^{-4} \,.\, t + 0.26637.10^{-9} \,.\, t^2.$$

With the same order of exactness (1.5 — 5 pro mille) the values of Q_0 can also be represented by the linear function:

$$Q_0 = 0.04561 \,.\, t + 0.05559.10^{-4} \,.\, t^2$$

and c_p, therefore, by:

$$c_p = 0.04561 + 0.1118.10^{-4} \,.\, t.$$

The true specific heats c_p and the corresponding "molecular" heats C_p are, for a series of temperatures, calculated according to the latter formula and the values obtained are in Table II compared with the sum Σ of the atomic heats of the components.

TABLE II.

Temperature t in °C.:	Specific Heats c_p observed:	'Molecular' Heats C_p observed:	Sum Σ of the atom. Heats of the Components:	Difference (Σ-C_p) in percentages:
100°	0.04693	24.926	24.942	+ 0.14 %
200	0.04785	25.415	25.475	+ 0.24
300	0.04896	26.005	26.000	— 0.02
400	0.05008	26.599	26.513	— 0.32
500	0.05120	27.195	27.012	— 0.67
600	0.05232	27.789	27.500	— 1.05
700	0.05344	28.384	27.979	— 1.44
800	0.05455	28.973	28.463	— 1.79

For *silver* and *gold* the values of the atomic heats C_p were calculated from the formulae previously [2]) given by us for the molten, solidified and stabilized metals.

The data of Table II prove, that even in the case of mixed crystals, there are *small* deviations from the rule of additive atomic heats, which

[1]) The greater deviations between the values observed and calculated occur between 250° and 450° C., because of the fact, that within this interval of temperatures the curve of the mean specific heats $\bar{c}_p$ in function of t shows a change of its curvature which proves to be a real one. The deviations are, however, not greater than about 0.5 %; the major part of the curve, more particularly at higher temperatures, is almost a straight line.

[2]) F. M. JAEGER, E. ROSENBOHM and J. A. BOTTEMA, these Proceedings, **35**, (1932), 763, 772.

clearly increase with augmenting temperatures. But these deviations are, for the greater part, *so small, that they remain within the limits of the uncertainties of the calculation itself;* only at temperatures surpassing 600° C. they become somewhat greater. In this respect, the mixed crystal certainly behaves differently from the true intermetallic compounds hitherto studied.

Groningen, Laboratory for Inorganic and Physical Chemistry of the University.

Astronomy. — *Mittlere Lichtkurven von langperiodischen Veränderlichen.* VIII. *R Leonis minoris.* Von A. A. NIJLAND.

(Communicated at the meeting of September 24, 1932.)

Instrumente: *S* und *R*. Die Beobachtungen wurden alle auf *R* reduziert: die Reduktion *R*—*S* beträgt —0^m.35. Spektrum M7—8e (*Harv. Ann.* 79 S. 170). Gesamtzahl der hier zu besprechenden Beobachtungen 592, von 2416836 bis 2426791). Der Stern ist von Mitte Juni bis Mitte August nicht beobachtbar, und die Lichtkurve (s. Fig. 1) zeigt Lücken, welche den Kurvenzug des öfteren unsicher machen und überdies die Gesamtzahl der Schätzungen von etwa 27 pro Jahr auf 22 herabdrücken.

Karte: HAGEN, *Atlas Stell. var. Series III.*

Die Stufenskala bezieht sich auf die Helligkeit 10^{m}0. Die Vergleichsterne sind in *Harv. Ann.* 29 schwer zu identifizieren, da die Koordinaten hier sehr ungenau angegeben sind. Die Helligkeit 10^m.86 für *k* fällt ganz aus der Skala heraus und blieb unberücksichtigt.

Nach MITCHELL (*Mem. Am. Ac.* **14**, IV, 284) bezieht sich die Helligkeit 12^m.97 aus *Harv. Ann.* 74 auf Stern *m*; ganz sicher ist das allerdings nicht, da die Koordinaten nur in Zehnteln Bogensekunden und ganzen Bogenminuten gegeben sind. Nach *Harv. Ann.* 37 wäre vielleicht *n* wahrscheinlicher. Die Grössen der *Harv. Ann.* 94 sind scheinbar den *Harv. Ann.* 37 entnommen; Stern *b* wird aber als 7^m.94 gegeben. Die Grössen von MITCHELL findet man a. a. O.

Stern *j* wurde fünf-mal, entweder direkt oder mittels des schwächeren Sterns *k*, an die Grenze 11^m.60 des Suchers *S* angeschlossen; das Mittel der schlecht stimmenden Resultate ist 11^m.11. Es ist kaum anzunehmen, dass der Stern viel schwächer wäre, denn tatsächlich habe ich den Stern *k* zweimal ganz bequem im Sucher sehen können. Vielleicht liegt in den *Harvard*-Grössen ein systematischer Fehler vor. Ich habe mich schliesslich an die Skala der *HP* gehalten. Der Stufenwert wird dann 0^m.101; tatsächlich hat dabei die nur 6-mal beobachtete Differenz *np* nicht mitgestimmt.

Es liegen 104 Schätzungen der Farbe vor, welche aber für vier

TABELLE I. Vergleichsterne.

	BD	HAGEN	St.	HA 29	HA 37	HA 74	Sp. HA 94	PD	PD *red.*	*H*
C	+35°.2042	—	72.1	6.06	6.03	—	F 2	6.38 GW +	6.17	6.27
A	34.2035	—	65.1	7.01	7.10	—	A 3	7.48 GW —	7.18	6.98
a	34.2022	3	63.9	7.33	7.34	7.40	K 0	7.38 WG —	7.23	7.11
b	35.2046	4	56.8	7.99	7.91	7.88	Ma	—	—	7.83
c	35.2041	6	51.8	—	8.00	8.49	F 8	—	—	8.33
d	35.2054	9	45.5	9.27	9.22	9.12	—	—	—	8.97
e	35.2059	10	39.5	9.78	9.47	9.60	—	—	—	9.58
f	35.2057	15	33.3	10.27	—	10.10	—	—	—	10.22
g	35.2053	19	28.3	10.40	—	10.60	—	—	—	10.72
h	—	21	25.4	10.75	11.00	11.04	—	—	—	11.02
j	—	24	19.9	11.52	11.46	11.53	—	MITCHELL	—	11.57
k	—	26	13.7	[10.86]	11.94	12.29	—	12.35	—	12.20
m	—	30	8.0	—	12.64	12.97	—	12.89	—	12.77
n	—	29	3.5	—	12.90	—	—	13.09	—	13.23
p	—	37	[0.0]	—	13.10	—	—	—	—	13.35

Fünftel aus den Jahren 1905—1912 stammen. Aus der Tabelle IIa scheint hervorzugehen, dass die Farbe sich in den Jahren 1905—1909 um etwa

TABELLEN IIa und II*b*. Farbenschätzung.

Zeitraum	*m*	Farbe	Grösse	*m*	Farbe
241 6906—7560	19	c 3.66	m 6.36	12	c 3.79
7572—7980	18	3.94	6.84	12	3.83
7987—8409	19	4.68	7.10	12	4.67
8630—9496	18	4.83	7.34	11	4.14
242 9755—2358	15	4.60	7.69	11	4.23
3111—5741	15	4.53	8.27	12	4.29
	104	4.37	9.17	12	4.96
			9.73	11	4.55
			10.32	11	4.82
				104	4.36

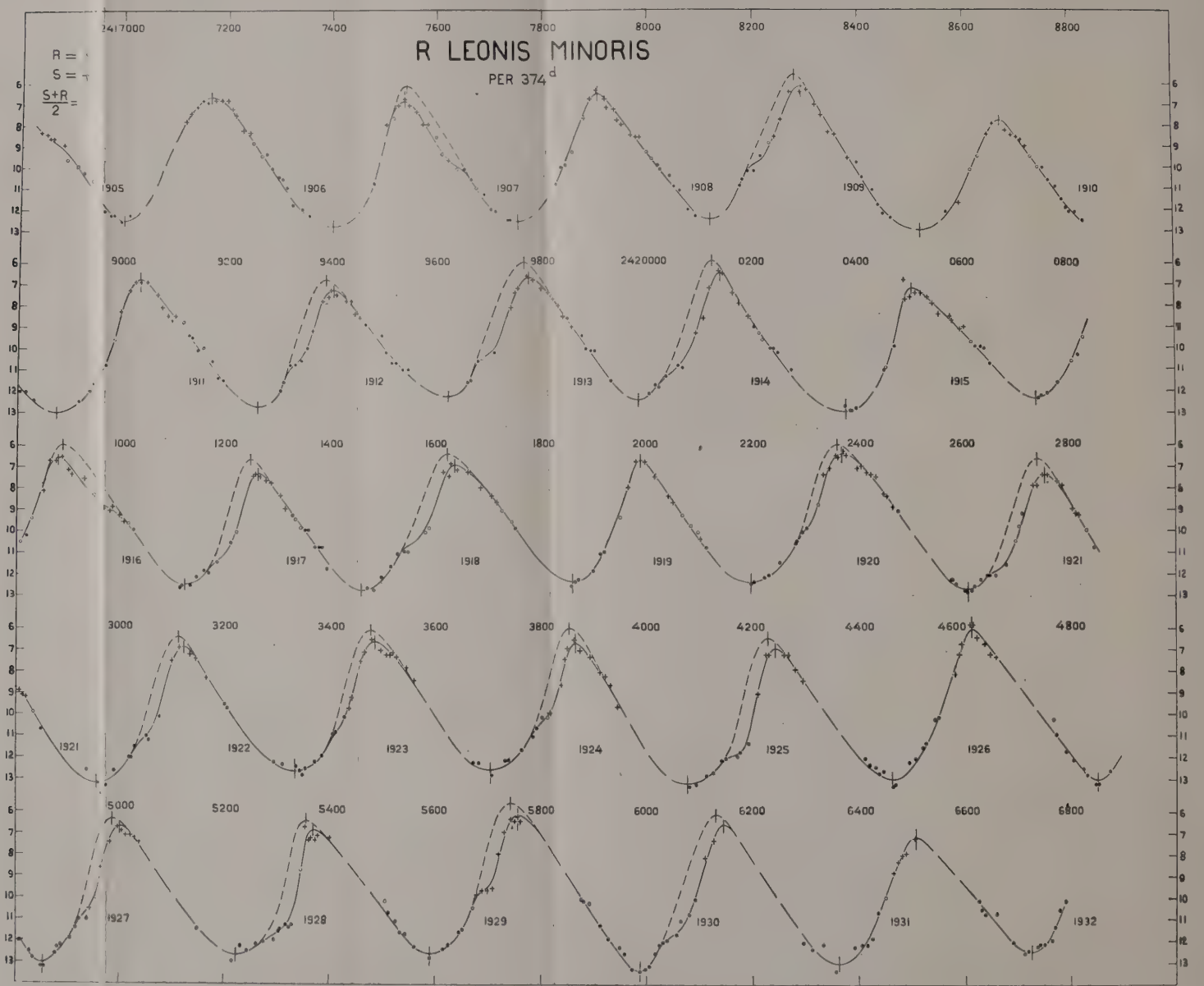
R LEONIS MINORIS
PER 374d
R =
S =
S+R / 2 =
2417000
7200
7400
7600
7800
8000
8200
8400
8600
8800
1905
1906
1907
1908
1909
1910
9000
9200
9400
9600
9800
2420000
0200
0400
0600
0800
1911
1912
1913
1914
1915
1000
1200
1400
1600
1800
2000
2200
2400
2600
2800
1916
1917
1918
1919
1920
1921
3000
3200
3400
3600
3800
4000
4200
4400
4600
4800
1921
1922
1923
1924
1925
1926
5000
5200
5400
5600
5800
6000
6200
6400
6600
6800
1927
1928
1929
1930
1931
1932

Fig. 1

1^c vertieft hat, von da aber nahezu konstant blieb. Auch eine Abhängigkeit von der Helligkeit ist schwach angedeutet, und zwar in diesem Sinne (s. die Tabelle II*b*), dass die schwächste Färbung der grössten Helligkeit entspricht. Das allgemeine Mittel ist 4^c.36.

Die Figur 1 enthält die Beobachtungen, alle auf R reduziert. Die Reihe der Abweichungen (Beobachtung minus Kurve) zeigt 230 Plus-, 235 Minuszeichen, 127 Nullwerte, 237 Zeichenfolgen, 227 Zeichenwechsel. Das Mittel der absoluten Werte der Abweichungen ist 0.143.

Ein Einfluss des Mondscheines auf die Helligkeitsschätzung ist nicht bemerkbar. Es verteilen sich auf 190 bei Mondschein angestellte Beobachtungen die Abweichungen wie folgt: 80 Plus-, 68 Minuszeichen, 42 Nullwerte.

Die Tabelle III enthält die aus der Kurve abgelesenen Epochen der Minima m und der Maxima M, nebst der Vergleichung mit den einfachen Elementen:

$$2421858^d + 374^d\,E \text{ (für die Minima)}$$

und $$2422010 + 374\,E \text{ (für die Maxima).}$$

Die übrigbleibenden $B—R$ sind gross und zeigen einen ausgeprägt systematischen Charakter; es wurde für Maxima und Minima zusammen auf graphischem Wege ein Sinusglied abgeleitet, und die definitiven Elemente F lauten dann:

$$\left.\begin{array}{l}\text{Minimum: } 2421857^d \\ \text{Maximum: } 2422010\end{array}\right\} + 374^d\,E - 18^d\,\sin 15^\circ\,(E+2);$$

$$\frac{M-m}{P} = 0.409.$$

Auf eine genauere Rechnung habe ich verzichtet.

PRAGER's Katalog für 1932 gibt den Periodenwert 377^d.9, und das aus sämtlichen von mir seit d. J. 1905 in den *Astr. Nachr.* mitgeteilten Epochen der Minima und Maxima abgeleitete allgemeine Mittel ist 373^d.5. Da die Berücksichtigung des Sinusgliedes die Quadratsumme der Abweichungen für die Minima und die Maxima zusammen von 12913 auf 5653 herabdrückt, kann die Formel F für den hier besprochenen Zeitraum als gut verbürgt gelten. Für die älteren Epochen gelten andere Elemente (s. *G.* und *L.* I, S. 278). Das daselbst zitierte Sinusglied mit einer Periode von 40 Perioden, das sämtliche Maxima und Minima aus den Jahren 1866 bis 1912 sehr befriedigend darstellt, verträgt sich aber offenbar wieder nicht mit meinen Epochen. Vielleicht wird man auch hier erst nach viel längerer Zeit das wahre Gesetz des Lichtwechsels ausfindig machen können. Die extremen Werte des Lichtwechsels sind:

$$\left.\begin{array}{l}\text{Minimum: } v = 12^m.66 \pm 0^m.070 \\ \text{Maximum: } v = \quad 6.72 \pm \quad 0.077\end{array}\right\} \text{(m.F.).}$$

Die Amplitude beträgt somit 5^m.94. Sowohl beim Minimum wie beim

TABELLE III.

Minima *m*						Maxima *M*				
E	*B*	*v*	*R*	*B*−*R*	*B*−*F*	*B*	*v*	*R*	*B*−*R*	*B*−*F*
		m					m			
−13	241 6999	12.4	6996	+ 3	− 1	241 7167	6.6	7148	+19	+14
−12	7402	12.7	7370	+32	+24	7537	6.8	7522	+15	+ 6
−11	7754	12.5	7744	+10	− 2	7907	6.5	7896	+11	− 2
−10	8121	12.3	8118	+ 3	−12	8293	6.1	8270	+23	+ 7
− 9	8519	12.9	8492	+27	+11	8671	7.7	8644	+27	+10
− 8	8873	13.0	8866	+ 7	−10	9032	6.7	9018	+14	− 4
− 7	9262	12.7	9240	+22	+ 6	9403	7.2	9392	+11	− 6
− 6	9623	12.2	9614	+ 9	− 6	9775	6.6	9766	+ 9	− 7
− 5	9985	12.3	9988	− 3	−15	242 0140	6.4	0140	0	−13
− 4	242 0379	12.9	0362	+17	+ 9	0502	7.1	0514	−12	−21
− 3	0739	12.3	0736	+ 3	− 1	0877	6.5	0888	−11	−16
− 2	1120	12.4	1110	+10	+11	1260	7.2	1262	− 2	− 2
− 1	1458	12.7	1484	−26	−20	1636	6.9	1636	0	+ 5
0	1860	12.3	1858	+ 2	+12	1989	6.6	2010	−21	−12
+ 1	2198	12.3	2232	−34	−20	2370	6.3	2384	−14	− 1
+ 2	2609	12.7	2606	+ 3	+20	2754	7.3	2758	− 4	+12
+ 3	2952	13.2	2980	−28	−10	3120	6.9	3132	−12	+ 5
+ 4	3333	12.6	3354	−21	− 2	3484	6.6	3506	−22	− 4
+ 5	3703	12.5	3728	−25	− 7	3865	6.6	3880	−15	+ 2
+ 6	4078	13.1	4102	−24	− 7	4243	6.9	4254	−11	+ 5
+ 7	4468	13.0	4476	− 8	+ 6	4615	6.0	4628	−13	−10
+ 8	4853	13.0	4850	+ 3	+13	4998	6.7	5002	− 4	+ 5
+ 9	5222	12.6	5224	− 2	+ 4	5367	6.8	5376	− 9	− 4
+10	5590	12.5	5598	− 8	− 7	5754	6.1	5750	+ 4	+ 4
+11	5987	13.3	5972	+15	+11	6145	6.5	6224	+21	+16
+12	6362	13.0	6346	+16	+ 8	6509	7.2	6498	+11	+ 2
+13	6725	12.4	6720	+ 5	− 7	—	—	—	—	—
		12.66			±9.5		6.72			± 7

Maximum scheinen die Abweichungen vom Mittelwert regellos aufzutreten.

Es wurde wieder der mittlere Verlauf der Lichtkurve in der Nähe der beiden Hauptphasen durch Ablesung der Helligkeit für je 10^d abgeleitet. Die beiden Teilkurven schliessen sich fast genau an einander an (s. die Figur 2), und geben zusammen den Verlauf der mittleren Kurve *B* (Tabelle IV).

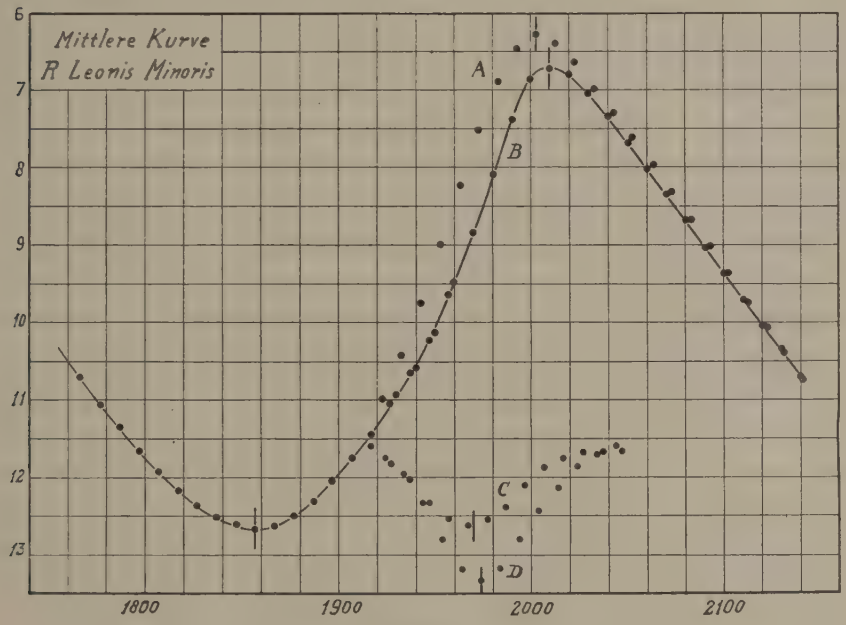

Fig. 2.

TABELLE IV. Die mittlere Kurve.

Phase	v	Phase	v	Phase	v	Phase	v	Phase	v
d	m	d	m	d	m	d	m	d	m
— 100	10.39	— 20	12.52	+ 60	11.46	+ 140	6.97	+ 220	8.58
— 90	10.73	— 10	12.61	+ 70	11.10	+ 150	6.73	+ 230	8.92
— 80	11.06	0	12.66	+ 80	10.70	+ 160	6.77	+ 240	9.25
— 70	11.37	+ 10	12.62	+ 90	10.24	+ 170	6.98	+ 250	9.58
— 60	11.66	+ 20	12.50	+ 100	9.68	+ 180	7.25	+ 260	9.91
— 50	11.92	+ 30	12.32	+ 110	9.02	+ 190	7.57	+ 270	10.24
— 40	12.16	+ 40	12.06	+ 120	8.30	+ 200	7.91	+ 280	10.58
— 30	12.36	+ 50	11.78	+ 130	7.59	+ 210	8.25		

Obwohl die mittlere Kurve glatt verläuft, so bekommt man dennoch

bei der Betrachtung der Fig. 1 die Ueberzeugung, dass auch *R Leonis minoris* beim Aufstieg eine Störung erleidet. Zwar ist diese Störung nicht immer deutlich ausgeprägt: die durch zahlreiche Schätzungen gut verbürgten Maxima 2417907, 8671, 9032, 2421989 und 4615 z. B. zeigen sogar keine Spur davon, während in anderen Fällen (2419403, 9775, 2421636, 4243, 5754, 6145) der Stillstand im aufsteigenden Aste ins Auge springt.

Ich habe es diesmal nicht wie bei *S Ursae Majoris* und *R Cygni* gewagt, für sämtliche Maxima nebst dem wirklich beobachteten einen "ungestörten" Kurvenzug zu konstruieren, mich aber, — etwas willkürlich und daher nicht sehr befriedigend — auf die deutlich sprechenden Fälle beschränkt, und dabei zwei Maxima (2417537 und 2420877) mit in den Kauf genommen, bei denen die Störung im Abstieg auftritt. Allerdings fühle ich mich hier nicht sicher. Zieht man bei diesen beiden Maxima den absteigenden Kurvenast glatt durch, so kommt das auf eine an sich gar nicht unwahrscheinliche Anhäufung von drei oder höchstens vier Zeichenfolgen heraus.

Hier folgt nun (Tabelle V) die Zusammenstellung der ungestörten Maxima: im Mittel fällt das ungestörte Maximum M' 7^d früher als das wirklich beobachtete M, und also auf 2422003. Das grösste Licht wird jetzt $6^m.33 \pm 0^m.098$ (m. F.).

TABELLE V. Die ungestörten Maxima M'.

E	M	M'	v	$M'-M$	E	M	M'	v	$M'-M$
	241		m			242		m	
— 13	7167	—	6.6	0	0	1989	—	6.6	0
— 12	7537	7541	6.1	[+ 4]	+ 1	2370	2361	5.9	— 9
— 11	7907	—	6.4	0	+ 2	2754	2740	6.6	— 14
— 10	8293	8280	5.5^5	— 13	+ 3	3120	3109	6.4	— 11
— 9	8671	—	7.7	0	+ 4	3484	3476	6.0	— 8
— 8	9032	—	6.7	0	+ 5	3865	3853	6.0	— 12
— 7	9403	9389	6.7	— 14	+ 6	4243	4229	6.4	— 14
— 6	9775	9766	5.9	— 9	+ 7	4615	—	6.0	0
— 5	242 0140	0125	5.8	— 15	+ 8	4998	4984	6.3	— 14
— 4	0502	—	7.1	0	+ 9	5367	5354	6.4	— 13
— 3	0877	0886	5.9	[+ 9]	+ 10	5754	5740	5.5	— 14
— 2	1260	1246	6.6	— 14	+ 11	6145	6131	6.0	— 14
— 1	1636	1622	6.3	— 14	+ 12	6509	—	7.1^5	0
								6.33	— 7

Auch die mittlere Kurve A des ungestörten Maximums, bei deren Bildung selbstverständlich auch die ungestörten Maxima 2417167, 7907, 8671, 9032, 2420502, 1989, 4615 und 6509 mitstimmten, schliesst sich der Kurve des Minimums wieder vorzüglich an (s. Figur 2). Die Schiefe wird jetzt

$$\frac{M-m}{P} = 0.390.$$

Schliesslich wurde noch die Differenzkurve $C = A - B$ gebildet, welche sich wieder so gut wie symmetrisch gestaltet; ich hatte das in diesem besonderen Falle eigentlich kaum erwartet. Die Verfinsterung, deren Mitte, zu $1^m.12$, auf 2421970 fällt und also 33^d vor dem (ungestörten) Maximum, beraubt den Stern von 64% seines Lichtes.

Man kann die beobachtete Störung auch so deuten, dass der Stern in gewissen Fällen bei der Aufhellung nicht gestört wird, in anderen Fällen aber um so stärker. Werden die Verfinsterungskurven, 18 an der Zahl, einzeln bestimmt, und dann zu einer mittleren Kurve vereinigt, indem man die Minima zur Deckung bringt, so entsteht die Kurve D (s. Fig. 2) deren Minimum, zu $1^m.84$, auf 2421974 fällt, 29^d vor dem Maximum M': bei dieser intermittierenden Verfinsterung büsst der Stern 82% seiner Helligkeit ein. Ich wäre geneigt, die beiden fraglichen Maxima 7537 und 0877 lieber ausser Acht zu lassen: dann fällt die Mitte der Verfinsterung auf 1963, oder 40^d vor dem ungestörten Maximum; das Minimum vertieft zich zu $1^m.94$ und der Stern wird von 83% seines Lichtes beraubt. Diese Deutung der beobachteten Erscheinung kommt mir die wahrscheinlichste vor.

Zu bemerken ist schliesslich noch, dass ich in meinen früheren Berichten über *R Leonis minoris* die Lichtkurve wiederholt als "schlängelnd" typiert habe. Diese Charakteristik kann jetzt, wie man sieht, aufgegeben werden: die Lichtkurve unterscheidet sich nach der neuen Bearbeitung nicht wesentlicht mehr von den Kurven, welche wie z.B. bei *T Cassiopeiae* und *T Cephei* regelmässig einen Buckel im Aufstieg aufweisen.

Zusammenfassung.

Aus 592 in den Jahren 1905 bis 1932 (2416836 bis 2426791) angestellten Beobachtungen von *R Leonis minoris* sind die folgenden Elemente des Lichtwechsels abgeleitet worden:

$$\left.\begin{array}{l}\text{Minimum: } 2421857^d \\ \text{Maximum: } 2422010\end{array}\right\} + 374^d\,E - 18^d\,\sin 15^\circ\,(E+2); \quad \begin{array}{l} v = 12^m.66 \\ v = 6\ .72 \\ \hline \text{Amplitude} = 5\ .94.\end{array}$$

Der Stern scheint bei den meisten Aufhellungen eine Verdunkelung von $1^m.94$ zu erfahren, deren Minimum auf 2421963 fällt.

Utrecht, Juli 1932.

Chemistry. — *Osmotic systems with water, NaCl and Na_2CO_3 in which one invariant liquid.* I. By F. A. H. SCHREINEMAKERS and L. J. VAN DER WOLK.

(Communicated at the meeting of September 24, 1932).

I. *Systems with a ternary invariant liquid.*

In the ternary osmotic system :

$$L(z) \mid inv.\ L'(X+Y+W) \ldots\ldots\ldots (1)$$

is a membrane permeable for the three substances X, Y and W(water). On the right side of this membrane is an invariant liquid L', containing the three substances X, Y and W ; we imagine this liquid represented in fig. 1 by point i ; the angle-points and sides of this XYW-diagram have not been drawn in this figure. On the left side of the membrane is a variable liquid $L(z)$, also containing the substances X, Y and W or in which at the beginning of the osmosis one or two of these substances may also be missing.

If we leave this system alone, the variable liquid $L(z)$ will change its composition and will during the osmosis consequently travel along a path in the XYW-diagram. As we have assumed that the membrane is permeable for all substances, the variable liquid will towards the end of the osmosis get the same composition as the invariant one [1] ; so the path of the variable liquid will end in point i (fig. 1).

As at the beginning of the osmosis we may give an infinite number of varying compositions to the variable liquid $L(z)$ (e.g.: f, u, p, q, etc. fig. 1), an infinite number of paths may meet in point i ; together they form the bundle of point i. We now may deduce [2] :

all paths meeting in an invariant point i have only two tangents in this point, which we may call the axes of this bundle ;

an infinite number of paths touches one of these axes (the principal axis) ; the other axis (the secondary axis) is touched only by two paths and in special cases by one only ;

the position of these axes is defined by the nature and the composition of the invariant liquid i and by the nature of the membrane.

If in fig. 1 we imagine the principal axis represented by kik' and the secondary axis by hih', then all paths will touch the axis kik' in i ; only the paths fi and $f'i$ touch the axis hih' in i.

---

[1] We assume namely that in the system $X+Y+W$ no dimixture into two liquids can occur.

[2] F. A. H. SCHREINEMAKERS, These Proceedings **34**, 341, 524 and 823 (1931).

During the osmosis the variable liquid will not only change its composition, but also its quantity ; in connection with experimental investigations, to be discussed further on, we shall also consider this change in quantity.

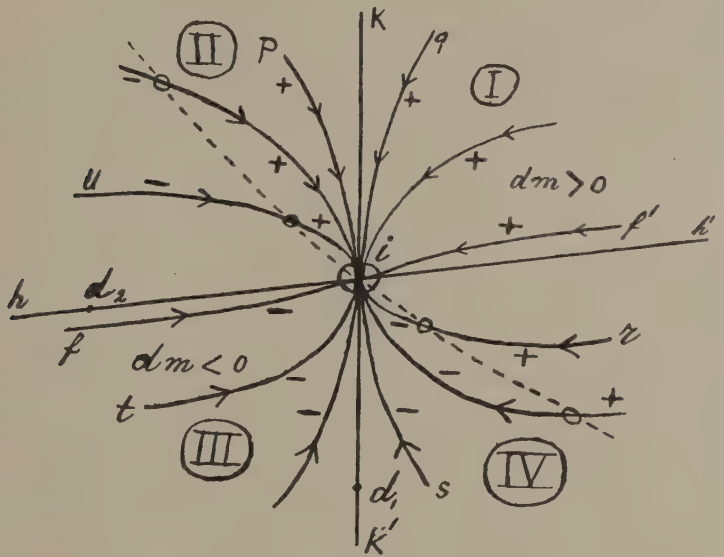

Fig. 1

At some moment of the osmosis we imagine the variable liquid of system (1) represented by a point z of one of the paths of fig. 1 ; the mixture diffusing at this moment is then represented by a point d of the tangent, which in this point z may be drawn to the path of the variable liquid.

If we take point z in one of the paths, touching the principal axis kik', then this tangent will coincide with the principal axis towards the end of the osmosis, namely when point z has arrived in the immediate vicinity of point i. So the mixture diffusing at this moment, and which we shall call the diffusing final-mixture, will be represented by a point of the principal axis ; we are able to deduce that all paths, touching the principal axis, must have the same diffusing final mixture. In accordance with experimental determinations to be discussed later on in an osmotic system containing the substances NaCl, Na_2CO_3 and water, this mixture has been represented in fig. 1 by a point d_1 on the part ik' of the principal axis.

We now shall first consider the paths touching part ik of the principal axis in i (e.g. path $u\,i$ or pi or qi). It follows from the position of point d_1 that a liquid, travelling along one of these paths, must take in this mixture d_1 towards the end of the osmosis ; consequently the quantity of the

variable liquid increases towards the end of the osmosis. This has been indicated in fig. 1 by the sign +, put with these paths.

As according to our deduction this increase of quantity is only valid, however, when the variable liquid has arrived in the vicinity of point *i*; it is of course possible that this quantity will decrease at some distance from point *i*. Further on we shall see that this happens indeed, so that we can distinguish two cases, viz.:

a. the quantity of the variable liquid increases during the entire osmosis (e.g. in paths *pi* and *qi* with which only the sign + has been placed).

b. during the osmosis the quantity of the variable liquid first decreases, next remains constant for a moment and then increases until the end of the osmosis (e.g. along path *ui* with which we find the signs — and +; the sign o indicates the liquid, the quantity of which does not change; we shall call this point the "zeropoint" of this path).

We now take the paths touching part *ik'* of the principal axis in point *i* (e.g. the paths *ri*, *si* and *ti*). It now follows from the position of point d_1 that a liquid travelling along one of these paths will give off this mixture d_1 towards the end of the osmosis; consequently the quantity of the variable liquid decreases towards the end of the osmosis. This has been indicated in the figure by placing the sign — with these paths.

Now it is clear that also here we may distinguish two cases, namely

c. the quantity of the variable liquid decreases during the entire osmosis (e.g. in the paths *si* and *ti*, with which only the sign — has been placed).

d. during the osmosis the quantity of the variable liquid first increases, next remains constant for a moment and then decreases until the end of the osmosis (e.g. along path *ri* with the signs +, o and —).

We now imagine the variable liquid *z* of system (1) represented by a point *z* of path *fi* or *f'i*, touching the secondary axis *hih'*. In a similar way as indicated above we now find that the diffusing final mixture must be situated somewhere on this secondary axis *hih'*. In accordance with the experimental determinations to be discussed later on (and the position of the zero-points in the paths touching the principal axis) this mixture has been represented in fig. 1 by a point d_2 on part *ih* of the secondary axis. From this it follows that the quantity of the variable liquid of path *fi* will decrease towards the end of the osmosis and the quantity of the variable liquid of path *f'i* will increase towards the end of the osmosis.

If we summarise the above considerations on the change in quantity of the variable liquid, it appears that in fig. 1 we may distinguish four groups of paths, namely

1. paths, along which the quantity of the variable liquid increases continuously (e.g. the paths *pi* and *qi*).

2. paths, along which the quantity of the variable liquid decreases continuously (e.g. the paths *si* and *ti*).

3. paths, along which during the osmosis the quantity of the variable liquid first increases and afterwards decreases (e.g. path *ri*).

4. paths, along which during the osmosis the quantity of the variable liquid first decreases and afterwards increases (e.g. path *ui*).

In order to illustrate the above, we represent the composition of the variable liquid $L(z)$ of the osmotic system:

$$L(z) \mid inv.\, L'(X+Y+W) \quad . \quad . \quad . \quad . \quad . \quad . \quad . \quad (2)$$

by

$$x\, gr\, X + y\, gr\, Y + (1-x-y)\, gr\, W \quad . \quad . \quad . \quad . \quad . \quad (3)$$

We now assume that in this system

$$(\alpha \,.\, dt)\, gr.\, X + (\beta \,.\, dt)\, gr.\, Y + (\gamma \,.\, dt)\, gr.\, W \quad . \quad . \quad . \quad . \quad (4)$$

flow through the membrane between the moments t and $t+dt$. We take α positive when the substance X diffuses towards the left and is consequently taken in by the variable liquid; if, however, the substance X diffuses towards the right and is consequently given off by the variable liquid, α will be negative. The same obtains for β and γ with respect to the directions in which Y and W diffuse.

If we represent the quantity of the variable liquid at the moment t by m and at the moment $t+dt$ by $m+dm$, we have, therefore:

$$dm = (\alpha+\beta+\gamma)\, dt \quad . \quad . \quad . \quad . \quad . \quad . \quad . \quad . \quad (5)$$

The quantity of the variable liquid will increase, therefore, between the moments t and $t+dt$ when $\alpha+\beta+\gamma>0$, decrease when $\alpha+\beta+\gamma<0$ and remain constant when $\alpha+\beta+\gamma=0$.

The quantity of X, running through the membrane in system (2) between the moments t and $t+dt$, depends upon the composition of the variable liquid, on the composition of the invariant liquid and on the nature of the membrane. So we may put:

$$\alpha = \varphi(x\, y) \quad . \quad . \quad . \quad . \quad . \quad . \quad . \quad . \quad . \quad . \quad . \quad (6)$$

which function also contains the composition of the invariant liquid and the magnitudes, determining the nature of the membrane. For the diffusing quantities Y and W obtains also:

$$\beta = f(x\, y) \quad \text{and} \quad \gamma = F(x\, y) \quad . \quad . \quad . \quad . \quad . \quad . \quad (7)$$

for which functions the same obtains as for (6). Instead of (5) we may write, therefore:

$$dm = [\varphi(x\, y) + f(x\, y) + F(x\, y)]\, dt \quad . \quad . \quad . \quad . \quad . \quad (8)$$

From this it appears that the quantity of a variable liquid will not change during a moment dt, when its composition (xy) satisfies:

$$\varphi(x\,y) + f(x\,y) + F(x\,y) = 0 \quad . \quad . \quad . \quad . \quad . \quad . \quad (9)$$

From this it follows that in fig. 1 there is an infinite number of variable liquids, the quantity of which does not change at a certain moment of the osmosis; or in other words: there must be an infinite number of zero-points in fig. 1. All these zero-points are situated on a curve, determined by (9); we shall call this curve the "zero-curve".

We imagine this zero-curve drawn in fig. 1 through the points, indicated by the sign o (the zeropoints of the paths). It is clear that this curve must also run through point i; if namely we imagine the variable liquid in point i, then, as both liquids will have the same composition at that time, the osmosis has ended and the quantity of the variable liquid consequently will remain constant (in this special case not only $\alpha + \beta + \gamma = 0$, but also at the same time $\alpha = 0$, $\beta = 0$ and $\gamma = 0$).

The shape of the zerocurve, as we have seen above, is determined by (9); as each of the three functions of (9) besides contains the magnitudes determining the nature of the membrane, this curve may have different shapes.

Above namely we have tacitly assumed that every path intersecting this curve, has only one single point of intersection with this curve. We may also suppose, however, that there are paths, intersected by this curve in two points; this will surely be the case e.g. when the zerocurve is a closed curve. Then we have paths with two zeropoints, so that during the osmosis the quantity of the variable liquid of such a path does not change for a moment in two points. If e.g. we imagine still another zeropoint in path ui (fig. 1), then during the osmosis the quantity of the variable liquid will first increase, afterwards it will decrease for some time and at last it will increase again until the end of the osmosis.

It also appears from the preceding considerations that between the position of the two diffusing final mixtures d_1 and d_2 and the direction of the zerocurve in point i there will exist some relation. We may deduce namely:

the points d_1 and d_2 are situated on the same side of the tangent that can be drawn to the zerocurve in point i.

From this it follows that the zerocurve (at least in the vicinity of point i) must be situated in fig. 1 within the angles hik and $h'ik'$; as we shall see later on, our experimental investigations agree with this.

We now shall discuss some of the paths, which have been experimentally determined in an osmotic system with the substances

$$X = NaCl \quad Y = Na_2CO_3 \quad \text{and} \quad W = \textit{water}.$$

From the determinations of these paths etc. it appears that the bundle of the system

$$L\,(z)\,|\,inv.\,L'\,(W + NaCl + Na_2CO_3)$$

can be represented schematically by fig. 1, in which we imagine the X-axis (NaCl-axis) horizontal and the Y-axis (Na_2CO_3-axis) vertical. The principal axis *kik'* and the paths *fi* and *f'i*, touching the secondary axis *hih'*, divide fig. 1 into four fields, which have been indicated by the encircled ciphers I, II, III and IV; in order to simplify the subsequent discussion we shall call them the fields I, II etc.

First we take the osmotic system

$$L\,(z)\,|\,inv.\,L'\,(i)\quad M = pig's\ bladder\ \alpha \quad . \quad . \quad . \quad . \quad (10)$$

in which a membrane of pig's bladder, which we shall call α and an invariant liquid $L'(i)$ with the composition:

$$11.72\ \%\ NaCl + 6.72\ \%\ Na_2CO_3 + 81.56\ \%\ H_2O$$

which we imagine represented in fig. 1 by point *i*.

For the variable liquid $L(z)$ we took the liquids *a*, *b*, *c* and *d*, which at the beginning of the osmosis had the compositions indicated in table 1.

TABLE I.

	% NaCl	% Na_2CO_3	% H_2O
L (beg a)	6.053	3.474	90.473
L (beg b)	5.496	6.686	87.818
L (beg c)	18.150	3.502	78.348
L (beg d)	18.014	6.863	75.123

So we determined the paths of the systems:

$$L\,(beg\ a)\,|\,inv\,L'\,(i) \qquad L\,(beg\ b)\,|\,inv\,L'\,(i)$$
$$L\,(beg\ c)\,|\,inv\,L'\,(i) \qquad L\,(beg\ d)\,|\,inv\,L'\,(i)$$

The data for these systems are found in the tables 2—5. In the first column we find the numbers of the successive determinations, in the second column the time, viz. the number of hours passed after the beginning of the osmosis. In the third, fourth and fifth columns we find the composition of the variable liquid in procents of weight ($X = NaCl$, $Y = Na_2CO_3$); in the three following columns we find sub X, Y and W the number of grams of NaCl, Na_2CO_3 and Water, which have passed through the membrane between two successive determinations: the sign + indicates that this quantity has been taken in by the variable liquid; the sign — indicates that this quantity has been given off by the variable liquid.

TABLE 2. L (*beg.* a) | *inv.* L' (*i*)

N⁰.	t in hours	Comp. of the variable liquid % X	% Y	% W	Diffused to the variable liquid gr X	gr Y	gr W	$\triangle m$
1	0	6.053	3.474	90.473				
2	16.5	7.069	3.625	89.206	+ 3.088	+ 0.127	— 16.146	— 12.931
3	39.5	8.391	3.846	87.763	+ 3.502	+ 0.197	— 19.623	— 15.924
4	64.3	9.555	4.090	86.355	+ 2.622	+ 0.257	— 16.713	— 13.834
5	110.	11.002	4.505	84.493	+ 2.510	+ 0.473	— 21.426	— 18.443
6	157.6	11.777	4.874	83.349	+ 0.755	+ 0.448	— 13.445	— 12.242
7	252.3	12.183	5.483	82.334	— 0.727	+ 0.776	— 14.646	— 14.597
8	419.3	11.992	6.153	81.855	— 1.772	+ 0.899	— 10.159	— 11.032
9	634.3	11.820	6.512	81.668	— 1.051	+ 0.400	— 5.097	— 5.748

From these three columns follows at once what has been indicated in the last column, namely the total quantity ($\triangle m$) taken in (sign +) by the variable liquid between two successive determinations or given off (sign —).

If we now draw the osmosis-paths with the aid of these tables we see that they have the same tangent in their final point i; this tangent, therefore, is the principal axis *kik'* of the bundle.

We now see that path *ai* is situated in field III. The W-amount of the variable liquid decreases during the entire osmosis, as is apparent from table 2 (column 3—5), whereas the Y-amount increases; the X-amount, however, first increases (nos 1—7) and afterwards decreases.

So the X-amount of the variable liquid passes through a maximum, consequently the path must have a vertical tangent somewhere.

From table 2 (column 6—8) it appears besides that during the entire osmosis water is given off by the variable liquid, whereas the substance Y is taken in; the substance X, however, is first taken in (nos 2—6) and afterwards given off.

From the last column it appears that during the entire osmosis the variable liquid gives off the diffusing mixture, so that the quantity of the variable liquid decreases continuously; this is in accordance with the position of this path *ai* in field III.

Path *bi* is situated in field II. It appears from table 3, that this path has a maximum Y-amount; that during the entire osmosis the variable liquid takes in the substance X, gives off the substance Y, but first gives off water and afterwards takes water in again. It appears from the last column that the quantity of the variable liquid first decreases and increases again

towards the end of the osmosis; consequently the path has a zeropoint in the vicinity of point *i*, like e.g. path *ui* of fig. 1.

TABLE 3. *L (beg b) | inv L('i).*

N°.	*t* in hours	Composition of the variable liq. % *X*	% *Y*	% *W*	Diffused to the varable liq. gr. *X*	gr. *Y*	gr. *W*	Δ *m*
1	0	5.496	6.686	87.818				
2	22.7	6.769	6.796	86.435	+ 4.324	— 0.228	— 13.799	— 9.703
3	45.7	7.827	6.856	85.317	+ 3.345	— 0.310	— 10.826	— 7.791
4	81.5	9.088	6.928	83.984	+ 3.768	— 0.322	— 11.801	— 8.355
5	127.7	10.163	6.961	82.876	+ 2.993	— 0.326	— 8.962	— 6.295
6	211.5	11.130	6.984	81.886	+ 2.628	— 0.215	— 6.551	— 4.138
7	287	11.446	6.939	81.615	+ 0.910	— 0.164	— 1.179	— 0.433
8	497.3	11.656	6.823	81.521	+ 0.810	— 0.221	+ 1.120	+ 1.709

The paths *ci* and *di* are both situated in field IV. It appears from table 5 that path *di* has a minimum *Y*-amount. It appears from the tables 4 and 5 that during the entire osmosis the variable liquids of the two paths give off the substance *X*, take in the substance *Y*, but first take in the water and afterwards give it off. It appears from the last column that during the osmosis the quantity of the variable liquid of both paths first increases and

TABLE 4. *L (beg. c) | inv. L'(i).*

N°.	*t* in hours	Composition of the variable liq. % *X*	% *Y*	% *W*	Diffused to the variable liq. gr. *X*	gr. *Y*	gr. *W*	Δ *m*
1	0	18.150	3.502	78.348				
2	22.2	17.039	3.637	79.324	— 4.230	+ 0.630	+ 5.649	+ 2.049
3	46.7	16.052	3.779	80.169	— 3.794	+ 0.592	+ 3.957	+ 0.755
4	86.5	14.883	4.044	81.073	— 4.647	+ 0.946	+ 2.236	— 1.465
5	153	13.650	4.473	81.877	— 5.421	+ 1.255	— 2.643	— 6.809
6	246.5	12.772	5.039	82.189	— 4.469	+ 1.358	— 8.353	— 11.464
7	415.7	12.154	5.841	82.005	— 3.696	+ 1.717	— 12.261	— 14.240
8	558	11.906	6.260	81.834	— 1.659	+ 0.729	— 6.959	— 7.889
9	743	11.809	6.510	81.681	— 0.855	+ 0.354	— 4.489	— 4.990

afterwards decreases. Consequently both paths have a zeropoint as e.g. path *ri* of fig. 1.

From this we see that the variable liquids of the paths *ci* and *di* behave in all respects differently (viz. reversely) from the one of path *bi*.

TABLE 5. *L (beg. d) | inv. L'(i).*

N⁰.	*t* in hours	Composition of the variable liq. % *X*	% *Y*	% *W*	Diffused to the variable liq. gr. *X*	gr. *Y*	gr. *W*	Δ *m*
1	0	18.014	6.863	75.123				
2	16	17.268	6.773	75.959	− 1.938	+ 0.074	+ 8.436	+ 6.572
3	39.5	16.222	6.698	77.080	− 2.878	+ 0.277	+ 11.390	+ 8.789
4	66.5	15.195	6.612	78.193	− 3.025	+ 0.177	+ 10.881	+ 8.033
5	109.6	14.061	6.510	79.429	− 3.315	+ 0.165	+ 12.023	+ 8.873
6	168.5	13.114	6.483	80.403	− 2.936	+ 0.330	+ 9.371	+ 6.765
7	277	12.256	6.450	81.294	− 2 941	+ 0.140	+ 7.047	+ 4.246
8	346.7	12.068	6.491	81.441	− 0.701	+ 0.189	+ 0.930	+ 0.418
9	658.2	11.808	6.609	81.583	− 1.300	+ 0.300	− 1.424	− 2.424

If we substitute the pig's bladder α, used in system (10) by an other pig's bladder β or by parchment or cellophane, we get the three systems

$$L\,(z)\,|\,inv.\,L'\,(i) \quad M = pig's\ bladder\ \beta \quad . \quad . \quad . \quad . \quad . \quad (11)$$

$$L\,(z)\,|\,inv.\,L'\,(i) \quad M = parchment \quad . \quad . \quad . \quad . \quad . \quad . \quad (12)$$

$$L\,(z)\,|\,inv.\,L'\,(i) \quad M = cellophane \quad . \quad . \quad . \quad . \quad . \quad . \quad (13)$$

in which the invariant liquid has the same composition as in system (10). It appears from the experimental[1]) determinations that the bundle of each of these systems can be represented again schematically by fig. 1; the principal axis *kik'* (and the secondary axis *hih'*), however, has in each of these systems a slightly different direction, as was to be expected.

A system

$$L\,(z)\,|\,inv\,L'\,(i) \qquad M = pig's\ bladder\ \gamma \quad . \quad . \quad . \quad . \quad (14)$$

was also examined, in which the invariant liquid had a composition differing entirely from that in the preceding systems; it contained namely

$$4.68\ \%\ NaCl + 10.10\ \%\ Na_2CO_3 + 85.22\ \%\ H_2O.$$

It appeared from the experimental determinations that the bundle of

[1]) Comp. L. J. v. D. WOLK, Diss. Leiden 1932. The bundles of this system and of the system (10) already discussed above are found in the figs. 8, 9, 10 and 12.

this system [1]), in which only paths were determined, situated in the fields III and IV, can also be represented schematically by fig. 1.

We shall not discuss these systems here, but only summarise some results; see table 6. In the first column we find the number, by which these systems have been indicated in this communication; in the last column we find the number of the figures in the dissertation (l.c.).

TABLE 6

Syst.	*Sign of dm*				Diss. l. c.
	+	−0+	−	+0−	
10	*n*	1	1	2	fig. 9
11	1	2	2	1	fig. 8
12	*n*	1	1	*n*	fig. 10
13	*n*	*n*	1	1	fig. 12
14	*n*	*n*	5	2	fig. 7

Above we have seen that, according to the change (dm) in the quantity of the variable liquid during the osmosis, we can divide the paths into four groups; we find these groups indicated in the columns 2—5 by the sign of dm and also the number of the paths determined in every group; n means that no path of this group has been determined.

Among other things it now appears from this table 6 that in system (11) six paths have been determined; along one of these paths the quantity of the variable liquid increases during the entire osmosis ($dm = +$); along two of these paths the quantity of the variable liquid first decreases and afterwards increases till the end of the osmosis ($dm = -0+$); along two paths the quantity of the variable liquid decreases ($dm = -$) during the entire osmosis and along one of these paths the quantity of the variable liquid first increases and afterwards decreases till the end of the osmosis ($dm = +0-$).

For normal and anormal changes in concentration, positive and negative osmosis and other phenomena, which may occur in these systems during the osmosis, we refer to the dissertation (l.c.).

(To be continued).

Leiden, Lab. of Inorg. Chemistry.

[1]) L. J. v. d. Wolk l. c. fig. 7.

Mathematics. — *Asymptotische Entwicklungen von* BESSELschen, HANKELschen *und verwandten Funktionen.* III [1]). Von C. S. MEIJER. (Communicated by Prof. J. G. VAN DER CORPUT).

(Communicated at the meeting of September 24, 1932).

Hilfssatz 14. *Ist* $w \neq 0$, $-\pi < arg\, w < \pi$ *und*

$$Max\left(-\frac{\pi}{2}, -\frac{\pi}{2}+arg\, w\right) < \mu < Min\left(\frac{\pi}{2}, \frac{\pi}{2}+arg\, w\right), \quad . \quad (76)$$

dann kann:

1. *Für jedes ganze* $N > \frac{|\Re(\nu)|}{2} - \frac{1}{2}$ *die in* (9) *definierte Funktion* $A_\nu(w)$ *auf die Gestalt*

$$\left.\begin{aligned} A_\nu(w) = {} & \sum_{l=0}^{N-1} \frac{1}{w^{2l+1}} \prod_{h=0}^{l-1} (\nu^2 - (2h+1)^2) + \\ & \frac{\cos\frac{\nu\pi}{2}}{(-1)^N \pi w^{2N+1}} \int_0^{\infty e^{i\mu}} e^{-u} u^{2N}\, du \int_{-\infty}^{\infty} \frac{w^2 \cosh^2 x \cosh \nu x\, dx}{(\cosh x)^{2N+1} (w^2 \cosh^2 x + u^2)} \end{aligned}\right\} \quad (77)$$

gebracht werden.

2. *Für jedes ganze* $N > \frac{|\Re(\nu)|}{2} - 1$ *die in* (10) *definierte Funktion* $B_\nu(w)$ *auf die Gestalt*

$$\left.\begin{aligned} B_\nu(w) = {} & \nu \sum_{l=0}^{N-1} \frac{1}{w^{2l+2}} \prod_{h=0}^{l-1} (\nu^2 - (2h+2)^2) + \\ & \frac{\sin\frac{\nu\pi}{2}}{(-1)^N \pi w^{2N+2}} \int_0^{\infty e^{i\mu}} e^{-u} u^{2N+1}\, du \int_{-\infty}^{\infty} \frac{w^2 \cosh^2 x \cosh \nu x\, dx}{(\cosh x)^{2N+2} (w^2 \cosh^2 x + u^2)} \end{aligned}\right\} \quad (78)$$

gebracht werden.

Beweis. 1. Wir gehen von der Integraldarstellung (9) von $A_\nu(w)$ aus. Wir setzen $z = x + iy$ und betrachten nur den Streifen der z-Ebene zwischen den Geraden R_7 und R_8, worauf $y = \frac{\pi}{2}$ bez. $y = -\frac{\pi}{2}$ (einschliesslich R_7 und R_8). Die Gleichung der Kurve $\Im(e^{-i\mu} w \sinh z) = 0$ ist

$$\cos(arg\, w - \mu) \cosh x \sin y + \sin(arg\, w - \mu) \sinh x \cos y = 0 \; . \quad (79)$$

[1]) Erste und zweite Mitteilung: These Proceedings, Vol. 35 (1932), S. 656—667 und S. 852—866.

Diese Kurve geht durch $z=0$ und ist symmetrisch in Bezug auf diesen Punkt. Die Tangente in $z=0$ bildet einen Winkel gleich $-\arg w+\mu$ mit der positiven Achse.

Ist $\arg w-\mu=0$, dann besteht der im betrachteten Streifen liegende Teil der Kurve nur aus der reellen Achse.

Ist $\arg w-\mu\neq 0$, dann schneidet die Gerade $x=0$ die Kurve (79) zwischen R_7 und R_8 nur im Punkte $z=0$. Die Gerade $x=a$ schneidet, falls $a>0$ und $0<\arg w-\mu<\frac{\pi}{2}$ ist, die Kurve (79) nur in einem Punkt und dieser Punkt liegt zwischen der reellen Achse und R_8. Denn setzt man die linke Seite von (79) gleich $f(x, y)$, dann ist $f(a, y)>0$ für $0\leqq y<\frac{\pi}{2}$ und $f(a, y)$ monoton steigend im Intervall $-\frac{\pi}{2}<y\leqq 0$. Wegen $f\left(a,-\frac{\pi}{2}\right)<0$ und $f(a, 0)>0$ hat $f(a, y)$ also eine und nur eine Nullstelle im Intervall $-\frac{\pi}{2}<y<0$. Ebenso beweist man, dass die Gerade $x=a$, falls $a>0$ und $-\frac{\pi}{2}<\arg w-\mu<0$ ist, die Kurve (79) nur in einem Punkt schneidet und zwar in einem Punkt zwischen der reellen Achse und R_7. Der zwischen R_7 und R_8 liegende Teil der Kurve (79) besteht also, falls $\arg w-\mu\neq 0$ ist, nur aus einem Zweig, der die reelle Achse nur im Punkte $z=0$ schneidet und R_7 und R_8 weder schneidet noch berührt. Aus (79) folgt, dass bei unbeschränkt wachsendem x y nach einem Grenzwert η strebt mit $\sin(\eta+\arg w-\mu)=0$; wegen (76) ist $-\frac{\pi}{2}<\arg w-\mu<\frac{\pi}{2}$. Also sind die Punkte $\infty-i(\arg w-\mu)$

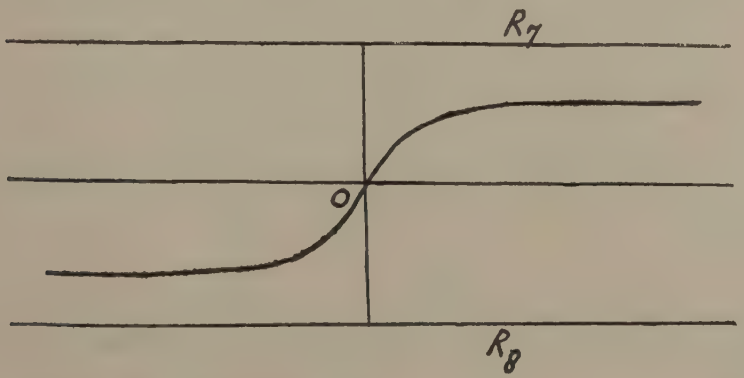

und (wegen der Symmetrie in Bezug auf $z=0$) $-\infty+i(\arg w-\mu)$ die im Unendlichen liegenden Punkte des obengemeinten Zweiges.

Wir nennen jetzt N den Teil der Kurve (79), der die Punkte 0 und $\infty-i(\arg w-\mu)$ verbindet. Ist $\arg w-\mu=0$, dann ist N die positive Achse.

Nehmen wir nun in (9) N als Integrationsweg, dann bekommen wir

$$A_\nu(w) = \int_N e^{-w \sinh z} \cosh \nu z \, dz \quad . \quad . \quad . \quad . \quad . \quad . \quad . \quad (80)$$

Setzt man

$$u = \Psi(z) = w \sinh z, \quad . \quad . \quad . \quad . \quad . \quad . \quad . \quad . \quad . \quad (81)$$

dann ist $e^{-i\mu} u$ reell für jedes z auf N; im Punkte $z = 0$ ist $u = 0$, und im Punkte $z = \infty - i(\arg w - \mu)$ ist $u = \infty e^{i\mu}$. Da auf N kein Sattelpunkt von $\sinh z$ liegt, läuft also $u e^{-i\mu}$ monoton von 0 nach ∞, wenn z die Kurve N von 0 nach $\infty - i(\arg w - \mu)$ durchläuft. Aus (80) und (81) folgt daher

$$A_\nu(w) = \int_0^{\infty e^{i\mu}} e^{-u} \cosh \nu z \frac{dz}{du} du \quad . \quad . \quad . \quad . \quad . \quad . \quad (82)$$

Wir betrachten nun die Kurve C_2, bestehend aus R_7, R_8 und den Geraden $x = k_1$ und $x = -k_2$, worin k_1 und k_2 unbeschränkt wachsen $\left(x = k_1 \text{ verbindet } \infty - \frac{\pi i}{2} \text{ mit } \infty + \frac{\pi i}{2},\ x = -k_2 \text{ verbindet } -\infty - \frac{\pi i}{2}\right.$ $\left.\text{mit } -\infty + \frac{\pi i}{2}\right)$. Wir wenden (41) von Hilfssatz 5 an mit $C = C_2$ und $F(z) = \Psi(z)$, also mit $p = w$ und $q = 1$, und finden dann für jedes z innerhalb C_2

$$\cosh \nu z \frac{dz}{du} = \frac{1}{2\pi i} \sum_{l=0}^{N-1} u^{2l} \int_{C_2} \frac{\cosh \nu t \, dt}{\Psi(t)^{2l+1}} + \frac{u^{2N}}{2\pi i} \int_{C_2} \frac{\cosh \nu t \, dt}{\Psi(t)^{2N}(\Psi(t) - u)}.$$

Aus Hilfssatz 4 folgt, dass $\Psi(t) \neq \Psi(z)$ ist, falls t auf C_2 und z innerhalb C_2 liegt; daher ist wegen (45) von Hilfssatz 6, mit $p = w$, $q = 1$ und $d = \Psi(z) = u$ angewendet, für jedes z innerhalb C_2 und jedes ganze $N > \frac{|\Re(\nu)|}{2} - \frac{1}{2}$

$$\int_{C_2} \frac{\cosh \nu t \, dt}{\Psi(t)^{2N}(\Psi(t) - u)} = \frac{2i \cos \frac{\nu\pi}{2}}{(-1)^N w^{2N+1}} \int_{-\infty}^{\infty} \frac{w^2 \cosh^2 x \cosh \nu x \, dx}{(\cosh x)^{2N+1}(w^2 \cosh^2 x + u^2)}.$$

Aus (38) von Hilfssatz 3 mit $a = 1$ und $m = 2l$ ergibt sich

$$\int_{C_2} \frac{\cosh \nu t \, dt}{\Psi(t)^{2l+1}} = \frac{1}{w^{2l+1}} \int_{(0+)} \frac{\cosh \nu t \, dt}{(\sinh t)^{2l+1}} = \frac{2\pi i}{w^{2l+1}(2l)!} \prod_{h=0}^{l-1} (\nu^2 - (2h+1)^2$$

also

$$\cosh \nu z \frac{dz}{du} = \sum_{l=0}^{N-1} \frac{u^{2l}}{w^{2l+1}(2l)!} \prod_{h=0}^{l-1} (\nu^2 - (2h+1)^2) +$$

$$\frac{u^{2N} \cos \frac{\nu\pi}{2}}{(-1)^N \pi w^{2N+1}} \int_{-\infty}^{\infty} \frac{w^2 \cosh^2 x \cosh \nu x \, dx}{(\cosh x)^{2N+1} (w^2 \cosh^2 x + u^2)}.$$

Hieraus und aus (82) folgt wegen

$$\int_0^{\infty e^{i\mu}} e^{-u} u^{2l} \, du = (2l)!$$

die erste Behauptung von Hilfssatz 14.

2. Wir gehen von der Integraldarstellung (10) aus und nehmen als Integrationsweg die Kurve N. Wir erhalten dann

$$B_\nu(w) = \int_N e^{-w \sinh z} \sinh \nu z \, dz$$

also, wenn wir (81) benutzen,

$$B_\nu(w) = \int_0^{\infty e^{i\mu}} e^{-u} \sinh \nu z \frac{dz}{du} \, du, \quad . \quad . \quad . \quad . \quad . \quad . \quad (83)$$

worin $u = \Psi(z)$ durch (81) definiert ist.

Wegen (42) von Hilfssatz 5, mit $C = C_2$ und $F(z) = \Psi(z)$, also mit $p = w$ und $q = 1$ angewendet, hat man für jedes z innerhalb C_2

$$\sinh \nu z \frac{dz}{du} = \frac{1}{2\pi i} \sum_{l=0}^{N-1} u^{2l+1} \int_{C_2} \frac{\sinh \nu t \, dt}{\Psi(t)^{2l+2}} + \frac{u^{2N+1}}{2\pi i} \int_{C_2} \frac{\sinh \nu t \, dt}{\Psi(t)^{2N+1} (\Psi(t) - u)}.$$

Wegen (46) von Hilfssatz 6, mit $p = w$, $q = 1$ und $d = \Psi(z) = u$ angewendet, hat man für jedes z innerhalb C_2 und jedes ganze $N > \frac{|\Re(\nu)|}{2} - 1$

$$\int_{C_2} \frac{\sinh \nu t \, dt}{\Psi(t)^{2N+1} (\Psi(t) - u)} = \frac{2i \sin \frac{\nu\pi}{2}}{(-1)^N w^{2N+2}} \int_{-\infty}^{\infty} \frac{w^2 \cosh^2 x \cosh \nu x \, dx}{(\cosh x)^{2N+2} (w^2 \cosh^2 x + u^2)}.$$

Aus (39) von Hilfssatz 3 mit $a = 1$ und $m = 2l + 1$ folgt

$$\int_{C_2} \frac{\sinh \nu t \, dt}{\Psi(t)^{2l+2}} = \frac{1}{w^{2l+2}} \int_{(0+)} \frac{\sinh \nu t \, dt}{(\sinh t)^{2l+2}} = \frac{2\pi \nu i}{w^{2l+2} (2l+1)!} \prod_{h=0}^{l-1} (\nu^2 - (2h+2)^2);$$

also

$$\sinh vz\,\frac{dz}{du}=\sum_{l=0}^{N-1}\frac{vu^{2l+1}}{w^{2l+2}(2l+1)!}\prod_{h=0}^{l-1}(v^2-(2h+2)^2)+$$

$$\frac{u^{2N+1}\sin\frac{v\pi}{2}}{(-1)^N\pi w^{2N+2}}\int_{-\infty}^{\infty}\frac{w^2\cosh^2 x\cosh vx\,dx}{(\cosh x)^{2N+2}(w^2\cosh^2 x+u^2)}.$$

Hieraus und aus (83) folgt wegen

$$\int_0^{\infty e^{i\mu}} e^{-u}u^{2l+1}\,du=(2l+1)!$$

die zweite Behauptung des Hilfssatzes.

Hilfssatz 15. *Ist $r>0$, $d\geqq 0$ und $-\pi<\beta<\pi$, dann hat man*

$$\left|\frac{re^{\beta i}}{re^{\beta i}+d}\right|\leqq\frac{1}{|\sin\beta|},\quad\ldots\ldots\quad(84)$$

und sogar, falls $-\frac{\pi}{2}\leqq\beta\leqq\frac{\pi}{2}$ ist,

$$\left|\frac{re^{\beta i}}{re^{\beta i}+d}\right|\leqq 1.\quad\ldots\ldots\quad(85)$$

Beweis. Man hat

$$\left.\begin{aligned}\left|\frac{re^{\beta i}+d}{re^{\beta i}}\right|&=\left|1+\frac{d}{r}e^{-\beta i}\right|=\sqrt{1+2\frac{d}{r}\cos\beta+\frac{d^2}{r^2}}\\&=\sqrt{\sin^2\beta+\left(\frac{d}{r}+\cos\beta\right)^2}\geqq|\sin\beta|,\end{aligned}\right\}\quad..\quad(86)$$

womit (84) bewiesen ist. Ist $-\frac{\pi}{2}\leqq\beta\leqq\frac{\pi}{2}$, dann ist $\cos\beta\geqq 0$, sodass dann aus (86) ausserdem noch folgt

$$\left|\frac{re^{\beta i}+d}{re^{\beta i}}\right|\geqq 1.$$

Hiermit ist Hilfssatz 15 bewiesen.

Hilfssatz 16. *Ist $r>0$, $d\geqq 0$ und $-\pi<\beta<\pi$, dann ist*

$$0\leqq\arg\left(\frac{re^{\beta i}}{re^{\beta i}+d}\right)\leqq\beta,\ \textit{falls}\ 0\leqq\beta<\pi\ \textit{ist},\quad\ldots\quad(87)$$

und

$$\beta \leqq arg\left(\frac{re^{\beta i}}{re^{\beta i}+d}\right) \leqq 0, \text{ falls } -\pi < \beta \leqq 0 \text{ ist.} \quad . \quad . \quad . \quad (88)$$

Beweis. Falls $d=0$, und auch falls $\beta=0$ ist, hat $\frac{re^{\beta i}}{re^{\beta i}+d}$ einen positiven Wert, also ein Argument $=0$. Ich darf also $d>0$ und $\beta \neq 0$ annehmen. Ich betrachte im Dreieck mit den Eckpunkten 0, $re^{\beta i}$ und $re^{\beta i}+d$ den Winkel α, dessen Spitze mit dem Koordinatenursprung zusammenfällt. Ist $0<\beta<\pi$, dann ist dieser Winkel α absolut genommen gleich $arg\,(re^{\beta i}) - arg\,(re^{\beta i}+d) = arg\left(\frac{re^{\beta i}}{re^{\beta i}+d}\right)$, sodass dieses Argument dann positiv und kleiner als β ist. Hiermit ist (87) bewiesen. Der Beweis von (88) geht auf analoge Weise.

Hilfssatz 17. *Es sei* $\varkappa > 0$, $-\frac{3\pi}{2} < \sigma < \frac{3\pi}{2}$,

$$Max\left(-\frac{\pi}{2}, -\pi+\sigma\right) < \mu < Min\left(\frac{\pi}{2}, \pi+\sigma\right), \quad . \quad . \quad . \quad (89)$$

$A=1$, *falls* $-\frac{\pi}{2} \leqq \sigma-\mu \leqq \frac{\pi}{2}$ *ist,*

$A = |\sin(\sigma-\mu)|$, *falls* $-\pi < \sigma-\mu < -\frac{\pi}{2}$ *und falls* $\frac{\pi}{2} < \sigma-\mu < \pi$ *ist,*

$$K(\mu) = A \,.\, (\cos\mu)^{\varkappa}, \qquad M = \underset{Max\left(-\frac{\pi}{2}, -\pi+\sigma\right) < \mu < Min\left(\frac{\pi}{2}, \pi+\sigma\right)}{Max} K(\mu)\ ^{1}).$$

Behauptungen:

1. *Ist* $-\frac{\pi}{2} \leqq \sigma \leqq \frac{\pi}{2}$, *dann ist* $M=1$.

2. *Ist* $-\frac{3\pi}{2} < \sigma < -\frac{\pi}{2}$, *dann ist*

$$M = \sin(\mu_1-\sigma)\,(\cos\mu_1)^{\varkappa};$$

hierin bezeichnet μ_1 *den durch*

$$\cos(\sigma-2\mu_1) = \frac{\varkappa-1}{\varkappa+1}\cos\sigma \quad . \quad . \quad . \quad . \quad . \quad . \quad . \quad . \quad (90)$$

---

[1]) D. h.: M ist der grösste Wert von $K(\mu)$ im Intervall

$$Max\left(-\frac{\pi}{2}, -\pi+\sigma\right) < \mu < Min\left(\frac{\pi}{2}, \pi+\sigma\right).$$

eindeutig bestimmten, im Falle $-\frac{3\pi}{2} < \sigma \leqq -\pi$ *zwischen* $-\frac{\pi}{2}$ *und* $\pi + \sigma$ *und im Falle* $-\pi < \sigma < -\frac{\pi}{2}$ *zwischen* $\frac{\pi}{2} + \sigma$ *und 0 liegenden Winkel.*

3. *Ist* $\frac{\pi}{2} < \sigma < \frac{3\pi}{2}$, *dann ist*

$$M = \sin(\sigma - \mu_2)(\cos\mu_2)^\varkappa;$$

hierin bezeichnet μ_2 *den durch*

$$\cos(\sigma - 2\mu_2) = \frac{\varkappa - 1}{\varkappa + 1}\cos\sigma$$

eindeutig bestimmten, im Falle $\pi \leqq \sigma < \frac{3\pi}{2}$ *zwischen* $-\pi + \sigma$ *und* $\frac{\pi}{2}$ *und im Falle* $\frac{\pi}{2} < \sigma < \pi$ *zwischen 0 und* $-\frac{\pi}{2} + \sigma$ *liegenden Winkel.*

Beweis. Wir unterscheiden drei Fälle:

1. Es sei $-\frac{\pi}{2} \leqq \sigma \leqq \frac{\pi}{2}$. Man hat $K(0) = 1$, wegen $K(\mu) \leqq 1$ folgt hieraus die erste Behauptung von Hilfssatz 17.

2. Es sei $-\frac{3\pi}{2} < \sigma < -\frac{\pi}{2}$. Hierbei unterscheiden wir wiederum zwei Fälle:

2*. Es sei $-\frac{3\pi}{2} < \sigma \leqq -\pi$. Wegen (89) ist dann $-\frac{\pi}{2} < \mu < \pi + \sigma$, also $-\pi < \sigma - \mu < \frac{\pi}{2} + \sigma \leqq -\frac{\pi}{2}$, somit

$$K(\mu) = \sin(\mu - \sigma)(\cos\mu)^\varkappa.$$

Hieraus ergibt sich

$$\left.\begin{aligned} K'(\mu) = \cos(\mu-\sigma)(\cos\mu)^\varkappa - \varkappa\sin(\mu-\sigma)(\cos\mu)^{\varkappa-1}\sin\mu = \\ (\cos\mu)^{\varkappa-1}(\cos(\mu-\sigma)\cos\mu - \varkappa\sin(\mu-\sigma)\sin\mu) = \\ \tfrac{1}{2}(\cos\mu)^{\varkappa-1}((\varkappa+1)\cos(\sigma-2\mu) - (\varkappa-1)\cos\sigma). \end{aligned}\right\} \quad (91)$$

Es existiert ein eindeutig bestimmter zwischen $-\sigma - 2\pi$ und $\sigma + \pi$ liegender Winkel φ mit der Eigenschaft

$$\cos\varphi = \frac{\varkappa - 1}{\varkappa + 1}\cos\sigma \quad . \quad . \quad . \quad . \quad . \quad . \quad . \quad . \quad (92)$$

Wegen $-\frac{\pi}{2} < \mu < \pi + \sigma$ ist $-\sigma - 2\pi < \sigma - 2\mu < \sigma + \pi$; es gibt also

einen eindeutig bestimmten zwischen $-\frac{\pi}{2}$ und $\pi+\sigma$ liegenden Winkel μ_1 mit (90). Aus (91) folgt nun

$$\underset{-\frac{\pi}{2}<\mu<\pi+\sigma}{Max} K(\mu)=K(\mu_1).$$

2**. Es sei $-\pi<\sigma<-\frac{\pi}{2}$, also wegen (89) $-\frac{\pi}{2}<\mu<\sigma+\pi$. Nun hat man, falls $-\frac{\pi}{2}<\mu\leqq\sigma+\frac{\pi}{2}$, also $-\frac{\pi}{2}\leqq\sigma-\mu<\sigma+\frac{\pi}{2}$ ist,

$$K(\mu)=(\cos\mu)^{\varkappa}\leqq\left(\cos\left(\sigma+\frac{\pi}{2}\right)\right)^{\varkappa}=K\left(\sigma+\frac{\pi}{2}\right). \quad . \quad . \quad (93)$$

und, falls $0\leqq\mu<\sigma+\pi$, also $-\pi<\sigma-\mu\leqq\sigma<-\frac{\pi}{2}$ ist,

$$K(\mu)=-\sin(\sigma-\mu)(\cos\mu)^{\varkappa}\leqq-\sin\sigma=K(0) \quad . \quad . \quad . \quad (94)$$

Aus (93) und (94) folgt, dass $K(\mu)$ seinen grössten Wert erreicht im Intervall $\sigma+\frac{\pi}{2}\leqq\mu\leqq 0$. Liegt μ in diesem Intervall, dann ist

$$K(\mu)=\sin(\mu-\sigma)(\cos\mu)^{\varkappa},$$
$$K'(\mu)=\tfrac{1}{2}(\cos\mu)^{\varkappa-1}((\varkappa+1)\cos(\sigma-2\mu)-(\varkappa-1)\cos\sigma). \quad . \quad . \quad (95)$$

Es existiert nun ein eindeutig bestimmter zwischen σ und $-\pi-\sigma$ liegender Winkel φ mit (92). Ist $\sigma+\frac{\pi}{2}<\mu<0$, dann ist $\sigma<\sigma-2\mu<-\sigma-\pi$; es gibt also einen eindeutig bestimmten zwischen $\sigma+\frac{\pi}{2}$ und 0 liegenden Winkel μ_1 mit (90). Aus (95) folgt jetzt

$$\underset{\sigma+\frac{\pi}{2}\leqq\mu\leqq 0}{Max} K(\mu)=K(\mu_1).$$

Hiermit ist die zweite Behauptung des Hilfssatzes bewiesen.

3. Es sei $\frac{\pi}{2}<\sigma<\frac{3\pi}{2}$. Die dritte Behauptung von Hilfssatz 17 folgt aus der zweiten, wenn man σ durch $-\sigma$ und μ durch $-\mu$ ersetzt.

Hilfssatz 18. *Es sei* $\varkappa > 0$, $-2\pi < \sigma < 2\pi$,

$$Max\left(-\frac{\pi}{2}, -\frac{\pi}{2}+\frac{\sigma}{2}\right) < \mu < Min\left(\frac{\pi}{2}, \frac{\pi}{2}+\frac{\sigma}{2}\right), \quad . \quad . \quad . \quad (96)$$

$B = 1$, *falls* $-\frac{\pi}{2} \leqq \sigma - 2\mu \leqq \frac{\pi}{2}$ *ist,*

$B = |\sin(\sigma - 2\mu)|$, *falls* $-\pi < \sigma - 2\mu < -\frac{\pi}{2}$ *und falls* $\frac{\pi}{2} < \sigma - 2\mu < \pi$ *ist,*

$$L(\mu) = B \cdot (\cos\mu)^{\varkappa}, \quad M^* = \underset{Max\left(-\frac{\pi}{2}, -\frac{\pi}{2}+\frac{\sigma}{2}\right) < \mu < Min\left(\frac{\pi}{2}, \frac{\pi}{2}+\frac{\sigma}{2}\right)}{Max} L(\mu)\ ^{1}).$$

Behauptungen:

1. *Ist* $-\frac{\pi}{2} \leqq \sigma \leqq \frac{\pi}{2}$, *dann ist* $M^* = 1$.

2. *Ist* $-2\pi < \sigma < -\frac{\pi}{2}$, *dann ist*

$$M^* = \sin(2\mu_3 - \sigma)(\cos\mu_3)^{\varkappa};$$

hierin bezeichnet μ_3 *den durch*

$$(\varkappa + 2)\cos(3\mu_3 - \sigma) = (\varkappa - 2)\cos(\mu_3 - \sigma) \quad . \quad . \quad . \quad . \quad (97)$$

eindeutig bestimmten, im Falle $-2\pi < \sigma \leqq -\frac{3\pi}{2}$ *zwischen* $-\frac{\pi}{2}$ *und* $\frac{\pi}{2}+\frac{\sigma}{2}$, *im Falle* $-\frac{3\pi}{2} < \sigma \leqq -\pi$ *zwischen* $\frac{\pi}{4}+\frac{\sigma}{2}$ *und* $\frac{\pi}{2}+\frac{\sigma}{2}$ *und im Falle* $-\pi < \sigma < -\frac{\pi}{2}$ *zwischen* $\frac{\pi}{4}+\frac{\sigma}{2}$ *und* 0 *liegenden Winkel.*

3. *Ist* $\frac{\pi}{2} < \sigma < 2\pi$, *dann ist*

$$M^* = \sin(\sigma - 2\mu_4)(\cos\mu_4)^{\varkappa};$$

hierin bezeichnet μ_4 *den durch*

$$(\varkappa + 2)\cos(3\mu_4 - \sigma) = (\varkappa - 2)\cos(\mu_4 - \sigma)$$

eindeutig bestimmten, im Falle $\frac{3\pi}{2} \leqq \sigma < 2\pi$ *zwischen* $-\frac{\pi}{2}+\frac{\sigma}{2}$ *und* $\frac{\pi}{2}$, *im Falle* $\pi \leqq \sigma < \frac{3\pi}{2}$ *zwischen* $-\frac{\pi}{2}+\frac{\sigma}{2}$ *und* $-\frac{\pi}{4}+\frac{\sigma}{2}$ *und im Falle* $\frac{\pi}{2} < \sigma < \pi$ *zwischen* 0 *und* $-\frac{\pi}{4}+\frac{\sigma}{2}$ *liegenden Winkel.*

---

[1]) D. h.: M^* ist der grösste Wert von $L(\mu)$ im Intervall

$$Max\left(-\frac{\pi}{2}, -\frac{\pi}{2}+\frac{\sigma}{2}\right) < \mu < Min\left(\frac{\pi}{2}, \frac{\pi}{2}+\frac{\sigma}{2}\right).$$

Beweis. Wir unterscheiden drei Fälle:

1. Es sei $-\frac{\pi}{2} < \sigma \leqq \frac{\pi}{2}$. Man hat $L(0) = 1$, wegen $L(\mu) \leqq 1$ folgt hieraus die erste Behauptung des Hilfssatzes.

2. Es sei $-2\pi < \sigma < -\frac{\pi}{2}$. Hierbei unterscheiden wir wiederum drei Fälle:

2*. Es sei $-2\pi < \sigma \leqq -\frac{3\pi}{2}$. Wegen (96) ist dann $-\frac{\pi}{2} < \mu < \frac{\pi}{2} + \frac{\sigma}{2}$, also $-\pi < \sigma - 2\mu < \pi + \sigma \leqq -\frac{\pi}{2}$, somit

$$L(\mu) = \sin(2\mu - \sigma)(\cos\mu)^{\varkappa}.$$

Hieraus folgt

$$\left.\begin{aligned} L'(\mu) = 2\cos(2\mu - \sigma)(\cos\mu)^{\varkappa} - \varkappa \sin(2\mu - \sigma)(\cos\mu)^{\varkappa-1}\sin\mu = \\ (\cos\mu)^{\varkappa-1}(2\cos(2\mu - \sigma)\cos\mu - \varkappa\sin(2\mu - \sigma)\sin\mu) = \\ \tfrac{1}{2}(\cos\mu)^{\varkappa-1}((\varkappa+2)\cos(3\mu - \sigma) - (\varkappa - 2)\cos(\mu - \sigma)). \end{aligned}\right\} \quad . \quad . \quad (98)$$

Nun ist

$$\frac{d}{d\mu}((\varkappa+2)\cos(3\mu - \sigma) - (\varkappa - 2)\cos(\mu - \sigma)) =$$

$$-(2\varkappa + 4)\sin(3\mu - \sigma) - 2\varkappa\cos(2\mu - \sigma)\sin\mu - 4\sin(2\mu - \sigma)\cos\mu$$

und dieser Ausdruck ist < 0, falls $-\frac{\pi}{2} < \mu < \frac{\pi}{2} + \frac{\sigma}{2}$ ist, da dann

$$0 \leqq -\frac{3\pi}{2} - \sigma < 3\mu - \sigma < \frac{\sigma}{2} + \frac{3\pi}{2} \leqq \frac{3\pi}{4}$$

und

$$\frac{\pi}{2} \leqq -\sigma - \pi < 2\mu - \sigma < \pi$$

ist. Wegen $(\varkappa+2)\cos(3\mu - \sigma) - (\varkappa - 2)\cos(\mu - \sigma) > 0$ für $\mu = -\frac{\pi}{2}$ und < 0 für $\mu = \frac{\pi}{2} + \frac{\sigma}{2}$ liegt also im Intervall $-\frac{\pi}{2} < \mu < \frac{\pi}{2} + \frac{\sigma}{2}$ ein und nur ein Punkt μ_3 mit (97) und aus (98) folgt

$$\underset{-\frac{\pi}{2} < \mu < \frac{\pi}{2} + \frac{\sigma}{2}}{Max} L(\mu) = L(\mu_3).$$

2**. Es sei $-\frac{3\pi}{2} < \sigma \leqq -\pi$, also wegen (96) $-\frac{\pi}{2} < \mu < \frac{\pi}{2} + \frac{\sigma}{2}$.

Nun hat man, falls $-\frac{\pi}{2} < \mu \leqq \frac{\pi}{4} + \frac{\sigma}{2}$, also $-\frac{\pi}{2} \leqq \sigma - 2\mu < \sigma + \pi \leqq 0$ ist,

$$L(\mu) = (\cos \mu)^x \leqq \left(\cos\left(\frac{\sigma}{2} + \frac{\pi}{4}\right)\right)^x = L\left(\frac{\sigma}{2} + \frac{\pi}{4}\right).$$

Hieraus folgt, dass $L(\mu)$ seinen grössten Wert erreicht im Intervall $\frac{\pi}{4} + \frac{\sigma}{2} \leqq \mu < \frac{\pi}{2} + \frac{\sigma}{2}$. Auf analoge Weise wie im Falle 2* beweist man nun, dass im Intervall $\frac{\pi}{4} + \frac{\sigma}{2} < \mu < \frac{\pi}{2} + \frac{\sigma}{2}$ ein und nur ein Punkt μ_3 mit (97) liegt und dass

$$\underset{\frac{\pi}{4} + \frac{\sigma}{2} \leqq \mu < \frac{\pi}{2} + \frac{\sigma}{2}}{Max} L(\mu) = L(\mu_3)$$

ist.

2***. Es sei $-\pi < \sigma < -\frac{\pi}{2}$, also wegen (96) $-\frac{\pi}{2} < \mu < \frac{\pi}{2} + \frac{\sigma}{2}$. Ebenso wie im Falle 2** hat man, falls $-\frac{\pi}{2} < \mu \leqq \frac{\pi}{4} + \frac{\sigma}{2}$ ist,

$$L(\mu) \leqq L\left(\frac{\pi}{4} + \frac{\sigma}{2}\right) \quad . \quad . \quad . \quad . \quad . \quad . \quad . \quad (99)$$

Ist $0 \leqq \mu < \frac{\pi}{2} + \frac{\sigma}{2}$, dann ist $-\pi < \sigma - 2\mu \leqq \sigma < -\frac{\pi}{2}$, also

$$L(\mu) = \sin(2\mu - \sigma)(\cos \mu)^k \leqq -\sin \sigma = L(0) \quad . \quad . \quad . \quad (100)$$

Aus (99) und (100) folgt, dass $L(\mu)$ seinen grössten Wert erreicht im Intervall $\frac{\pi}{4} + \frac{\sigma}{2} \leqq \mu \leqq 0$. Auf analoge Weise wie im Falle 2* beweist man jetzt, dass zwischen $\frac{\pi}{4} + \frac{\sigma}{2}$ und 0 ein und nur ein Punkt μ_3 mit (97) liegt und dass

$$\underset{\frac{\pi}{4} + \frac{\sigma}{2} \leqq \mu \leqq 0}{Max} L(\mu) = L(\mu_3)$$

ist. Hiermit ist die zweite Behauptung von Hilfssatz 18 bewiesen.

3. Es sei $\frac{\pi}{2} < \sigma < 2\pi$. Die dritte Behauptung des Hilfssatzes folgt aus der zweiten, wenn man σ durch $-\sigma$ und μ durch $-\mu$ ersetzt.

Mathematics. — *Ein mengentheoretischer Satz aus dem Gebiete der diophantischen Approximationen.* Von J. F. KOKSMA. (Communicated by Prof. J. G. VAN DER CORPUT).

(Communicated at the meeting of September 24, 1932.)

Bekanntlich heisst eine Folge reeller Zahlen

$$z(1),\ z(2),\ z(3),\ldots\ldots$$

gleichverteilt modulo 1, wenn für jedes feste γ $(0 \leqq \gamma \leqq 1)$ die Anzahl N_γ der natürlichen Zahlen $x \leqq N$ mit [1])

$$0 \leqq z(x) - [z(x)] < \gamma. \quad \ldots\ldots\ldots \quad (1)$$

die Eigenschaft

$$\lim_{N\to\infty} \frac{N_\gamma}{N} = \gamma \quad \ldots\ldots\ldots \quad (2)$$

besitzt. Statt (1) schreiben wir immer die *diophantische Ungleichung* (in x)

$$0 \leqq z(x) < \gamma \quad (mod.\ 1).$$

Ist θ eine reelle irrationale Zahl und $f(x)$ eine für jedes ganze $x > 0$ definierte ganzzahlige positive Funktion mit

$$f(1) < f(2) < f(3) < \ldots\ldots, \quad \ldots\ldots\ldots \quad (3)$$

so braucht die Folge

$$\theta f(1),\quad \theta f(2),\quad \theta f(3),\ldots\ldots \quad \ldots\ldots\ldots \quad (4)$$

nicht gleichverteilt modulo 1 zu sein. In der Tat, man konstruiert z. B. zu $f(x) = 10^x$ leicht einen Dezimalbruch θ, mit der Eigenschaft [2])

$$\lim_{x\to\infty} \theta f(x) - [\theta f(x)] = 0.$$

---

[1]) $[u]$ bezeichne für reelles u die grösste ganze Zahl $\leqq u$.

[2]) Vgl. z. B. G. H. HARDY and J. E. LITTLEWOOD. Some problems op diophantine approximation. Acta Math. **37** (1914) S. 155—190, i.B. S. 156.

Herr A. KHINTCHINE [1]) bewies sogar, dass es zu jeder positiven ganzzahligen Funktion $f(x)$ mit (3), die schneller wächst als eine gewisse geometrische Progression, wenigstens ein irrationales θ gibt, derart, dass die Folge (4) nicht gleichverteilt *mod.* 1 ist, sogar derart, dass die Zahlen der Folge

$$\theta f(1) - [\theta f(1)], \quad \theta f(2) - [\theta f(2)], \ldots\ldots \quad . \quad . \quad . \quad . \quad (5)$$

nicht einmal in Einheitsintervall überall dicht liegen.

Herr H. WEYL [2]) jedoch bewies, dass für fast alle θ, bei beliebig gegebenem ganzzahligem positivem $f(x)$ mit (3), die Folge (4) gleichverteilt *mod.* 1 ist.

"Fast alle θ" heisst: die Ausnahme-Zahlen θ sind enthalten in einer Menge vom Mass Null im BORELschen Sinne. Nach Herrn WEYLs Kriterium ist die Folge (4) gleichverteilt *mod.* 1, wenn für jedes ganze $h \neq 0$

$$\lim_{N \to \infty} \frac{1}{N} \sum_{x=1}^{N} e^{2\pi i h \theta f(x)} = 0 . \quad . \quad . \quad . \quad . \quad . \quad . \quad . \quad . \quad (6)$$

ist. Der Nachweis von (6) geschieht mit einer Methode, wobei das RIESZ-FISCHERsche Theorem benutzt wird.

Es wird hier jetzt bewiesen:

Satz 1. *Ist $f(x)$ für positives ganzes x eine beliebige ganzzahlige positive Funktion mit* (3) *und ist $w(x)$ eine für hinreichend grosses ganzes x definierte, unbeschränkt wachsende Funktion, dann hat für jedes reelle α und für fast jedes reelle θ die diophantische Ungleichung*

$$\alpha < \theta f(x) < \alpha + \frac{\log x}{\sqrt[3]{x}} w(x) \,(\text{mod. } 1) \quad . \quad . \quad . \quad . \quad . \quad (7)$$

unendlich viele ganzzahlige Lösungen.

Bemerkung I: Genau gesagt: *Es gibt eine Menge $\mathfrak{M}$ vom Mass Null im Sinne von* BOREL, *die durch die Definition von $f(x)$ und $w(x)$ völlig bestimmt ist, derart, dass für jedes reelle, nicht zu $\mathfrak{M}$ gehörige θ und für jedes reelle α die Ungleichung* (7) *unendlich viele ganzzahlige Lösungen x hat.*

Bemerkung II: Ich beweise Satz 1 sogar unter der weniger fordernden Voraussetzung für $f(x)$, *dass $f(x)$ für jedes ganze $x > 0$ einen ganzzahligen Wert hat mit $f(x) \neq f(x')$ für $x \neq x'$.*

Satz 1 besagt also, wie dicht jedes α im Intervall $0 \leqq \alpha < 1$ wenigstens durch unendlich viele Glieder der Folge (5) angenähert wird.

Der Beweis beruht auf zwei Sätzen: Hilfssatz 1, und dem grundlegenden

---

[1]) A. KHINTCHINE. Ueber eine Klasse linearer diophantischer Approximationen. Rendic. di Palermo **50** (1926) S. 170—195, i.B. S. 182.

[2]) H. WEYL. Ueber die Gleichverteilung von Zahlen mod. Eins. Math. Ann. **77** (1916) S. 312—352.

VAN DER CORPUTschen Satz 2 [1]). Ich beweise Hilfssatz 1, ausgehend von dem Ansatz, der Herrn WEYL zu dem schon genannten Beweis der Limesbeziehung (6) für fast alle θ führte.

Hilfssatz 1. *Ist (I_σ) eine Folge von Intervallen*

$$I_\sigma \ldots . a_\sigma \leqq x < b_\sigma \quad (\sigma = 1, 2, \ldots .),$$

wo a_σ und b_σ ganz sind mit $a_\sigma < b_\sigma$, ist (Λ_σ) eine Folge von positiven Zahlen $\Lambda_1, \Lambda_2, \ldots$ mit der Eigenschaft, dass

$$\sum_{\sigma=1}^{\infty} \frac{1}{\Lambda_\sigma} \quad . \quad . \quad . \quad . \quad . \quad . \quad . \quad . \quad . \quad . \quad (8)$$

konvergiert, bezeichnet (r_σ) eine Folge natürlicher Zahlen $r_1, r_2, \ldots$, und ist (S_σ) eine Folge von Funktionensystemen

$$S_\sigma = (f_{\sigma 1}(x),\ f_{\sigma 2}(x), \ldots, f_{\sigma r_\sigma}(x)) \quad (\sigma = 1, 2, \ldots),$$

wo $f_{\sigma\varrho}(x)$ für $\sigma \geqq 1$, $1 \leqq \varrho \leqq r_\sigma$ eine für jedes ganze, in I_σ liegende x definierte, ganzzahlige Funktion bedeutet mit $f_{\sigma\varrho}(x) \neq f_{\sigma\varrho}(x')$ für $x \neq x'$, dann gibt es eine im Intervall $0 \leqq \theta \leqq 1$ liegende Menge $\mathfrak{M}$ vom Mass Null im Sinne von BOREL, *die durch die Definition der genannten Folgen eindeutig bestimmt ist, mit folgender Eigenschaft:*

Jedem θ $(0 < \theta \leqq 1)$, das nicht zu $\mathfrak{M}$ gehört, kann man einen durch θ und die Definition der genannten Folgen eindeutig bestimmten Index σ_0 zuordnen, derart, dass für $\sigma \geqq \sigma_0$ und $1 \leqq \varrho \leqq r_\sigma$ die Ungleichung

$$\left| \frac{1}{b_\sigma - a_\sigma} \sum_{x=a_\sigma}^{b_\sigma - 1} e^{2\pi i \theta f_{\sigma\varrho}(x)} \right| < \sqrt{\frac{r_\sigma \Lambda_\sigma}{b_\sigma - a_\sigma}} \quad . \quad . \quad . \quad . \quad . \quad (9)$$

gilt.

Beweis. Wird für jedes θ im Intervall $0 \leqq \theta \leqq 1$

$$\Omega_{\sigma\varrho}(\theta) = \frac{1}{b_\sigma - a_\sigma} \sum_{x=a_\sigma}^{b_\sigma - 1} e^{2\pi i f_{\sigma\varrho}(x)} \quad (\sigma = 1, 2, \ldots;\ \varrho = 1, 2, \ldots, r_\sigma) \quad (10)$$

gesetzt, dann ist

$$\int_0^1 |\Omega_{\sigma\varrho}(\theta)|^2 d\theta = \frac{1}{(b_\sigma - a_\sigma)^2} \int_0^1 \left\{ \sum_{x=a_\sigma}^{b_\sigma - 1} e^{2\pi i \theta f_{\sigma\varrho}(x)} \cdot \sum_{x=a_\sigma}^{b_\sigma - 1} e^{-2\pi i \theta f_{\sigma\varrho}(x)} \right\} d\theta = \left. \right\} \quad (11)$$

$$= \frac{b_\sigma - a_\sigma}{(b_\sigma - a_\sigma)^2} = \frac{1}{b_\sigma - a_\sigma},$$

[1]) Den Beweis von Satz 2 wird Herr J. G. VAN DER CORPUT demnächst veröffentlichen in den Acta Math. und zwar im dritten Teil seiner Abhandlung: Diophantische Ungleichungen. Erschienen sind schon:

Teil I. Zur Gleichverteilung modulo Eins. Acta **56** (1931) S. 373—456.

Teil II, Abschnitte *A* und *B*. Rhytmische Systeme. Acta **59**, (1932) S. 210—328.

denn in I_σ ist $f_{\sigma\varrho}(x) \neq f_{\sigma\varrho}(x')$ für $x \neq x'$, sodass bei Ausmultiplizierung und Integration genau $b_\sigma - a_\sigma$ Glieder den Wert 1, und die übrigen Glieder den Wert 0 ergeben.

Bedeutet $\mathfrak{M}_{\sigma\varrho}$ für jedes Zahlenpaar σ und ϱ mit $\sigma \geqq 1$; $1 \leqq \varrho \leqq r_\sigma$ die Menge aller θ in $0 \leqq \theta \leqq 1$ mit

$$|\Omega_{\sigma\varrho}(\theta)| \geqq \sqrt{\frac{r_\sigma \Delta_\sigma}{b_\sigma - a_\sigma}} \quad \ldots\ldots\ldots \quad (12)$$

dann ist weil $|\Omega_{\sigma\varrho}(\theta)|$ wegen (10) eine stetige Funktion ist, $\mathfrak{M}_{\sigma\varrho}$ messbar. Also gilt, wenn wir das Mass einer Menge $\mathfrak{E}$ mit $\mathfrak{m}(\mathfrak{E})$ andeuten

$$\int_0^1 |\Omega_{\sigma\varrho}(\theta)|^2 \, d\theta \geqq \mathfrak{m}(\mathfrak{M}_{\sigma\rho}) \cdot \frac{r_\sigma \Delta_\sigma}{b_\sigma - a_\sigma} \quad (\sigma \geqq 1;\ 1 \leqq \varrho \leqq r_\sigma),$$

sodass aus (11) folgt

$$\mathfrak{m}(\mathfrak{M}_{\sigma\rho}) \leqq \frac{1}{b_\sigma - a_\sigma} \cdot \frac{b_\sigma - a_\sigma}{r_\sigma \Delta_\sigma} = \frac{1}{r_\sigma \Delta_\sigma} \quad (\sigma \geqq 1;\ 1 \leqq \varrho \leqq r_\sigma) \ . \quad (13)$$

Es sei jetzt σ_1 eine beliebige natürliche Zahl und es bezeichne $\mathfrak{M}_{\sigma_1}$ die Menge der θ die wenigstens einer der Mengen $\mathfrak{M}_{\sigma\varrho}$ $(\sigma \geqq \sigma_1;\ 1 \leqq \varrho \leqq r_\sigma)$ angehören. Für das äussere Mass $\overline{\mathfrak{m}}(\mathfrak{M}_{\sigma_1})$ dieser Menge gilt

$$\overline{\mathfrak{m}}(\mathfrak{M}_{\sigma_1}) \leqq \sum_{\sigma=\sigma_1}^{\infty} \sum_{\rho=1}^{r_\sigma} \mathfrak{m}(\mathfrak{M}_\sigma) \quad (\sigma_1 \geqq 1),$$

also wegen (13)

$$\overline{\mathfrak{m}}(\mathfrak{M}_{\sigma_1}) \leqq \sum_{\sigma=\sigma_1}^{\infty} \frac{1}{\Delta_\sigma} \quad (\sigma_1 \geqq 1) \ . \quad \ldots\ldots \quad (14)$$

Ueberdies gilt wegen der Definition von $\mathfrak{M}_{\sigma_1}$ $(\sigma_1 \geqq 1)$

$$\mathfrak{M}_{\sigma_1} \succ \mathfrak{M}_{\sigma_1+1} \succ \mathfrak{M}_{\sigma_1+2} \succ \ldots\ldots \quad (\sigma_1 \geqq 1) \ . \quad \ldots \quad (15)$$

Ist nun ε eine beliebige feste positive Zahl, so kann man, weil die Summe (8) konvergiert, nach (14) σ_1 immer so gross wählen, dass

$$\overline{\mathfrak{m}}(\mathfrak{M}_{\sigma_1}) < \varepsilon$$

ist. Wegen (15) hat also die Durchschnittmenge $\mathfrak{M}$ der Mengen

$$\mathfrak{M}_1, \mathfrak{M}_2, \mathfrak{M}_3, \ldots\ldots \quad \ldots\ldots\ldots \quad (16)$$

das BORELsche Mass Null. Wir zeigen nun, dass $\mathfrak{M}$ uns das im Hilfssatz 1 Behauptete liefert.

1. $\mathfrak{M}$ ist nach der obigen Konstruktion durch die Definition der Folgen $(I_\sigma), (\Lambda_\sigma), (r_\sigma)$ und (S_σ) eindeutig bestimmt.

2. $\mathfrak{M}$ hat das BORELsche Mass Null.

3. Es sei θ eine Zahl mit $0 \leqq \theta < 1$, aber nicht zu $\mathfrak{M}$ gehörig. Wegen der Tatsache, dass $\mathfrak{M}$ Durchschnittmenge der Mengen (16) ist, gibt es eine durch θ und die Definition der Folgen $(I_\sigma), (\Lambda_\sigma), (r_\sigma)$ und (S_σ) eindeutig bestimmte natürliche Zahl σ_0 derart, dass θ in keinem $\mathfrak{M}_\sigma$ liegt für $\sigma \geqq \sigma_0$. Wegen der Definition von $\mathfrak{M}_\sigma$ kann also θ in keinem $\mathfrak{M}_{\sigma\varrho}$ liegen mit $\sigma \geqq \sigma_0$ und $1 \leqq \varrho \leqq r_\sigma$. Dies besagt aber, dass es zu θ kein Zahlenpaar σ und ϱ mit $\sigma \geqq \sigma_0$; $1 \leqq \varrho \leqq r_\sigma$ gibt mit (12). Also gilt

$$|\Omega_{\sigma\varrho}(\theta)| < \sqrt{\frac{r_\sigma \Lambda_\sigma}{b_\sigma - a_\sigma}} \quad (\sigma \geqq \sigma_0;\ 1 \leqq \varrho \leqq r_\sigma).$$

Wegen (10) ist diese Ungleichung identisch mit (9), sodass Hilssatz 1 völlig bewiesen ist.

Satz 2. *Es sei eine Folge natürlicher Zahlen $m_1, m_2, \ldots$ gegeben, und es sei F eine Folge von m_σ-dimensionalen Quadern*

$$Q_\sigma \ldots a_{\sigma\mu} \leqq x_\mu < b_{\sigma\mu} \quad (\sigma = 1, 2, \ldots;\ \mu = 1, 2, \ldots, m_\sigma),$$

wo $a_{\sigma\mu}$ und $b_{\sigma\mu}$ ganz sind und $a_{\sigma\mu} < b_{\sigma\mu}$ ist. Jedem Q_σ seien zugeordnet eine natürliche Zahl n_σ, $2n_\sigma$ reelle Zahlen $\alpha_{\sigma\nu}$ und $\beta_{\sigma\nu}$ mit $\alpha_{\sigma\nu} < \beta_{\sigma\nu} \leqq \alpha_{\sigma\nu} + 1$ und n_σ Funktionen

$$f_{\sigma\nu}(x) = f_{\sigma\nu}(x_1, x_2, \ldots, x_{m_\sigma}) \quad (\sigma = 1, 2, \ldots;\ \nu = 1, 2, \ldots n_\sigma),$$

definiert für jeden Gitterpunkt $(x) = (x_1, x_2, \ldots, x_{m_\sigma})$ von Q_σ.

Es werde für $\sigma \geqq 1$

$$T_\sigma(c) = \sum_{(h)}{}' \left| \frac{1}{A(Q_\sigma)} \sum_{(x) \text{ in } Q_\sigma} e^{2\pi i (h_1 f_{\sigma 1}(x) + h_2 f_{\sigma 2}(x) + \ldots + h_{n_\sigma} f_{\sigma n_\sigma}(x))} \right| \ldots \quad (17)$$

gesetzt, wo $A(Q_\sigma)$ die Anzahl der Gitterpunkte (x) in Q_σ bedeutet, und wo $\sum_{(h)}{}'$ erstreckt wird über alle Gitterpunkte $(h) = (h_1, h_2, \ldots, h_{n_\sigma}) \neq (0, 0, \ldots, 0)$ mit

$$|h_\nu| \leqq \frac{c\, n_\sigma}{\beta_{\sigma\nu} - \alpha_{\sigma\nu}} \log \frac{2\, n_\sigma}{\beta_{\sigma\nu} - \alpha_{\sigma\nu}} \quad (\sigma \geqq 1;\ 1 \leqq \nu \leqq n_\sigma). \ldots \quad (18)$$

Wir nehmen an

$$\lim_{\sigma \to \infty} T_\sigma(c) = 0. \ldots \quad (19)$$

für jedes feste $c>0$. *Es sei* $A^*(Q_\sigma)$ *die Anzahl der Gitterpunkte* (x) *in* Q_σ, *die dem diophantischen System*

$$\alpha_{\sigma\nu} < f_{\sigma\nu}(x) < \beta_{\sigma\nu} \,(\mathrm{mod.}\ 1) \quad (\sigma \geqq 1;\ \nu = 1, 2, \ldots, n_\sigma) \quad . \quad . \quad (20)$$

genügen. Unter diesen Bedingungen ist

$$\lim_{\sigma \to \infty} \frac{A^*(Q_\sigma)}{A(Q_\sigma)(\beta_{\sigma 1} - \alpha_{\sigma 1}) \ldots\ldots (\beta_{\sigma n_\sigma} - \alpha_{\sigma n_\sigma})} = 1 \quad . \quad . \quad . \quad (21)$$

Beweis von Satz 1. Ohne Beschränkung der Allgemeinheit kann ich bei dem Beweis von Satz 1

$$0 \leqq \theta \leqq 1$$

annehmen. Gemäss Satz 1 kann ich die ganze Zahl $x_0 > e^3$ so wählen, dass $w(x)$ für jedes ganze $x \geqq x_0$ definiert und $\leqq 1$ ist. Wird nun für jedes ganze $x \geqq x_0$ gesetzt

$$\varphi(x) = \frac{\sqrt[3]{x}}{\log x} \cdot \frac{\underset{\substack{x_0 \leqq y \leqq x \\ y\ \mathrm{ganz}}}{\mathrm{Min}} \frac{\log y}{\sqrt[3]{y}} w(y)}{1 + \frac{\log x_0}{\sqrt[3]{x_0}} w(x_0)}, \quad . \quad . \quad . \quad . \quad . \quad (22)$$

dann ist für jedes ganze $x \geqq x_0$

$$\frac{\log x}{\sqrt[3]{x}} \varphi(x) < \frac{\underset{\substack{x_0 \leqq y \leqq x \\ y\ \mathrm{ganz}}}{\mathrm{Min}} \frac{\log y}{\sqrt[3]{y}} w(y)}{\frac{\log x_0}{\sqrt[3]{x_0}} w(x_0)} \leqq 1 \quad . \quad . \quad . \quad . \quad . \quad (23)$$

Unser nächstes Ziel ist jetzt die Relation

$$\lim_{x \to \infty} \varphi(x) = \infty \quad . \quad . \quad . \quad . \quad . \quad . \quad . \quad . \quad . \quad (24)$$

zu zeigen. Ich bemerke dazu zuerst, dass die Funktion $\frac{\log y}{\sqrt[3]{y}}$ für $y > e^3$ monoton abnimmt, weil ihre Ableitung gleich

$$\frac{1}{3 y^{4/3}} (3 - \log y) < 0$$

ist. Für jedes y im Intervall $x_0 \leqq y \leqq x$ gilt somit

$$\frac{\log y}{\sqrt[3]{y}} \geqq \frac{\log x}{\sqrt[3]{x}} \quad (x_0 \leqq y \leqq x). \quad . \quad . \quad . \quad . \quad . \quad (25)$$

Weiter bemerke ich, dass man nach der Definition (22) von $\varphi(x)$, jedem ganzen $x \geqq x_0$ ein ganzes y_x zuordnen kann mit

$$\varphi(x) = \frac{\sqrt[3]{x}}{\log x} \cdot \frac{\frac{\log y_x}{\sqrt[3]{y_x}} \cdot w(y_x)}{1 + \frac{\log x_0}{\sqrt[3]{x_0}} w(x_0)}; \quad x_0 \leqq y_x \leqq x, \quad . \quad . \quad . \quad (26)$$

sodass wegen (25)

$$\varphi(x) \geqq \frac{w(y_x)}{1 + \frac{\log x_0}{\sqrt[3]{x_0}} w(x_0)} \quad . \quad . \quad . \quad . \quad . \quad . \quad . \quad (27)$$

ist.

Weil $w(x)$ mit x unbeschränkt wächst, kann man jedem konstanten K ein ganzes $\xi \geqq x_0$ zuordnen, mit der Eigenschaft, dass für jedes ganze $x \geqq \xi$

$$w(x) \geqq K$$

ist. Es sei jetzt K eine beliebige positive Konstante. Wir unterscheiden zwei verschiedene Fälle.

1. Es sei in (26) $y_x \geqq \xi$. Dann ist also wegen (27)

$$\varphi(x) \geqq \frac{K}{1 + \frac{\log x_0}{\sqrt[3]{x_0}} w(x_0)} \quad (x \geqq x_0;\ y_x \geqq \xi) \, . \quad . \quad . \quad . \quad (28)$$

2. Es sei in (26) $y_x < \xi$, sodass ξ eine der Zahlen $x_0, x_0+1, \ldots, \xi-1$ ist. Es gibt dann wegen $x_0 > e^3$ eine nur von K und von der Definition von $w(x)$ abhängige positive Zahl K_1, derart dass

$$\frac{\log y_x}{\sqrt[3]{y_x}} w(y_x) \geqq K_1$$

ist, sodass aus (26) folgt

$$\varphi(x) \geqq \frac{K_1}{1 + \frac{\log x_0}{\sqrt[3]{x_0}} w(x_0)} \cdot \frac{\sqrt[3]{x}}{\log x} \quad (x \geqq x_0;\ y_x < \xi) \, . \quad . \quad . \quad (29)$$

Man hat also für jedes ganze $x \geqq x_0$, wegen (28) und (29)

$$\varphi(x) \geqq \frac{1}{1 + \frac{\log x_0}{\sqrt[3]{x_0}} w(x_0)} \, Min\left(K, \frac{K_1 \sqrt[3]{x}}{\log x}\right)$$

d. h. weil K_1 von x unabhängig ist, x_0

$$\underset{x \to \infty}{Lim}\ \varphi(x) \geqq \frac{K}{1 + \frac{\log x_0}{\sqrt[3]{x_0}}\, w(x_0)}$$

Weil diese Ungleichung für jede positive Konstante K gilt, folgt aus ihr erst recht die zu beweisende Beziehung (24).

Bezeichnet c irgend eine positive Zahl, bezeichnet b_σ für $\sigma \geqq 1$ die kleinste ganze Zahl $> x_0$ mit $\varphi(b_\sigma) \geqq \sigma$ (b_σ existiert wegen (24)), bezeichnet (I_σ) die Folge der Intervalle

$$I_\sigma \ldots a_\sigma = x_0 \leqq x < b_\sigma \quad (\sigma = 1, 2 \ldots .),$$

bezeichnet A_σ die Folge der Zahlen

$$A_\sigma = \{\varphi(b_\sigma)\}^2 \quad (\sigma = 1, 2, \ldots .), \quad . \quad . \quad . \quad . \quad . \quad (30)$$

bezeichnet (r_σ) die Folge der Zahlen

$$r_\sigma = \left[\frac{c \sqrt[3]{b_\sigma}}{\varphi(b_\sigma) \log b_\sigma} \log \frac{2 \sqrt[3]{b_\sigma}}{\varphi(b_\sigma) \log b_\sigma} + 1 \right] (\sigma = 1, 2, \ldots .) \quad , \quad (31)$$

und bedeutet (S_σ) die Folge der Funktionensysteme

$$S_\sigma = (f_{\sigma 1}(x),\ f_{\sigma 2}(x), \ldots ., f_{\sigma r_\sigma}(x)),$$

wo

$$f_{\sigma\varrho}(x) = \varrho f(x) \quad (\sigma \geqq 1,\ \varrho = 1, 2, \ldots ., r_\sigma) \quad . \quad . \quad . \quad . \quad (32)$$

gesetzt ist, so können wir zeigen, dass die Bedingungen von Hilfssatz 1 erfüllt sind. In der Tat es sind a_σ und b_σ ganze Zahlen mit $a_\sigma < b_\sigma$, es sind $A_1, A_2, \ldots$ wegen (30) positiv und es konvergiert die Summe (8) wegen $A_\sigma = \{\varphi(b_\sigma)\}^2 \geqq \sigma^2$, es sind wegen (31) $r_1, r_2, \ldots$ natürliche Zahlen und es ist wegen (32) und Bemerkung II bei Satz 1 $f_{\sigma\varrho}(x) = \varrho f(x)$ eine für jedes ganze x in I_σ definierte, ganzzahlige Funktion mit $f_{\sigma\varrho}(x) \neq f_{\sigma\varrho}(x')$ für $x \neq x'$.

Hilfssatz 1 lehrt also die Existenz einer in $0 \leqq \theta \leqq 1$ liegender Menge $\mathfrak{M}$ vom Mass Null, die durch die obige Definition der Folgen (I_σ), (A_σ), (r_σ) und (S_σ), also durch die Definition der Funktionen $f(x)$ und $w(x)$ in Satz 1 eindeutig bestimmt ist, mit folgender Eigenschaft:

Jedem θ $(0 \leqq \theta \leqq 1)$, das nicht zu $\mathfrak{M}$ gehört, kann ein Index σ_0 zugeordnet werden, derart, dass für $\sigma \geqq \sigma_0$ und $1 \leqq \varrho \leqq r_\sigma$

$$\left| \frac{1}{b_\sigma - x_0} \sum_{x = x_0}^{b_\sigma - 1} e^{2\pi i \theta \varrho f(x)} \right| < \sqrt{\frac{r_\sigma \{\varphi(b_\sigma)\}^2}{b_\sigma - x_0}}$$

ist. Die linke Seite ändert sich nicht, wenn ϱ durch $-\varrho$ ersetzt wird, sodass

$$\left.\begin{aligned}\sum_{\substack{|h|\leqq r_\tau \\ h\neq 0,\ ganz}} \left|\frac{1}{b_\sigma - x_0}\sum_{x=x_0}^{b_\sigma-1} e^{2\pi i h\theta f(x)}\right| &< 2\,r_\sigma\sqrt{\frac{r_\sigma\{\varphi(b_\sigma)\}^2}{b_\sigma - x_0}} = \\ &= 2\sqrt{\frac{r_\sigma^3\{\varphi(b_\sigma)\}^2}{b_\sigma - x_0}}\end{aligned}\right\} \quad (33)$$

ist.

Wegen $b_\tau > e^3$ ist $2 < b_\tau^{\frac{2}{3}}$; wegen der Definition von b_τ ist $\varphi(b_\tau) \geqq \sigma \geqq 1$, sodass aus (31) folgt

$$r_\tau \leqq \frac{c\sqrt[3]{b_\sigma}}{\varphi(b_\sigma)\log b_\tau}\log\frac{b_\sigma^{2/3}\cdot b_\sigma^{1/3}}{1} + 1 = c\frac{\sqrt[3]{b_\sigma}}{\varphi(b_\sigma)} + 1 \leqq (c+1)\frac{\sqrt[3]{b_\sigma}}{\varphi(b_\sigma)} \quad (34)$$

wegen $b_\sigma > x_0 > e^3$ und (23) mit $x = b_\sigma$.

Aus (33) und (34) geht hervor

$$\sum_{\substack{|h|\leqq r_\tau \\ h\neq 0,\ ganz}} \left|\frac{1}{b_\tau - x_0}\sum_{x=x_0}^{b_\sigma-1} e^{2\pi i h\theta f(x)}\right| < 2\sqrt{\frac{(c+1)^3 b_\sigma}{\{\varphi(b_\tau)\}^3}\cdot\frac{\{\varphi(b_\sigma)\}^2}{b_\tau - x_0}} =$$

$$= 2\sqrt{(c+1)^3\cdot\frac{b_\sigma}{b_\sigma - x_0}\cdot\frac{1}{\varphi(b_\sigma)}} \leqq 2\sqrt{(c+1)^3\cdot\frac{b_\sigma}{b_\sigma - x_0}\cdot\frac{1}{\sigma}},$$

weil b_τ so gewählt worden ist, dass $\varphi(b_\tau) \geqq \sigma$ $(\sigma \geqq 1)$. Es gilt also, weil $\frac{b_\tau}{b_\sigma - x_0}$ beschränkt ist

$$\sum_{\substack{|h|\leqq r_\sigma \\ h\neq 0,\ ganz}} \left|\frac{1}{b_\sigma - x_0}\sum_{x=x_0}^{b_\tau-1} e^{2\pi i h\theta f(x)}\right| \to 0 \text{ für } \sigma\to\infty, \quad . \quad . \quad (35)$$

und zwar für jedes θ $(0 \leqq \theta \leqq 1)$, dass nicht zu $\mathfrak{M}$ gehört.

Ich behaupte jetzt, dass die Voraussetzungen von Satz 2 erfüllt sind, wenn

$$\left.\begin{aligned} &m_\sigma = 1,\ a_{\sigma\mu} = x_0,\ b_{\sigma\mu} = b_\sigma,\ n_\sigma = 1, \\ &\alpha_{\sigma\nu} = \alpha,\ \beta_{\sigma\nu} = \alpha + \frac{\log b_\tau}{\sqrt[3]{b_\sigma}}\varphi(b_\sigma),\ f_{\tau\nu}(x) = \theta f(x)\end{aligned}\right\} \quad (36)$$

gesetzt wird, sodass jetzt die Folge F der Quader Q_τ die Folge (I_τ) der Intervalle I_τ bedeutet. In (36) bezeichnet θ eine beliebige Zahl in

$0 \leqq \theta \leqq 1$, aber nicht zu $\mathfrak{M}$ gehörig. Die Behauptung ist wahr, denn es ist $m_\sigma \geqq 1$; $a_{\sigma\mu}$ und $b_{\sigma\mu}$ sind ganze Zahlen mit $a_{\sigma\mu} < b_{\sigma\mu}$, n_σ ist eine natürliche Zahl; wegen $b_\sigma > x_0$ gilt (23) mit $x = b_\sigma$, sodass $\alpha_{\sigma\nu} < \beta_{\sigma\nu} \leqq \alpha_{\sigma\nu} + 1$ ist; die Funktionen $f_{\sigma\nu}(x) = \theta f(x)$ sind für jedes ganze x im Intervall $I_\sigma \ldots a_\sigma \leqq x < b_\sigma$ definiert. Es braucht also nur noch gezeigt zu werden, dass (19) gilt, wo man wegen (36) die in Satz 2 definierte Summe

$$T_\sigma(c) = \sum_{(h)}{}' \left| \frac{1}{b_\sigma - x_0} \sum_{x=x_0}^{b_\sigma - 1} e^{2\pi i h \theta f(x)} \right|$$

für beliebiges feste $c > 0$ zu erstrecken hat über alle ganzen $h \neq 0$ mit

$$|h| \leqq \frac{c \sqrt[3]{b_\sigma}}{\varphi(b_\sigma) \log b_\sigma} \log \frac{2 \sqrt[3]{b_\sigma}}{\varphi(b_\sigma) \log b_\sigma} \quad (\sigma \geqq 1),$$

sodass wegen (31) h erst recht an

$$h \neq 0, \text{ganz}; \quad |h| \leqq r_\sigma$$

genügt. Aus (35) folgt somit a fortiori (19), womit gezeigt worden ist, dass alle Bedingungen von Satz 2 erfüllt sind.

Wegen (36) lehrt Satz 2 für jedes θ in $0 \leqq \theta \leqq 1$, dass nicht zu der oben konstruierten, durch die Definition von $f(x)$ und $w(x)$ eindeutig bestimmten Menge $\mathfrak{M}$ vom Mass Null gehört, die folgende Tatsache: die Anzahl $A^*(I_\sigma)$ der im Intervall I_σ liegenden ganzzahligen Lösungen der diophantischen Ungleichung

$$\alpha < \theta f(x) < \alpha + \frac{\log b_\sigma}{\sqrt[3]{b_\sigma}} \varphi(b_\sigma) \quad . \quad . \quad . \quad . \quad . \quad . \quad (37)$$

besitzt die Eigenschaft

$$\lim_{\sigma \to \infty} \frac{A^*(I_\sigma)}{(b_\sigma - x_0) \frac{\log b_\sigma}{\sqrt[3]{b_\sigma}} \varphi(b_\sigma)} = 1.$$

Wegen $\varphi(b_\sigma) \geqq \sigma$ wächst der Nenner

$$(b_\sigma - x_0) \frac{\log b_\sigma}{\sqrt[3]{b_\sigma}} \varphi(b_\sigma)$$

unbeschränkt mit σ, sodass also auch der Zähler $A^*(I_\sigma)$ unbeschränkt mit σ zunimmt, d.h. es ist

$$\lim_{\sigma \to \infty} A^*(I_\sigma) = \infty \quad . \quad . \quad . \quad . \quad . \quad . \quad . \quad . \quad (38)$$

Aus der Definition (22) von $\varphi(x)$ folgt für jedes Paar ganzer Zahlen x und $\bar{y}$ mit $x_0 \leqq \bar{y} \leqq x$

$$\frac{\log x}{\sqrt[3]{x}} \varphi(x) \leqq \frac{\log \bar{y}}{\sqrt[3]{\bar{y}}} w(\bar{y}).$$

Für jedes ganze x im Intervall $x_0 \leqq x < b_\sigma$ ist somit

$$\frac{\log b_\sigma}{\sqrt[3]{b_\sigma}} \varphi(b_\sigma) \leqq \frac{\log x}{\sqrt[3]{x}} w(x).$$

Eine ganzzahlige, im Intervall I_σ liegende Lösung x von (37) ist also erst recht eine ganzzahlige Lösung der diophantischen Ungleichung (7). Wegen (38) wächst also a fortiori die Anzahl der in I_σ liegenden ganzzahligen Lösungen x von (7) mit σ unbeschränkt ins Unendliche, sodass Satz 1 bewiesen ist.

Mathematics. — *Die Doppelfünfen von* R. WEITZENBÖCK *und* D. BARBILIAN. Von E. A. WEISS in Bonn. (Communicated by Prof. R WEITZENBÖCK.)

(Communicated at the meeting of Sept. 24, 1932.)

Es wird eine Parameterdarstellung aller regulären M_3^2 des R_4 angegeben, die dem Koordinatensimplex gleichzeitig ein- und umbeschrieben sind. Indem die Punkte einer solchen M_3^2 einerseits auf die Geraden eines linearen Komplexes, andererseits auf die orientierten Kreise einer Ebene abgebildet werden, ergeben sich im Linienraume die WEITZENBÖCKsche [1]), in der Ebene der orientierten Kreise die BARBILIANsche [2]) Doppelfünf.

I. In letzter Zeit sind von verschiedenen Seiten zwei spezielle Doppelfünfen untersucht worden: *Im Linienraume* ist die WEITZENBÖCKsche Doppelfünf dadurch ausgezeichnet, dass je vier windschiefe ihrer Geraden ein „singuläres Quadrupel" derart bilden, dass die Gerade der Doppelfünf, welche sie schneidet, die *einzige* gemeinsame Trefflinie der vier Geraden ist. Die 10 Geraden der Konfiguration gehören einem linearen Komplex an und je vier zusammengehörige Geraden bilden ein äquianharmonisches

[1]) R. WEITZENBÖCK, Über eine Konfiguration von 10 Geraden im projektiven R_3. Proc. Amsterdam Ak. d. Wet. **31**, 1928, S. 133—137. Ferner: G. SCHAAKE, ebenda, S. 715—717.

[2]) D. BARBILIAN, Les cas d'exception de certaines propriétés quadratiques. Bul. de Math. et de Phys. de l'Ecole Polyt. I. Bucarest, 1929. S. 12—16.
G. TZITZÉICA, Sur certaines propriétés quadratiques. Ebenda, S. 16—21.

KLUYVERsches Quadrupel [1]). *In der Ebene der orientierten Kreise* ist die BARBILIANsche Doppelfünf die Figur von zwei Kreisquintupeln derart, dass je vier Kreise eines Quintupels einen Kreis des anderen zum *einzigen* gemeinsamen Berührungskreis haben. Sie berühren ihn in einem äquianharmonischen Punktquadrupel.

Bildet man die Geraden des Komplexes und die orientierten Kreise der Ebene auf die Punkte einer M_3^2 im R_4 ab, so erhält man in beiden Fällen die Figur eines Simplexes, welcher der M_3^2 gleichzeitig ein- und umbeschrieben ist. Die Eckpunkte des Simplex entsprechen dem einen, die Berührungspunkte der Simplexflache dem anderen Quintupel der Doppelfünf. Es handelt sich also beide Male — im Grunde genommen — um dieselbe Figur und es liegt daher nahe, die Behandlung der beiden Doppelfünfen mit der Untersuchung ihrer gemeinsamen Bildfigur im R_4 zu beginnen. Es ist zweckmässig, hierbei von einem Simplex — dem Koordinatensimplex — auszugehen und nach allen M_3^2 zu fragen, die diesem Simplex gleichzeitig ein- und umbeschrieben sind.

II. Eine durch die Ecken des Koordinatensimplex laufende M_3^2 habe die Gleichung:

$$p_{01}^2 x_0 x_1 + p_{02}^2 x_0 x_2 + \ldots + p_{34}^2 x_3 x_4 = 0 \quad . \quad . \quad . \quad . \quad (1)$$

Soll sie die Flache des Koordinatensimplex berühren, so müssen die 5 Unterdeterminanten U_{ii} ihrer Matrix verschwinden. Es gilt, die 5 Gleichungen $U_{ii}=0$ identisch mit der Nebenbedingung zu erfüllen, dass die Determinante D der M_3^2 von Null verschieden ausfällt.

Nun lassen sich die Ausdrücke U_{ii} als symmetrische vierreihige Determinanten mit verschwindenden Diagonalelementen in Produkte von je vier in den p_{ik} linearen Formen zerlegen. Z. B.:

$$\left.\begin{aligned} U_{00} = (&+ p_{12}p_{34} + p_{13}p_{42} + p_{14}p_{23}) \cdot \\ \cdot (&+ p_{12}p_{34} - p_{13}p_{42} - p_{14}p_{23}) \cdot \\ \cdot (&- p_{12}p_{34} + p_{13}p_{42} - p_{14}p_{23}) \cdot \\ \cdot (&- p_{12}p_{34} - p_{13}p_{42} + p_{14}p_{23}) \cdot \end{aligned}\right\} \quad . \quad . \quad . \quad . \quad . \quad (2)$$

[1]) Davon verschieden ist die STUDYsche Doppelfünf, die durch die Geraden-Kugeltransformation aus der Figur von 5 (unorientierten), sich paarweise berührenden Kugeln entsteht und projektiv dadurch charakterisiert ist, dass sie eine Kollineationsgruppe vom Ikosaedertypus zulässt, dass ihre Gegengeraden sich in einem Nullsystem zugeordnet sind und jede Gerade von ihren Treffgeraden in einem äquianharmonischen Punktquadrupel geschnitten wird. Bei der Abbildung des Linienraumes auf M_4^2 im R_5 wird der ausgezeichnete Komplex auf einen R_4 abgebildet, der M_4^2 in einer regulären M_3^2 schneidet. Dieser M_3^2 ist ein Tangentenpentatop (ein solches, dessen 10 Geraden M_3^2 berühren) umbeschrieben. Die Eckpunkte des Pentatops sind mit dem Pole des R_4 (in Bezug auf M_4^2) verbunden und die Verbindungslinien schneiden M_4^2 in den Bildpunkten der Doppelfünfgeraden.

Vgl. E. STUDY, Vereinfachte Begründung von Lies Kugelgeometrie I. Sitzungsber. d. Preuss. Ak. d. Wiss. 1926, S. 380 und A. MAURER, Doppelvieren und Doppelfünfen. Diss. Bonn, 1929.

Die fünf zu erfüllenden Gleichungen lauten also:

$$\pm p_{12}\,p_{34} \pm p_{13}\,p_{42} \pm p_{14}\,p_{23} = 0 \quad . \quad . \quad . \quad . \quad . \quad . \quad (3)$$

und:

$$\left.\begin{aligned} &\ast \quad \pm p_{02}\,p_{34} \pm p_{03}\,p_{42} \pm p_{04}\,p_{23} = 0, \\ \pm p_{01}\,p_{34} \quad &\ast \quad \pm p_{03}\,p_{14} \pm p_{04}\,p_{13} = 0, \\ \pm p_{01}\,p_{42} \pm p_{02}\,p_{14} \quad &\ast \quad \pm p_{04}\,p_{12} = 0, \\ \pm p_{01}\,p_{23} \pm p_{02}\,p_{13} \pm p_{03}\,p_{12} \quad &\ast \quad = 0, \end{aligned}\right\} \quad . \quad . \quad . \quad . \quad (4)$$

wobei über die zu wählenden Vorzeichen noch entschieden werden muss.

Eine besonders einfache Annahme würde über diese Vorzeichen so verfügen, dass die p_{ik} Linienkoordinaten einer Geraden des R_4 würden. Dann aber würde keine reguläre M_3^2 geliefert werden. Eine Untersuchung sämtlicher Möglichkeiten verschiedener Vorzeichenverteilung zeigt nämlich folgendes. Setzt man voraus, dass alle p_{ik} von Null verschieden sind, (weil im anderen Falle $D = 0$ trivialerweise folgen würde) und nennt man zwei Systeme von Relationen (3), (4) *äquivalent*, wenn man das eine in das andere dadurch überführen kann, dass man in allen Relationen des ersten Systems gleichzeitig gewisse p_{ik} durch $-p_{ik}$ ersetzt, so gilt:

1. *In der vorgegebenen Determinante D sei $U_{ii} = 0$, aber $p_{ik} \neq 0$. Ferner seien die Vorzeichen der p_{ik} so gewählt, dass die Gleichung $U_{00} = 0$ durch das Bestehen der Relation:*

$$p_{12}\,p_{34} + p_{13}\,p_{42} + p_{14}\,p_{23} = 0 \quad . \quad . \quad . \quad . \quad . \quad . \quad (5)$$

erfüllt wird. Dann ist das System (4) der vier übrigen Relationen $U_{ii} = 0$, aufgefasst als homogenes Gleichungssystem für die vier fehlenden Grössen $p_{01}, p_{02}, p_{03}, p_{04}$ äquivalent mit einem der beiden Gleichungssysteme von schiefsymmetrischer oder symmetrischer Determinante:

$$\Delta_1 = \begin{vmatrix} \ast & -p_{34} & -p_{42} & -p_{23} \\ p_{34} & \ast & p_{14} & -p_{13} \\ p_{42} & -p_{14} & \ast & p_{12} \\ p_{23} & p_{13} & -p_{12} & \ast \end{vmatrix}, \qquad \Delta_2 = \begin{vmatrix} \ast & p_{34} & p_{42} & p_{23} \\ p_{34} & \ast & p_{14} & p_{13} \\ p_{42} & p_{14} & \ast & p_{12} \\ p_{23} & p_{13} & p_{12} & \ast \end{vmatrix}.$$

Im ersten Falle hat Δ_1 den Rang 2 und D den Rang 3. (Das System der p_{ik} ist äquivalent mit dem System der Linienkoordinaten einer Geraden des R_4).

Im zweiten Falle folgt:

$$\Delta_2 = 2\,(p_{12}^2\,p_{34}^2 + p_{13}^2\,p_{42}^2 + p_{14}^2\,p_{23}^2) = 0 \quad . \quad . \quad . \quad . \quad . \quad (6)$$

und:

$$D = -2^5 \cdot p_{01}\,p_{02}\,p_{03}\,p_{04}\,p_{12}\,p_{13}\,p_{14}\,p_{34}\,p_{42}\,p_{23} \neq 0 \quad . \quad . \quad . \quad (7)$$

Für uns ist nur der zweite Fall von Interesse. Wir wählen also von nun ab in (3), (4) überall die + Zeichen und sehen die Grössen

$p_{12}, p_{13}, p_{14}, p_{34}, p_{42}, p_{23}$ als Parameter an, die durch die Gleichungen (5), (6) verbunden sind. Die vier übrigen Grössen p_{ik} können dann aus (4) berechnet werden. So ergibt sich:

2. *Die ∞^4 regulären M_3^2 (1), die dem Koordinatensimplex des R_4 gleichzeitig ein- und umbeschrieben sind, können mit Hilfe von 6 inhomogenen Parametern $p_{12}, p_{13}, p_{14}, p_{34}, p_{42}, p_{23}$ erschöpfend angegeben werden. Diese müssen von Null verschieden sein und den Gleichungen (5), (6) genügen. Die fehlenden p_{ik} ergeben sich dann z.B. aus den Gleichungen:*

$$p_{01} = p_{12}\, p_{13}\, p_{14}, \; p_{02} = p_{12}^2\, p_{34}, \; p_{03} = p_{13}^2\, p_{42}, \; p_{04} = p_{14}^2\, p_{23} \quad . \quad . \quad (8)$$

Wegen der Gleichberechtigung aller Koeffizienten der M_3^2 folgt jetzt weiter:

3. *Zwischen den, mit geeigneten Vorzeichen versehenen Wurzeln p_{ik} aus den Koeffizienten einer M_3^2, die dem Koordinatensimplex im R_4 gleichzeitig ein- und umbeschrieben ist, bestehen nicht nur die Gleichungen (3), (4), sondern auch die Gleichungen, die — wie (6) — aus ihnen entstehen, wenn man p_{ik} durch p_{ik}^2 ersetzt.*

Für eine spätere Anwendung brauchen wir auch die Koordinaten der Berührungspunkte der Koordinatenflache. Sie ergeben sich aus den algebraischen Komplementen U_{ik} der p_{ik}^2 in der Matrix der M_3^2 und zwar gilt der Satz:

4. *Setzt man:*

$$P_{ik} = p_{ik}\, p_{mn}\, p_{nl}\, p_{lm}, \; (i, k, l, m, n = 0, 1, 2, 3, 4) \quad . \quad . \quad . \quad . \quad (9)$$

so folgt für die algebraischen Komplemente U_{ik} der Elemente p_{ik}^2 in der Matrix der M_3^2:

$$U_{ik} = -8\, P_{ik}^2 \quad . \quad . \quad . \quad . \quad . \quad . \quad . \quad . \quad . \quad (10)$$

Zwischen den P_{ik} bestehen die gleichen Relationen wie zwischen den p_{ik}.

III. Die Relationen zwischen den p_{ik} und P_{ik} sollen nun geometrisch gedeutet werden. Wir bezeichnen zu diesem Zwecke mit a_{ik} und A_{ik} die Ausdrücke (Relative Invarianten von zwei Geraden), welche verschwinden, wenn zwei Eckpunkte oder zwei Berührungspunkte des Simplexes zueinander in Bezug auf eine, von nun ab festgehaltene M_3^2 konjugiert sind. Man erhält a_{ik}, wenn man die Koordinaten des i^{ten} und k^{ten} Eckpunktes in die polarisierte Ordnungsgleichung und A_{ik}, wenn man die Koordinaten des i^{ten} und k^{ten} Simplexflaches in die polarisierte Klassengleichung der M_3^2 einsetzt. Es folgt dann:

5. *Zwischen den relativen Invarianten:*

$$a_{ik} = p_{ik}^2, \quad A_{ik} = P_{ik}^2 \quad . \quad . \quad . \quad . \quad . \quad . \quad . \quad . \quad (11)$$

zweier Eckpunkte oder zweier Berührungspunkte eines der M_3^2 gleich-

zeitig ein- und umbeschriebenen Simplexes bestehen die gleichen Relationen wie zwischen den p_{ik} und P_{ik}.

Wir betrachten nun einen bestimmten Eckpunkt, etwa 0. Die Berührungspunkte der durch ihn hindurchlaufenden Simplexflache liegen auf dem Kegel M_2^2, den sein Tangentialflach aus M_3^2 ausschneidet. Bildet man die relativen Invarianten der Berührungspunkte in Bezug auf diesen Kegel, so erhält man dieselben Ausdrücke A_{ik} wie bei Zugrundelegung der M_3^2. Zwischen diesen Grössen besteht dann nach 5 die Beziehung:

$$A_{12}^2 A_{34}^2 + A_{13}^2 A_{42}^2 + A_{14}^2 A_{23}^2 = 0, \quad . \quad . \quad . \quad . \quad . \quad (12)$$

deren geometrische Deutung den Satz von B. GAMBIER [1]) liefert:

6. *Ein Simplex sei einer M_3^2 gleichzeitig ein- und umbeschrieben. Das Tangentialflach in einem Eckpunkte schneidet dann M_3^2 in einem Kegel 2. Ordnung, der die Berührungspunkte der durch den ausgezeichneten Eckpunkt laufenden Simplexflache in einem äquianharmonischen Erzeugendenquadrupel projiziert.*

Bildet man jetzt die Punkte der M_3^2 auf die orientierten Kreise der Ebene ab, so folgt daraus der Satz von D. BARBILIAN:

7. *Ein Kreis des einen Quintupels einer* BARBILIAN*schen Doppelfünf wird von den vier Berührungskreisen des anderen Quintupels in einem äquianharmonischen Punktquadrupel berührt.*

Schliesslich deuten wir die Punkte der M_3^2 als Geraden eines linearen Komplexes im R_3. Die zwischen den a_{ik} und A_{ik} bestehenden Relationen führen dann zu dem Satze von R. WEITZENBÖCK:

8. *Vier windschiefe Geraden einer* WEITZENBÖCK*schen Doppelfünf bilden ein äquianharmonisches* KLUYVER*sches Quadrupel* [2]). (Quadrupel von Wendepunkttangenten einer äquianharmonischen Raumkurve 4. Ordnung erster Art) [3]).

---

[1]) B. GAMBIER, Propriétés quadratiques et leurs cas d'exception. Cycles tangents dans le plan ou paratactiques dans l'espace. Bull. des sc. math. **55**, 1931.

Hier wird die BARBILIANsche Doppelfünf als Minimalprojektion einer Punktfigur im Raume untersucht.

[2]) Vgl. H. MOHRMANN, Math. Zeitschr. **5**, 1919, S. 274.

[3]) *Zusatz bei der Korrektur*: Inzwischen habe ich auf einem, mir von Herrn B. SEGRE zugesandten Verzeichnis seiner Arbeiten die folgenden Abhandlungen bemerkt:

Intorno ad una proprietà dei determinanti simmetrici del 6^0 ordine. Rend. della R. Acc. dei Lincei, (6), **2**, 1925.

Le piramidi inscritte e circoscritte alle quadriche di S_4 e una notevole configurazione di rette dello spazio ordinario. Memorie della R. Acc. dei Lincei, (6), **2**, 1927.

In der ersten Arbeit wird die Existenz der hier — somit leider fälschlich — WEITZENBÖCKsche Doppelfünf genannten Konfiguration ähnlich wie oben durch den Nachweis der Existenz einer von Null verschiedenen 6-reihigen symmetrischen Determinante mit $p_{11} = P_{11} = 0$ bewiesen. Die zweite Arbeit habe ich nicht mehr rechtzeitig einsehen können.

Physics. — *On the* LORENTZ-LORENZ *Correction in Metallic Conductors.* By R. DE L. KRONIG and H. J. GROENEWOLD. (Communicated by Prof. H. A. KRAMERS).

(Communicated at the meeting of September 24, 1932.)

According to the theory of dispersion the index of refraction n of an isotropic substance for an electromagnetic wave of frequency ν is determined by the relation between the electric polarisation per unit volume P due to the wave and the macroscopic electric field E of the wave, entering into MAXWELL's equations, n being given by

$$n^2 - 1 = \frac{4\pi P}{E} \quad . \quad . \quad . \quad . \quad . \quad . \quad . \quad . \quad . \quad (1)$$

In order to apply this formula it is necessary to know the relationship between P and E.

In the case of an insulator the customary procedure to obtain P/E is the following. For a particular atom of the substance the electric moment induced by the wave will be

$$p = \alpha E_0 \quad . \quad . \quad . \quad . \quad . \quad . \quad . \quad . \quad . \quad . \quad (2)$$

where E_0 is the electric field of frequency ν acting on the atom and α the polarisability of the atom at that frequency. If we take as atom the harmonic oscillator usually employed in classical dispersion theory, i.e. an electron of charge $-e$ and mass m attached elastically to the electrical center of a fixed constellation of positive electricity with an equal total charge, then α is given by

$$\alpha = \frac{e^2}{4\pi^2 m (\nu_0^2 - \nu^2)}, \quad . \quad . \quad . \quad . \quad . \quad . \quad . \quad . \quad (3)$$

ν_0 being the natural frequency of vibration of the electron. E_0 may in general not be identified with E. It can most easily be calculated by imagining a sphere constructed around the center of the atom under consideration, the radius being chosen small compared to the wavelength of the radiation but still so large that the sphere contains many atoms. Then

$$E_0 = E + E' + E'', \quad . \quad . \quad . \quad . \quad . \quad . \quad . \quad . \quad (4)$$

where E' and E'' denote respectively the electric fields produced at the center of the atom considered by the polarisation of the atoms with centers

outside the sphere and by the polarisation of the other atoms with centers inside the sphere [1]). As LORENTZ [2]) showed, E' for an isotropic substance is given by

$$E' = \frac{4\pi}{3} P \quad . \quad . \quad . \quad . \quad . \quad . \quad . \quad . \quad . \quad . \quad (5)$$

In order to compute E'', the arrangement of the atoms has to be known. For a simple cubical arrangement LORENTZ [3]) could prove that

$$E'' = 0 \quad . \quad . \quad . \quad . \quad . \quad . \quad . \quad . \quad . \quad . \quad (6)$$

The same holds rigorously for a gas composed of independent atoms that can approach each other only up to a minimum distance [4]) and probably approximately for most isotropic substances. By combining eqs. (2), (4), (5) and (6) we get

$$P = Np = N\alpha\left(E + \frac{4\pi}{3} P\right),$$

where N is the number of atoms per unit volume. Solving for P/E and substituting in eq. (1) leads to the CLAUSIUS-MOSOTTI equation

$$3\frac{n^2 - 1}{n^2 + 2} = 4\pi N\alpha. \quad . \quad . \quad . \quad . \quad . \quad . \quad . \quad . \quad (7)$$

This equation differs from the equation

$$n^2 - 1 = 4\pi N\alpha. \quad . \quad . \quad . \quad . \quad . \quad . \quad . \quad . \quad . \quad (8)$$

which we would have obtained if we had neglected the LORENTZ-LORENZ correction, i.e. if we had identified E with E_0. Only when $4\pi N\alpha$ is small compared to unity is the difference between eqs. (7) and (8) inappreciable.

The question naturally arises as to how these considerations are altered when we are dealing with a metallic conductor. In order to illustrate the essential points we shall use as model of such a conductor a positive fluid of uniform charge density in which the electrons are situated at the corner points of a simple cubical lattice with a lattice constant a, so chosen that on the average the conductor is neutral. On the one hand it would seem as if the index of refraction ought now to be calculated in the following way: For a free electron in an electric field E_0 oscillating with frequency

---

[1]) H. A. LORENTZ, The Theory of Electrons, Teubner 1909; p. 137 et seq.
[2]) H. A. LORENTZ, l. c.; p. 303 et seq.
[3]) H. A. LORENTZ, l. c.; p. 306.
[4]) R. LUNDBLAD, Ann. d. Phys. 57. 183, 1918.

ν the product of its charge and its displacement from the original position of rest has the form

$$p = \beta E_0$$

with

$$\beta = -\frac{e^2}{4\pi^2 m\nu^2},$$

quite analogous to the relation (2) for an electron bound in an atom, so that replacing α by β in the CLAUSIUS-MOSOTTI equation (7) will give us n. On the other hand one can argue that no LORENTZ-LORENZ correction should be made in this case, or, expressing it differently, that eq. (8) with β instead of α should be applied, since all the electrons inside a region of linear dimensions small compared with the wave length suffer the same displacement, with the consequence that there are no electric forces of frequency ν acting on the electrons excepting the field E of the wave itself. In trying to decide between these two viewpoints it must be remembered that in the derivation of LORENTZ previously described it is essential that the substance be regarded as composed of neutral atoms in which the electrons are bound. By an artifice it is possible to look at our model of a metallic conductor in the same way, and it then appears that the force E', giving rise to the LORENTZ-LORENZ correction, just balances the elastic restoring force. In treating the electrons as free, the LORENTZ-LORENZ correction hence has already been taken into account so that the second method of calculating n proposed above is the correct one[1]).

We may imagine the positive fluid of our model subdivided into equal cubes by three mutually perpendicular sets of parallel planes. In particular we can chose these planes in such a way that in every cube there is one electron in the center. The length of the edge of the cubes will then be equal to the lattice constant a of the cubical lattice at the corner points of which we assumed the electrons to be located. If now, keeping the centers of the cubes, i.e. the positions of the electrons, fixed while letting the size of the cubes diminish (always retaining the positive charge with uniform density inside the cubes), we get a cubical lattice of "atoms" separated by finite intervals without any charge. The individual "atom", a cube filled with positive charge of uniform density and with an electron at its center, is such that we may apply eq. (3). Indeed, as will be shown in the note at the end of the paper, the electron for small displacements suffers an elastic

[1]) Prof. DARWIN first suggested to one of us in connection with a paper on the quantum theory of dispersion in metallic conductors (R. DE L. KRONIG, Proc. Roy. Soc. A. 124, 409, 1929; see especially the footnoote on p. 419) that n should be computed according to the first method. The discrepancy between theory and experiment resulting in this way immediately led to serious doubts regarding this suggestion and to a more thorough investigation of the whole problem. The choice of the model employed here to elucidate the relation to the case of an insulator is the result of a discussion with Prof. KRAMERS.

restoring force directed toward the center of its cube, the natural frequency of vibration being given by

$$4\pi^2 m\nu_0^2 = \frac{a^3}{b^3}\frac{4\pi Ne^2}{3}, \quad \ldots\ldots\ldots \quad (9)$$

where b is the edge of the cube reduced in size as described above, while the other symbols have their old meaning. On the basis of what has been said in the beginning of this paper we may apply to our model the equation (7), obtaining

$$3\frac{n^2-1}{n^2+2} = \frac{4\pi Ne^2}{\frac{a^3}{b^3}\frac{4\pi Ne^2}{3} - 4\pi^2 m\nu^2}.$$

Now if b becomes equal to a, i.e. if the positive cubes touch, forming one continuous positive fluid, then this reduces to

$$n^2 - 1 = 4\pi N \cdot \left(-\frac{e^2}{4\pi^2 m\nu^2}\right) = 4\pi N\beta.$$

We can summarize our result as follows: *The index of refraction of our simple model of a metallic conductor may be calculated as if the electrons were free while the* LORENTZ-LORENZ *correction is omitted.*

There is in this argument still one point requiring proof, viz. that the value of ν_0, given for the isolated "atom" by eq. (9), is not altered by the close proximity of the neighbouring atoms. The proof is given in the note at the end. One will also inquire how the foregoing considerations are to be modified when the electrons combine the properties both of free and bound electrons as they do in the quantum theoretical treatment of metallic conduction developed by BLOCH. A discussion of this question will be reserved for a later investigation.

Note. We imagine a charge distribution in space, symmetrical with respect to the three coordinate planes, the density ϱ being continuous at the origin and having there the value ϱ_0. We wish to determine the electric field in the neighbourhood of the origin.

Let ξ, η, ζ be the coordinates of a point in the charge distribution, x, y, z the coordinates of a point near the origin, where the field is to be determined. If r denotes the length of the line joining the two points, then the x-component of the electric field due to the charge distribution is given by

$$E_x = -\frac{\partial V}{\partial x},$$

where

$$V = \int \frac{\varrho(\xi, \eta, \zeta)}{r} d\xi\, d\eta\, d\zeta.$$

For small values of x, y, z we may develop E in a power series in x, y, z, obtaining

$$E_x = -\left(\frac{\partial V}{\partial x}\right)_0 - \left(\frac{\partial^2 V}{\partial x^2}\right)_0 x - \left(\frac{\partial^2 V}{\partial x\,\partial y}\right)_0 y - \left(\frac{\partial^2 V}{\partial x\,\partial z}\right)_0 z,$$

the derivatives to be taken at the origin. On account of the symmetry of the charge distribution E_x vanishes at the origin. For the same reason the coefficients of y and z vanish. We retain

$$E_x = -\left(\frac{\partial^2 V}{\partial x^2}\right)_0 x = -x \cdot \int \frac{\varrho \cdot (3\xi^2 - r_0^2)}{r_0^5}\, d\xi\, d\eta\, d\zeta =$$

$$= -x \cdot \int \frac{\varrho}{3} \triangle\left(\frac{1}{r_0}\right) d\xi\, d\eta\, d\zeta,$$

r_0 being the value of r when x, y and z are zero. Taking a little sphere around the origin and splitting the integral into the contributions from outside and from inside this sphere, we get naught for the first and $-4\pi\varrho_0/3$ for the second part, where ϱ_0 is the charge density at the origin. We thus have

$$E_x = \frac{4\pi\varrho_0}{3} x$$

for small displacements from the origin. In other words an electron will be elastically bound to the origin, the frequency of vibration being given by

$$4\pi^2 m \nu_0^2 = \frac{4\pi\varrho_0 e}{3} \quad . \quad . \quad . \quad . \quad . \quad . \quad . \quad . \quad (10)$$

In our model of a system of electrons situated at the points of a simple cubical lattice with lattice constant a, each electron being at the center of a cube with edge b, in which the positive charge e is uniformly distributed

$$\varrho_0 = \frac{a^3}{b^3} Ne.$$

Substitution in eq. (10) gives us eq. (9), and we also see now that the value ν_0 is the same whether we regard an isolated "atom" or an "atom" symmetrically surrounded by neighbours as in our model.

Natuurkundig Laboratorium der Rijks-Universiteit,
Groningen.

Physics. — *Line spectrum of samarium ion in crystals and its variation with the temperature.* By SIMON FREED and J. G. HARWELL. (Communicated by Prof. W. J. DE HAAS.)

(Communicated at the meeting of September 24, 1932.)

The magnetic behaviour of Sm^{+++} [1]) showed that there was an equilibrium distribution of the ions between different electronic configurations and as anticipated, the absorption spectra [2]) consisted of lines varying in their relative intensities with changing temperature. The present work was instituted with the view of obtaining quantitative data concerning the differences in energy between the various configurations. These differences have been looked upon as originating through the action of the electric fields about Sm^{+++} in the lattice. They are a measure of their symmetry and intensity. Recently, Miss AMELIA FRANK [3]) obtained rough agreement with the magnetic susceptibility at higher temperatures by taking into account the presence of the activated state ${}^6H_{7/2}$, presumably about 1000 cm^{-1} higher in energy than the basic state ${}^6H_{5/2}$. The agreement is rather surprising since both the basic state, ${}^6H_{5/2}$ and activated states, ${}^6H_{7/2}$ are probably decomposed into sub-levels of wide separation by the electric fields of the lattice. The specific heat of Sm^{+++} [4]) at low temperature has given a measure of these separations. It appeared that energy of about 160 cm^{-1} (450 cal/mole) had to be supplied to activate a mole of Sm^{+++}. Even greater intervals may have resulted in the decomposition of the ${}^6H_{5/2}$ term but they must be so great that relatively few ions exist in the upper level.

The present work is mainly concerned with the effect of the electric fields upon the state ${}^6H_{5/2}$ that is, with levels which are sufficiently occupied at ordinary temperatures to have their presence recorded in the absorption spectrum. They are identified by the change in the relative intensity of the lines as the temperature changes, more especially by those instances when a line increases in intensity apparently at the expense of a neighbouring line. When this line is of higher frequency than the one whose intensity is decreasing, there is considerable probability that the lines arise at two levels slightly different in energy and end in a common energy level. And the recurrence of the same interval in different regions of the spectrum practically establishes the existence and separation of the lower energy levels.

---

[1]) S. FREED, Journ. Am. Chem. Soc. **52**, 2702 (1930).
[2]) S. FREED and F. H. SPEDDING, Nature **123**, 525 (1929).
[3]) A. FRANK, Phys. Rev. **39**, 119 (1932).
[4]) J. E. AHLBERG and S. FREED, Phys. Rev. **39**, 540 (1932).

The experimental method has been described [1]) in another connection. A hydrogen discharge tube served as the source of the continuous radiation and the spectra extended from 4200 Å to about 2200 Å. A Hilger spectrograph of the type $E\,2$ was employed. The radiation was passed parallel to the optic axis of the hexagonal crystal [2]) Sm $(C_2H_5SO_4)_3 . 9H_2O$ which was about 0.5 mm. thick. For the purpose of lowering the temperature of the crystal, liquid hydrogen (20° K), liquid nitrogen (77° K), and liquid ethylene (169° K) were used, all boiling at atmospheric pressure. The average absolute error in the measurement of the lines is about 5 cm^{-1}. Some of the lines were faint or diffuse and there has been listed next to each line in the table, the number of times it was measured and the reproducibility of the measurement. The recorded intensities are visual estimates and should be trusted only as a measure of relative intensity within a restricted region of the spectrum and in spectra originating at the same temperature.

The groups of lines assigned to energy levels have undergone such changes in intensity that the increase or decrease in intensity of one line with respect to another could be told at a glance on an enlargement of the spectrogram.

For convenience, the groups have been numbered on the reproductions of the spectra. Below each diagram is given a list of the frequencies derived from the energy levels and these are compared with the observed frequencies for each group of lines. All the deviations are well within the errors of measurement. Groups 4, 7, 8 and 10 under low dispersion appear as doublets having the same energy difference at each temperature. Under higher dispersion, each line is found to be doubled and with the data in hand it is impossible to prove rigorously whether the "fine-structure" energy level belongs to the basic term system or not. More data, we are informed, will be available soon in a more extensive paper by SPEDDING and BEAR from Berkeley. If the "fine-structure" level is assigned to the basic multiplet, it becomes possible to include the quartet 5 and also the sextet 3 and 6. This arrangement of levels has a considerable degree of probability and by its aid all the multiplets in which marked intensity changes occur can be interrelated.

Below is a typical example of an energy level pattern which the quartets 4, 7, 8 and 10 accord with and also the basic separations which are valid for all of them. The intensities, too, agree with these assignments.

Some of the lines which one would normally expect from these levels were too faint to be measured. At higher temperatures, some of the lines were so diffuse that the average between two unresolved lines is given.

There can be no doubt concerning the existence of an interval of 60 cm^{-1} (at 20° K, 65 cm^{-1} at 77° K, and 60 cm^{-1} at 169° K) between

---

[1]) S. FREED, Phys. Rev. **38**, 2122 (1931).

[2]) F. M. JAEGER, Rec. des Trav. Chem. Pays Bas **33**, 362 (1914).

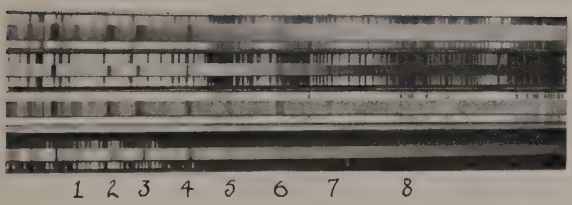

Absorption Spectrum of Sm^{+++} in $Sm(C_2H_5SO_4)_3 . 9 H_2O$).

Group	Temp. °K	Seperation of Upper Level, cm^{-1}	Calc. Line cm^{-1}	Observed Line cm^{-1}	Deviation cm^{-1}
4	20°	12		29.008 (accepted)	
			28,996	28,996 ± 3	0
			28,948	28,949 ± 1	1
			28,936	28,936 ± 1	0
	77°	12		29,010 (accepted)	
			28,998	28,996 ± ?	2
			28,945	28,945 ± 3	0
			28,933	28,936 ± ?	3
	169°			29,016 (accepted)	
			28,956	28,955 ± 0	1
7	20°	12		32,721 (accepted)	
			32,708 too faint		
	77°			32,723 ± 1 (accepted)	
			32,658	32,655 ± 2	3
	169°			32,728 ± 1 (accepted)	
			32,668	32,666 ± 1	2
8	20°	23		35,857 (accepted)	
			35,834	35,834 ± 2	0
	77°	12		35,846 ± 2 (accepted)	
			35,834	35,833 ± 0	1
			35,781	35,777 ± 3	4
	169°			35,838 ± 0	
			35,778	35,777 ± 0	1
10	20°			42,321 ± 1 (accepted)	
			42,261	42,260 ± 2	1
	77°			42,319 ± 1 (accepted)	
			42,254	42,251 ± 1	3

two energy levels in the basic multiplet. Also, there is little doubt but that this interval can be related to the influence of the electric fields of the lattice upon ${}^6H_{5/2}$. It may be predicted at this point that a close study of

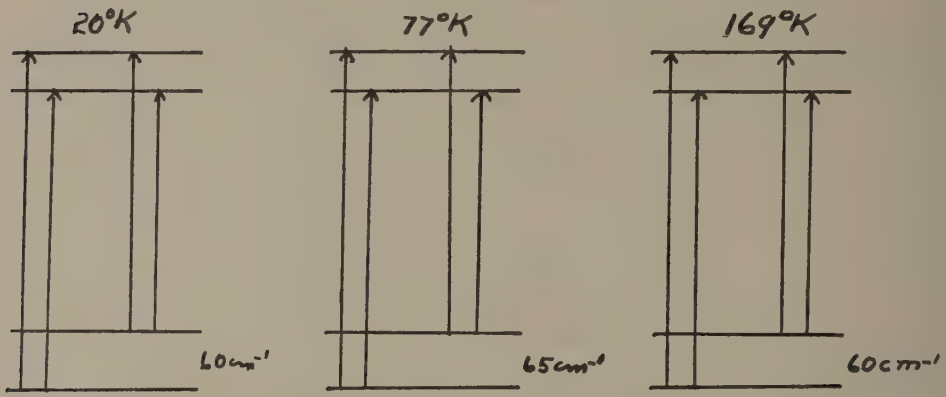

the specific heat measurements at low temperatures will confirm the existence of this interval.

Based upon the same pattern of levels as those given above, the quartet 5 will have the following basic intervals:

60 cm^{-1} at 20° K, 54 cm^{-1} at 77° K, and 43 cm^{-1} at 169° K.

Temp. °K	Calc. Line cm^{-1}	Observed Line cm^{-1}	Deviation
20		30,115 ± 2 (accepted)	
	30.130	30,133 ± ?	3
	30,070	30,071 ± 2	1
	30,055	30,058 ± 1	3
77		30.121 ± 2 (accepted)	
	30,067	30,067 ± 1	0
169		30,118 ± 1	
	30,075	30,072 ± 2	3

Now, it is clear that if the 12 cm^{-1} interval (the "fine-structure" interval) is inserted in the basic multiplet of 4, 7, 8, 10, the group 5 fits into the same scheme as groups 4, 7, 8, 10 and we shall see later the sextets 3 and 6 will also be associated with the same levels. As an example we shall give the energy levels of group 4 and 5 at 77° K employing the same basic multiplet for both.

The fact that the "fine-structure" interval is of the same magnitude in all groups (with the possible exception of 8) is evidence for including it

Quartet 4 and basic interval of 5
77° K.

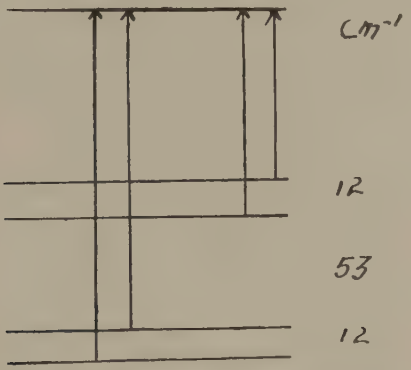

in the basic multiplet. Its inclusion results naturally in any attempt to superpose the levels of the groups for the purpose of obtaining all the components which ${}^6H_{5/2}$ has been split into. The total number can not exceed six. It must be stated again that more data are necessary for this purpose, especially spectra at the temperature of liquid helium.

Since the spectrum of Sm^{+++} consists of rather isolated groups, one would expect the lines within a group to originate and end at neighbouring levels. The intensities justify this point of view as the components of greater frequency always become more intense as the temperature is reduced. The sextets 3 and 6 contain the same energy interval as the quartet 5 and the intensities of corresponding lines behave in the same way with regard to temperature. We shall therefore associate 3 and 6 with the same basic states as 5. Below is the energy level pattern of 3 based upon that of 5.

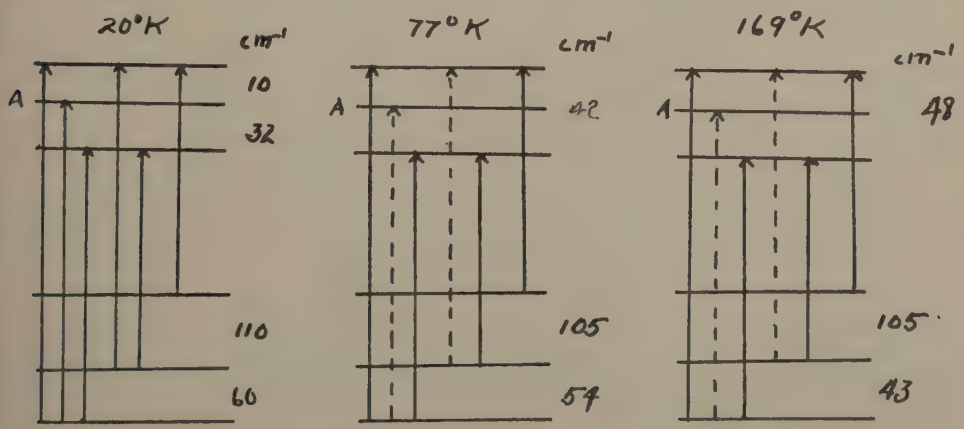

A is the "fine structure level" which can be inserted in the basic multiplet so that the interval 10 cm^{-1} (or 12 cm^{-1}) would be produced there (See page 982).

Temp. K	Calc. Line cm^{-1}	Obs. Line cm^{-1}	Deviation cm^{-1}
20°		27,639 ± 1 (accepted)	
	27,629	27,629 ± 1	0
	27,597	27,597 ± 0	0
	27,579	27,585 ± 6	6
	27,537	27,537 ± 0	0
	27,469	27,469 ± 1	0
77°		27,637 ± 1 (accepted)	
	27,595	27,595 ± 2	0
	27,541	27,540 ± 1	1
	27,478	27,478 ± 1	0
169°		27,639 ± 0	
	27,591	27,591 ± 1	0
	27,548	27,549 ± 0	0
	27,491	27,491 ± 0	0

The sextet 6 follows a similar pattern, its first interval being identical at each temperature with that of 3 but the over-all separation of the basic multiplet is slightly different. This difference can probably be ascribed to another "fine-structure" interval in the basic term system. The over-all separation of 170 cm^{-1} agrees with the interval evaluated from the specific heat measurements [1] [2].

The lines which have been studied here because of the variation in their intensities constitute about one half the prominent lines of the spectrum.

A part of this experimental work was done by one of us (S. F.) during his stay in the laboratory of Professor DE HAAS Leyden, Holland while he was a fellow of the JOHN SIMON GUGGENHEIM Memorial Foundation. He wishes to express his gratitude to Professor DE HAAS for the generous hospitality of his laboratory.

[1] J. E. AHLBERG and S. FREED, Phys. Rev. **39**, 540 (1932).

[2] Dr. SPEDDING has kindly called my attention to some unpublished spectra of $Sm_2(SO_4)_3\,8H_2O$ which he and Mr. BEAR have taken. It appears that the interval of about 165 cm^{-1} in this salt corresponds to the 60 cm^{-1} interval recorded here for the ethylsulfate and hence the interval 170 cm^{-1} found in the ethylsulfate is not to be identified with the interval found in the specific heat measurements.

Absorption Lines Obtained at 20° K.			
Intensity [1])	Wave Length	Wave Number	Measured
2 D	2328.1 ± ?	42,940 ± ?	1
2 D	2329.4 ± .05	42,915 ± 1	2
3 S	2332.1 ± .10	42,867 ± 2	4
3 B	2333.9 ± .05	42,834 ± 1	4
5 S	2349.9 ± .13	42,542 ± 3	3
5 S	2351.5 ± .20	42,513 ± 3	3
5 B	2354.6 ± .03	42,457 ± 1	4
5 B	2362.2 ± .05	42,321 ± 1	4
1 S	2365.6 ± .10	42,260 ± 2	4
2 S	2378.8 ± .10	42,025 ± 1	4
Faint	2380.1 ± ?	42,002 ± ?	1
3 B	2383.1 ± .03	41,949 ± 1	4
Faint	2604.7 ± ?	38,381 ± ?	1
2 S	2665.3 ± .05	37,508 ± 1	2
Faint	2666.9 ± ?	37,486 ± ?	1
2 S	2667.7 ± .10	37,474 ± 2	2
Faint	2735.9 ± ?	36,540 ± ?	1
Faint	2737.2 ± ?	36,523 ± ?	1
3 S	2788.0 ± .05	35,857 ± 1	2
3 B	2789.8 ± .20	35,834 ± 2	4
3 D	2900.7 ± .50	34,464 ± 6	4
Faint	2957.7 ± ?	33,800 ± ?	1
2 S	2970.4 ± .10	33,656 ± 1	2
2 D	2971.7 ± .05	33,641 ± 1	2
Faint	2978.1 ± .05	33,569 ± 1	2
Faint	2982.9 ± ?	33,515 ± ?	1
Faint	2985.1 ± .20	33,490 ± 2	2
1 S	3020.0 ± ?	33,103 ± ?	1
1 S	3022.6 ± ?	33,074 ± ?	1
3 S	3055.3 ± 0	32,721 ± 0	2

[1]) D = diffuse. S = sharp. B = broad.

Absorption Lines Obtained at 20° K. (*Continued*).

Intensity	Wave Length	Wave Number	Measured
4 B	3056.5 ± .10	32,708 ± 1	2
2 S	3058.1 ± .10	32,691 ± 1	2
Faint	3063.6 ± ?	32,632 ± ?	1
3 D	3170.7 ± .10	31,530 ± 1	2
2 B	3172.6 ± .05	31,511 ± 1	2
5 S	3177.4 ± 0	31,463 ± 0	2
4 B	3179.0 ± ?	31,448 ± ?	1
2 D	3183.7 ± .10	31,401 ± 1	3
1 D	3188.6 ± .4	31,353 ± 4	4
Faint	3308.3 ± ?	30,218 ± ?	1
2 S	3309.1 ± .15	30,211 ± 1.5	2
2 S	3317.7 ± ?	30,133 ± ?	1
3 D	3319.6 ± .20	30,115 ± 1.5	2
Faint	3320.6 ± .20	30,106 ± 1.5	2
1 D	3324.5 ± .15	30,071 ± 1.5	2
2 D	3326.0 ± .10	30,058 ± 1	2
Faint	3335.7 ± 0	29,970 ± 0	2
2 S	3337.6 ± .35	29,953 ± 2.5	2
Faint	3332.4 ± ?	30,000 ± ?	1
1 D	3339.4 ± ?	29,937 ± ?	1
1 D	3417.3 ± .10	29,255 ± .50	2
1 D	3426.8 ± 0	29,173 ± 0	2
Faint	3437.3 ± ?	29,084 ± ?	1
5 B	3446.3 ± 0	29,008 ± 0	2
7 S	3447.8 ± .30	28,996 ± 3	2
4 S	3451.6 ± .20	28,964 ± 1.5	2
4 D	3453.4 ± .15	28,949 ± 1	2
5 S	3454.9 ± .15	28,936 ± 1	2
5 D	3456.3 ± .10	28,924 ± 1	2
Faint	3538.7 ± .30	28,251 ± 2	2

Absorption Lines Obtained at 20° K. (*Continued*).

Intensity	Wave Length	Wave Number	Measured
2 D	3540.0 ± .25	28,241 ± 1	2
1 S	3547.1 ± ?	28,184 ± ?	1
3 D	3551.5 ± 0	28,149 ± 0	2
2 D	3552.9 ± .40	28,138 ± 3.5	2
7 D	3617.1 ± .15	27,639 ± 1	2
10 B	3618.3 ± .15	27,629 ± 1	2
7 B	3622.6 ± 0	27,597 ± 0	2
5 B	3624.0 ± .40	27,585 ± 3.5	2
5 B	3630.5 ± 0	27,537 ± 0	2
2 D	3639.4 ± .15	27,469 ± 1	2
Faint	3648.2 ± ?	27,403 ± ?	1
Faint	3711.7 ± ?	26,934 ± ?	1
Faint	3718.5 ± ?	26,885 ± ?	1
3 D	3739.3 ± .20	26,735 ± 2	3
1 S	3743.2 ± ?	26,708 ± ?	1
5 B	3748.4 ± .20	26,670 ± 1.5	4
4 B	3751.3 ± 0	26,650 ± 0	2
4 S	3755.4 ± 0	26,621 ± 0	2
10 B	3758.8 ± .30	26,597 ± 2	2
Faint	3763.2 ± ?	26,566 ± ?	1
Faint	3770.5 ± ?	26,514 ± ?	1
Faint	3774.4 ± ?	26,487 ± ?	1
Faint	3779.8 ± ?	26,449 ± ?	1
Faint	3785.6 ± ?	26,408 ± ?	1
Faint	3790.8 ± ?	26,372 ± ?	1
2 D	3801.8 ± ?	26,296 ± ?	1
2 S	3806.9 ± ?	26,261 ± ?	1
2 S	3811.4 ± ?	26,230 ± ?	1
2 S	3853.5 ± ?	25,943 ± ?	1
2 S	3857.7 ± ?	25,915 ± ?	1

Absorption Lines Obtained at 20° K. (*Continued*).

Intensity	Wave Length	Wave Number	Measured
2 S	3875.9 ± ?	25,793 ± ?	1
2 S	3878.7 ± .15	25,775 ± 1	2
2 S	3884.1 ± .60	25,739 ± 4	3
2 S	3887.9 ± ?	25,714 ± ?	1
Faint	3903.0 ± ?	25,614 ± ?	1
5 B	3907.3 ± .50	25,586 ± 3	4
5 B	3913.9 ± .20	25,543 ± 1.5	2
5 S	3915.0 ± .15	25,536 ± 2	2
1 S	3923.4 ± .80	25,485 ± 5	2
2 D	3969.3 ± 0	25,186 ± 0	2
1 S	3974.9 ± ?	25,151 ± ?	1
4 D	3981.8 ± 0	25,107 ± 0	2
2 S	3985.6 ± .40	25,083 ± 3	2
1 S	4001.0 ± ?	24,987 ± ?	1
1 S	4004.5 ± ?	24,965 ± ?	1
10 B	4011.8 ± 0	24,919 ± 0	3
10 B	4019.9 ± .50	24,869 ± 4	4
1 S	4042.5 ± .60	24,730 ± 4	3
1 S	4049.3 ± ?	24,681 ± ?	1
1 S	4052.6 ± .20	24,669 ± 1.5	2
5 B	4076.8 ± .20	24,522 ± 1	2
1 S	4082.6 ± ?	24,487 ± ?	1
1 S	4086.2 ± .60	24,466 ± 3	2
1 S	4088.6 ± ?	24,451 ± ?	1
3 D	4094.3 ± .60	24,417 ± 4	3
2 S	4101.2 ± .30	24,376 ± 2	3
2 D	4108.4 ± .30	24,334 ± 2	2
1 S	4151.3 ± .80	24,082 ± 5	2
1 S	4156.1 ± ?	24,054 ± ?	1
7 S	4162.7 ± 0	24,016 ± 0	4

Absorption Lines Obtained at 77° K.			
Intensity	Wave Length	Wave Number	Measured
Faint	2332.3 ± .05	42,862 ± 1	2
3 B	2333.9 ± .05	42,834 ± 1	4
2 S	2350.1 ± .05	42,538 ± 1	2
2 S	2351.5 ± ?	42,513 ± ?	1
3 B	2354.6 ± .20	42,457 ± 3	4
3 B	2356.1 ± .05	42,430 ± 1	2
3 D	2356.5 ± .05	42,423 ± 1	2
2 S	2359.2 ± ?	42,374 ± ?	1
2 S	2360.5 ± ?	42,351 ± ?	1
3 B	2362.3 ± .03	42,319 ± 1	4
2 S	2364.3 ± ?	42,283 ± ?	1
2 B	2366.1 ± .03	42,251 ± 1	4
Faint	2378.9 ± .10	42,023 ± 2	2
1 S	2381.6 ± ?	41,976 ± ?	1
3 B	2383.1 ± .05	41,949 ± 1	4
1 S	2660.3 ± ?	37,579 ± ?	1
1 S	2661.3 ± ?	37,564 ± ?	1
1 S	2663.3 ± .30	37,536 ± 3	2
1 S	2665.3 ± .30	37,508 ± 4	2
1 S	2667.2 ± ?	37,481 ± ?	1
2 D	2669.4 ± .05	37,450 ± 1	4
Faint	2672.7 ± ?	37,404 ± ?	1
Faint	2679.7 ± ?	37,306 ± ?	1
Faint	2681.1 ± ?	37,287 ± ?	1
Faint	2682.0 ± ?	37,275 ± ?	1
1 S	2701.9 ± .05	37,000 ± 1	2
2 D	2788.9 ± .20	35,846 ± 2	4
2 D	2789.9 ± 0	35,833 ± 0	2
2 D	2794.3 ± .30	35,777 ± 3	4
Faint	2879.8 ± ?	34,714 ± ?	1

Absorption Lines Obtained at 77° K. (*Continued*).

Intensity	Wave Length	Wave Number	Measured
Faint	2887.0 ± ?	34,628 ± ?	1
2 D	2900.5 ± .15	34,467 ± 2	4
1 S	2904.9 ± 0	34,415 ± 0	2
1 S	2905.4 ± .06	34,409 ± 1	3
1 S	2907.5 ± ?	34,384 ± ?	1
1 S	2908.7 ± ?	34,370 ± ?	1
1 S	2910.3 ± .20	34,351 ± 2	4
3 B	3055.1 ± .10	32,723 ± 1	4
1 S	3058.5 ± .20	32,686 ± 2	4
2 D	3061.4 ± .20	32,655 ± 2	4
2 D	3170.4 ± .10	31,533 ± 1	2
3 D	3172.6 ± ?	31,511 ± ?	1
2 D	3173.5 ± .10	31,502 ± 1	3
3 D	3174.0 ± ?	31,497 ± ?	1
3 D	3177.6 ± .10	31,461 ± 1	4
2 D	3183.0 ± .15	31,408 ± 2	4
3 D	3187.4 ± .15	31,364 ± 1	4
3 D	3319.0 ± .20	30,121 ± 2	2
1 B	3325.0 ± .20	30,067 ± 1	4
5 B	3446.0 ± .20	29,010 ± 2	4
5 S	3447.8 ± ?	28,996 ± ?	1
Faint	3449.9 ± ?	28,978 ± ?	1
5 B	3453.8 ± .30	28,945 ± 3	4
3 S	3454.9 ± ?	28,936 ± ?	1
Faint	3538.7 ± ?	28,251 ± ?	1
5 B	3617.3 ± .10	27,647 ± 1	4
2 D	3622.8 ± .30	27,595 ± 2	4
5 B	3630.0 ± .15	27,540 ± 1	4
5 B	3638.3 ± .15	27,478 ± 1	4
1 S	3739.1 ± .20	26,737 ± 1	3

Absorption Lines Obtained at 77° K. (*Continued*).

Intensity	Wave Length	Wave Number	Measured
1 S	3743.2 ± .15	26,708 ± 1	4
5 S	3749.4 ± .30	26,664 ± 2	3
5 S	3752.3 ± .30	26,643 ± 2	3
5 S	3755.1 ± .30	26,623 ± 2	3
10 B	3757.7 ± .10	26,604 ± 1	3
5 S	3761.0 ± .15	26,581 ± 1	2
Faint	3782.2 ± ?	26,432 ± ?	1
Faint	3790.0 ± ?	26,378 ± ?	1
1 S	3807.5 ± 0	26,257 ± 0	2
Faint	3848.6 ± .30	25,976 ± 2	2
Faint	3855.3 ± .15	25,931 ± 1	2
1 S	3877.0 ± .15	25,786 ± 1	2
1 S	3883.0 ± .15	25,746 ± 1	2
1 S	3895.4 ± ?	25,664 ± ?	1
2 S	3907.0 ± .40	25,588 ± 2.5	4
1 S	3913.7 ± ?	25,544 ± ?	1
2 S	3914.4 ± .20	25,532 ± 1	3
1 S	3920.0 ± .20	25,503 ± 1	2
2 D	3969.3 ± .80	25,186 ± 5	3
1 S	3974.5 ± 0	25,153 ± 0	3
2 D	3981.7 ± .40	25,108 ± 2	3
2 B	3986.6 ± 0	25,077 ± 0	2
1 S	3997.6 ± .50	25,008 ± 2	2
1 S	4001.9 ± .50	24,981 ± 3	3
1 S	4005.5 ± ?	24,959 ± ?	1
1 S	4009.3 ± 0	24,935 ± 0	2
1 S	4013.4 ± .40	24,910 ± 2	3
10 B	4016.9 ± .40	24,888 ± 2	2
10 B	4032.1 ± .20	24,794 ± 1	4
2 S	4043.3 ± ?	24,725 ± ?	1
5 B	4076.7 ± .15	24,532 ± 1	2
5 B	4081.7 ± .15	24,493 ± 1	2
2 S	4142.0 ± ?	24,136 ± ?	1
Faint	4157.4 ± ?	24,047 ± ?	1
7 S	4162.7 ± 0	24,016 ± 0	4

Absorption Lines Obtained at 169° K.			
Intensity	Wave Length	Wave Number	Measured
Faint	2664.9 ± ?	37,514 ± ?	1
2 D	2668.9 ± .10	37,457 ± 1	2
Faint	2789.5 ± 0	35,838 ± 0	2
Faint	2794.3 ± 0	35,777 ± 0	2
Faint	2882.7 ± ?	34,680 ± ?	1
Faint	2894.9 ± ?	34,533 ± ?	1
Faint	2900.5 ± .05	34,467 ± 1	2
Faint	2904.6 ± 0	34,418 ± 0	2
Faint	2909.5 ± .05	34,360 ± 1	2
3 D	3054.6 ± .10	32,728 ± 1	2
3 D	3060.4 ± .10	32,666 ± 1	2
1 D	3133.6 ± ?	31,903 ± ?	1
1 D	3135.6 ± ?	31,883 ± ?	1
Faint	3169.7 ± ?	31,540 ± ?	1
3 B	3172.7 ± ?	31,510 ± ?	1
Faint	3173.2 ± ?	31,505 ± ?	1
Faint	3174.3 ± ?	31,494 ± ?	1
2 D	3177.9 ± .15	31,458 ± 1.5	2
2 D	3182.2 ± .10	31,416 ± 1	2
3 D	3186.7 ± .10	31,371 ± 1	2
2 D	3194.5 ± ?	31,295 ± ?	1
1 D	3198.2 ± ?	31,259 ± ?	1
1 S	3313.7 ± ?	30,169 ± ?	1
Faint	3314.9 ± ?	30,158 ± ?	1
1 S	3319.3 ± .10	30,118 ± 1	2
2 D	3324.4 ± .20	30,072 ± 2	2
5 B	3445.4 ± .30	29,015 ± 2.5	2
7 B	3452.7 ± 0	28,955 ± 0	2
1 S	3486.6 ± ?	28,673 ± ?	1
1 S	3490.4 ± ?	28,642 ± ?	1

Absorption Lines Obtained at 169° K. (*Continued*).

Intensity	Wave Length	Wave Number	Measured
5 B	3617.1 ± 0	27,639 ± 0	2
1 S	3623.4 ± .10	27,591 ± 1	2
5 B	3628.8 ± 0	27,549 ± 0	2
5 B	3636.5 ± 0	27,491 ± 0	2
1 S	3643.4 ± ?	27,439 ± ?	1
1 S	3648.0 ± ?	27,405 ± ?	1
1 S	3655.4 ± ?	27,349 ± ?	1
1 S	3661.0 ± ?	27,307 ± ?	1
Faint	3723.3 ± ?	26,850 ± ?	1
Faint	3730.3 ± ?	26,800 ± ?	1
1 S	3735.6 ± ?	26,762 ± ?	1
1 S	3739.0 ± 0	26,738 ± 0	2
5 S	3750.7 ± .15	26,654 ± 1.5	2
5 B	3757.0 ± .30	26,609 ± 2.5	2
2 S	3905.7 ± .15	25,596 ± 2	2
1 D	3912.8 ± 0	25,550 ± 0	2
1 S	3967.1 ± 0	25,200 ± 0	2
1 D	3980.0 ± .30	25,119 ± 1.5	2
1 S	4009.1 ± .15	24,936 ± 1	2
1 S	4011.8 ± .35	24,919 ± 2	2
10 B	4015.7 ± .30	24,895 ± 2	2
10 B	4028.9 ± 0	24,814 ± 0	2
1 S	4040.6 ± ?	24,742 ± ?	1
1 S	4052.5 ± .15	24,669 ± 1	2
1 S	4059.5 ± .60	24,627 ± 3	2
3 D	4069.4 ± ?	24,567 ± ?	1
5 B	4075.7 ± .30	24,529 ± 3	2
5 B	4078.6 ± ?	24,511 ± ?	1
1 S	4091.4 ± .15	24,535 ± 1	2
1 S	4105.7 ± 0	24,350 ± 0	2
5 S	4159.1 ± .20	24,037 ± 1	2
3 S	4167.9 ± .20	23,986 ± 1.5	2
3 D	4175.0 ± .20	23,941 ± 1	2

Summary.

The absorption spectra of Sm^{+++} in the hexagonal crystal $Sm(C_2H_5SO_4)_3 . 9H_2O$ were taken parallel to the optic axis at 20° K, 77° K, and 169° K. Absorption lines are listed in the region of the spectrum between 4200 Å and 2200 Å.

This paper is principally concerned with the various electronic configurations in the basic multiplet, especially as they result from the inter-action of Sm^{+++} and the electric fields of the lattice. In consequence, all the lines whose relative intensities vary with the temperature have been studied in terms of energy level diagrams.

Physics. — *The Calibration of a Pressure Balance in Absolute Units.* (31st Communication of the VAN DER WAALS Fund). By A. MICHELS. (Communicated by Prof. J. D. VAN DER WAALS Jr.).

(Communicated at the meeting of September 24, 1932.)

Introduction. For the measurement of pressure in absolute units, as soon as the pressure is greater than some atmospheres, the only method that need be considered is that using a mercury column. This method, however, involves considerable difficulties when the pressures to be measured become appreciable. A few examples are known of high pressure mercury manometers such as those of AMAGAT in a mine-shaft at Verpilleux near St. Etienne, and of CAILLETET in the Eifel Tower, with which it was possible to measure up to about 400 atm. In the same group can be placed the so-called "gebroken manometer" designed by KAMERLINGH ONNES, which is still in use for measurements up to 120 atm. We are unaware of any direct measurements with a mercury column besides these.

Of the secondary gauges in use the most suitable for accurate measurement is the pressure balance which also allows measurements to be made at much higher pressures. For the most accurate work it should, however, be calibrated directly. Many types of this apparatus are known (AMAGAT, WIEBE, STÜCKRATH, WAGNER, LANGE, HOLBORN, BRIDGMAN and others) all of which are designed on the same principle: a piston is ground to fit as well as possible in a cylinder; the unknown hydrostatic pressure is applied under the piston and the force is measured necessary to keep the piston in equilibrium. The pressure can then be calculated from

$$p = \frac{K}{0}$$

where K is the force applied and 0 the area of the piston. By giving the piston a rotatory or to and fro motion the friction can be kept low.

In two previous publications [1]) the necessary conditions were considered, in terms of a theory there derived, to reduce the friction to a minimum and thus to make the sensitivity as high as possible. It has since been possible to increase the sensitivity from $2^1/_2$ g. to less than $^1/_2$ g. (on a maximum load of about 300 Kg. in the instrument here used). It follows from the same theoretical treatment that the measured surface of the piston cannot be taken as the effective surface area. This effective area was shown to be dependent on the internal diameter of the cylinder, rate of leaking, pressure etc., so that for really accurate measurements it appeared to be necessary to calibrate any pressure balance against an absolute manometer, thus against a mercury column. In the same publications a differential method was described for carrying out this calibration at higher pressures. The accuracy of the calibration is, however, dependent on the available height of the mercury column which on that occasion was limited to $4^1/_2$ M. On this account, and the then smaller sensitivity of the pressure balance, greater accuracy than $^1/_{2400}$ could not be obtained in the measurement of the effective area.

In order to put measurements in the field of higher pressures on a better basis, the VAN DER WAALS Fund in 1925 resolved to build up an equipment for the calibration of pressure gauges. Thanks to support received from many quarters, a start was made in the same year.

The use of the "Westertoren" was kindly given by the "Burgemeester en Wethouders" of Amsterdam for the erection of the necessary mercury column.

Although it would have been possible to make use directly of the full length of the tower, this would have made it necessary to bring a large part of the manometer tube through the open air which would have given rise to large temperature changes; it is further impossible in some places to carry the column upwards in a straight line which would involve difficulty in measuring the height. In order to avoid having to overcome so many difficulties, it was decided first to use a height of $27^1/_2$ M. which was available in a vertical line between the first and sixth floors. The intention, however, remains to make use later of the complete height of the tower.

The preparatory work is at present largely finished and a start could be made with the definite measurements. Calibrations using the differential method have, indeed, not yet been carried out for lack of certain pieces of apparatus, but the direct measurements against an open mercury manometer, which therefore only go to low pressures (about 40 atm.) have been completed. It was decided to publish these results for the following reasons:

1. All measurements carried out in this laboratory on the influence of pressure on physical constants published since 1924 are based on the

---

[1]) A. MICHELS, Ann. d. Phys. **72**, 285, 1923: **73** 577, 1924.

calibration made in that year. The accuracy obtained then was, as has been stated, $^1/_{2400}$, while it is by no means impossible that by wear or ageing effects the effective area then measured has altered. To this must be added the fact that the piston originally calibrated has been out of use for several years as the result of wear and there are only available comparison figures between the pistons at present in use and the calibrated one in its original state. All published results have therefore up to the present an element of uncertainty so that verification was very desirable.

2. The change of the effective area with pressure is very small, as appears from the theoretical treatment. The values measured at present at low pressures, can therefore temporarily be used also for higher pressures. Corrections for the effect of pressure can then be applied later when the differential method has been used.

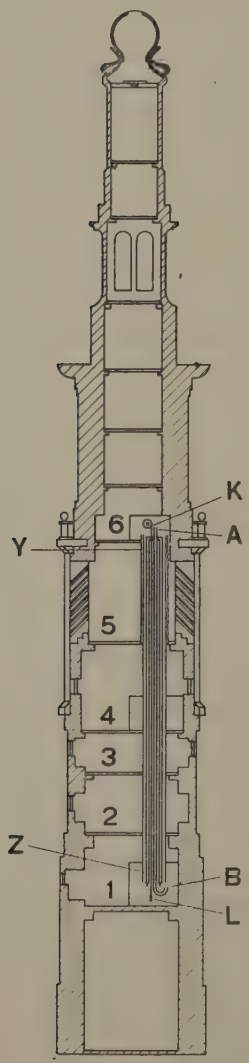

Fig. 1

The equipment of the "Westertoren".

A description will only be given of such apparatus as was used for the first measurements.

In order to carry out the work, laboratories were built and equiped on the first, fourth and sixth floors at heights of 10, 24 and 38 M. respectively and were connected by a vertical wooden case (30 × 50 cm.). In the lowest room, which is also the largest, the main part of the apparatus was set up.

For the direct calibration of a piston against an open mercury manometer it is in principle only necessary to have a pressure balance, press and mercury column of which the height and temperature can be accurately defined.

Fig. 1 shows a diagrammatic sketch of the arrangements, while fig. 2 shows better the apparatus on the first and sixth floors. The mercury is in a steel tube (*AB*) of about 11 mm. diameter. A short glass tube (*F*) is joined to the top of (*AB*) in which the mercury surface can be observed with a cathetometer. The second mercury surface is at (*C*) in a thick-walled glass tube. This surface is in direct contact with the oil which transmits the pressure through the press (*D*) to the effective surface of the piston (*O*). The steel vessel (*E*), the nitrogen cylinder (*R*) and the taps (*G*), (*H*) and (*I*) are only used in filling the apparatus with mercury. The steel tube (*AB*) is hung in the

wooden case (*YZ*). Where this case passes openings in the tower with the consequent possibility of rapid temperature changes, it is double walled. The height of the mercury column is measured with the invar

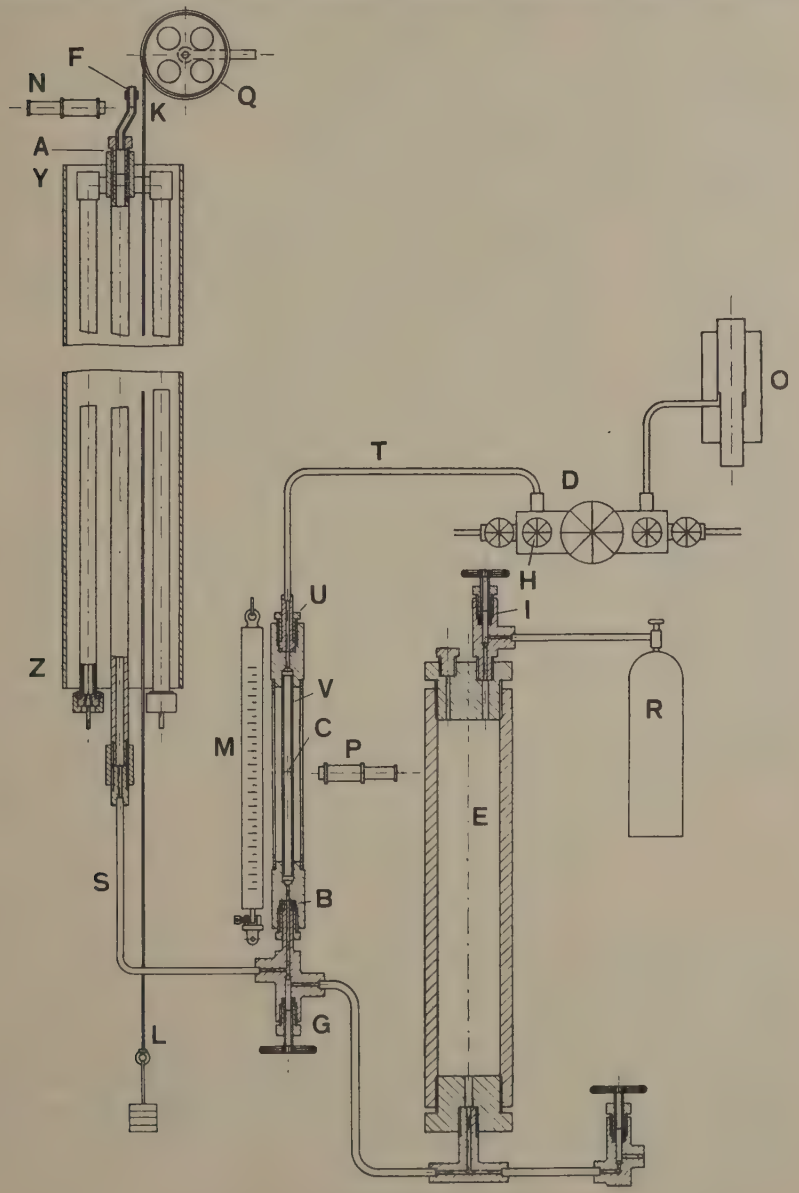

Fig. 2

tape (*KL*), the invar metre (*M*) and the cathetometers (*N*) and (*P*). The invar tape is divided in half metres and is suspended from one

end in the groove of a bronze wheel (Q) by which the height of the tape can be adjusted. The other end hangs free and is loaded with a weight of 10 Kg.

A blackened brass tube is pushed over the glass tube (*F*). The invar tape is so adjusted with the wheel (Q) that one of the divisions on it is at the same height as the bottom of the brass tube. During the measurements the distance of the mercury meniscus from the tube is read, this distance being always kept less than a few millimeters.

The position of the zero stripe on the invar tape is read with the cathetometer (*P*) on the invar metre (*M*). The position of the bottom meniscus in (*C*) is measured on (*M*) with the same cathetometer. In this way the height of the mercury column is found. Since (*O*) and (*C*) are not at the same height a correction must be applied for the pressure due to the oil column *OC*.

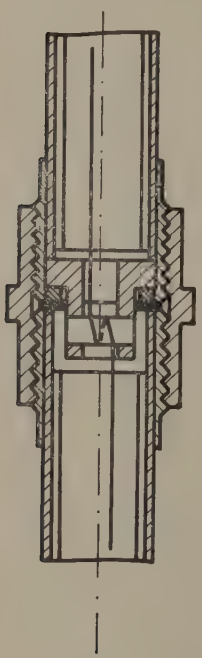

Fig. 3

In order to measure the temperature of the mercury, thermometers are placed through the wall of the case at intervals of 1 M. These thermometers can be read from outside the case and measurements were made simultaneously by six observers.

It is simpler to use a secondary thermometer consisting of a platinum wire stretched up and down along the whole length of the case so that the two halves lie on opposite sides of the mercury column. The wire is in a glass tube which in turn is placed inside a brass tube. By giving the walls suitable dimensions the temperature lag of the wire is made as nearly as possible the same as that of the mercury column. To remove strains due to its own weight the wire is wound every two metres on an ebonite rod in the manner shown in fig. 3.

From the resistance of the platinum wire it is possible to calculate its mean temperarure and therefore that of the mercury in the manometer since the two are always nearly enough alike. From this the mean density of the mercury follows directly, which can be multiplied with the height to give the pressure. In an appendix a deduction is given of the temperature limits within which this method is allowable; in the present case an allowable temperature variation of 14° was found for a final accuracy of $^1/_{100000}$. The readings of the platinum wire were calibrated by measurements with the ordinary mercury thermometers.

Calibration of the Invar Tape.

The division and temperature coefficient of the invar tape were compared with an invar metre calibrated at the Bureau International de

Poids et de Mesures at Paris. For this comparison an apparatus was constructed as shown in fig. 4.

Four wheels (*A*, *B*, *C* and *D*) supported on ball bearings, are hung

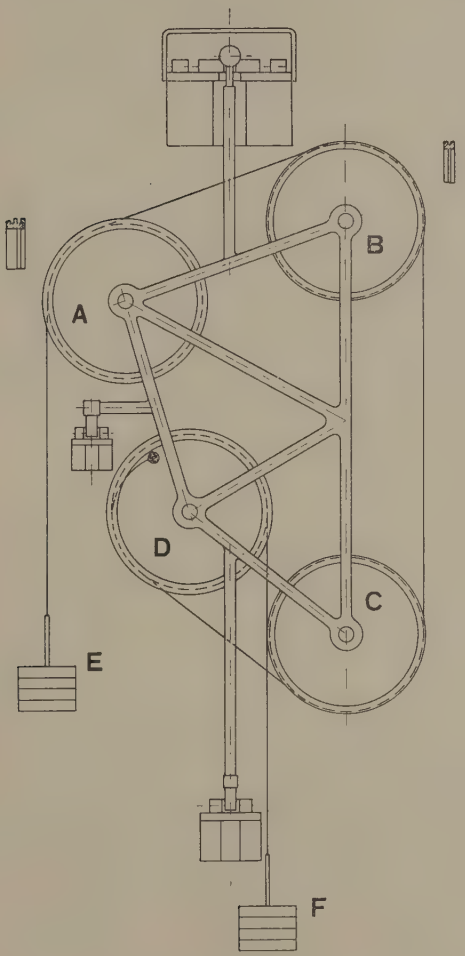

Fig. 4

in an iron frame. *B* and *C* have one, *A* and *D* two grooves cut in the circumference. At the beginning of the comparison the tape is rolled up on *A* and the end made fast as shown in the figure to the circumference of *D*, the tape lying in the groovés of *B* and *C*. In the second grooves of both *A* and *D* a steel tape is fitted from which hangs a weight of 10 Kg. (*E* and *F*) keeping the invar tape under tension. By means of a cathetometer (allowing measurements to be made to 0.001 mm.) the tape is now metre by metre compared with the standard metre. In the same way the distances $0—{}^1/_2$, ${}^1/_2—1\,{}^1/_2$, $1\,{}^1/_2—2\,{}^1/_2 \ldots . 28\,{}^1/_2—29\,{}^1/_2$,

$29^1/_2$—30 M. were measured. These measurements were carried out at two different temperatures.

Filling of the apparatus.

The filling is carried out as follows: with the tap G (fig. 2) shut, the mercury to be used is poured into the vessel E and a pressure of a few atmospheres is applied to the surface of the mercury from the gas cylinder R. The coupling U is loosened. By opening G the mercury is allowed to rise slowly in the tubes S and V till the surface reaches the top of V. G is now closed, the tube T filled with oil from the press and the coupling U again tightened. The press is then used to force the mercury so far back that the meniscus is about half way down V. H is now shut and G opened. The pressure in the vessel E is so adjusted with the tap I that the mercury slowly rises in the manometer tube till it is visible in F. G is then shut and the gas pressure let off.

The measurements.

The effective areas of the pistons A_2 250 and A 50 were determined with the following results:

Effective area of A_2 250 . . . . . 1.03210 cm²
„ „ „ A 50 . . . . . 5.5112^5 „ at 18° C.

The reproducibility of the measurements was found to be better than $^1/_{50000}$ corresponding with ± 0.5 mm. mercury or a variation of 0.1° in the temperature of the column.

The temperature of the wooden case was not the same over its whole length, being ± 0.7° higher at the top than at the bottom. The gradient was very regular. Apart from this, during the first hour of the measurements the temperature rose steadily about 0.25° and then remained constant within 0.02°.

Both pistons had been previously compared with the old piston A_1 250 calibrated 8 years ago. Taking the average of a large number of determinations of this piston as 0.9988^5 the values found by comparison were:

A_2 250 . . . . . 1.0318 cm²
A 50 . . . . . 5.5096 „

The difference amounts to $^3/_{10000}$. Since the accuracy of the old measurements was limited to $^1/_{2400}$ the agreement is satisfactory.

It may be of interest to mention that during the measurements the sun began to shine with the result that the tower increased in height.

Although the temperature rise inside remained less than 0.25°, the measured length in the tower, ± 27 M. increased by 0.8 mm. in 2 hours.

It may also be mentioned that the calibration could only be carried out in calm weather. Before the experiments were started the period and the amplitude of the movement of the tower were measured during a storm. The maximum double amplitude of the top was found to be 26 mm. with a period of ± 1 second [1]).

Appendix.

The use of the platinum thermometer is based on the following argument:

The total mercury pressure at the bottom of the mercury column is $P = \int_0^H \varrho \, dh$, where ϱ is the local density of the mercury. This is dependent on the temperature.

The total resistance of the platinum wire can also be written as $W = \int_0^H w dh$. where w is the resistance per cm. length.

Assuming that ϱ and w are linearly dependent on the temperature it is possible to measure the mean temperature by a simple calculation from the second integral, and from this the mean value of ϱ which determines the first integral.

Actually, however, neither ϱ nor w are strictly linear temperature functions and can be written

$$\varrho = \varrho_0 (1 + \alpha t + X) \qquad w = w_0 (1 + \alpha t + Y) \quad . \quad . \quad . \quad (1)$$

where ϱ_0 and w_0 are the specific quantities at the mean temperature and t is the local variation from this temperature. In order to see how great is the quantity omitted in considering the functions as linear (removal of X and Y) the following method may be used:

$$\left.\begin{aligned} P &= \int_0^H \varrho_0 (1 + \alpha t + X) \, dh = \\ &= \varrho_0 \int_0^H dh + \varrho_0 \alpha \int_0^H t \, dh + \varrho_0 \int_0^H X dh \\ &= \varrho_0 H + \varrho_0 \alpha \int_0^H t \, dh + \varrho_0 \int_0^H X dh \end{aligned}\right\} \quad . \quad . \quad . \quad . \quad (2a)$$

[1]) Our thanks are due to Prof. SCHERMERHORN of the Technische Hoogeschool Delft. for the loan of a theodolite used to measure the movement of the tower.

$$W = \int_0^H w_0 (1 + at + Y)\, dh =$$

$$= w_0 \int_0^H dh + w_0\, a \int_0^H t\, dh + w_0 \int_0^H Y\, dh =$$

$$w_0 H + w_0\, a \int_0^H t\, dh + w_0 \int_0^H Y\, dh \qquad \text{or}$$

$$\int_0^H t\, dh = \frac{W - w_0 H - w_0 \int_0^H Y\, dh}{w_0\, a} \quad . \quad . \quad . \quad . \quad . \quad . \quad . \quad (2b)$$

Substituting (2*b*), in (2*a*) gives

$$\left.\begin{aligned} P &= \varrho_0 H + \frac{\varrho_0 \alpha}{w_0 a}\left\{ W - w_0 H - w_0 \int_0^H Y dh \right\} + \varrho_0 \int_0^H X dh \\ &= \varrho_0 H + \frac{\varrho_0 \alpha}{w_0 a}(W - w_0 H) + \varrho_0 \int_0^H dh \left[X - \frac{\alpha}{a} Y \right] \end{aligned}\right\} \quad . \quad (2c)$$

If linearity is assumed therefore, the third term of the right hand side is omitted while the first is by far the largest. Then, if the error in P may not be for example greater than $^1/_{100000}$

$$\frac{\varrho_0 \int_0^H dh \left[X - \frac{\alpha}{a} Y \right]}{\varrho_0 H} < 10^{-5}$$

or

$$\int_0^H dh \left[X - \frac{\alpha}{a} Y \right] < 10^{-5} H \quad . \quad . \quad . \quad . \quad . \quad . \quad . \quad (3)$$

X and Y can be written in the following way

$$X = \beta t^2 + \gamma t^3 + \ldots . ; \qquad Y = b t^2 + c t^3 + \ldots . ;$$

as is seen by comparison of the expressions (1) with the full series development of ϱ and w with respect to temperature. If τ is the maximum-

deviation from the mean temperature, then expression (3) will certainly be satisfied if

$$\int_0^H dh\left[\left(\beta-\frac{\alpha}{a}b\right)\tau^2+\left(\gamma-\frac{\alpha}{a}c\right)\tau^3+\ldots.\right]<10^{-5}H \quad . \quad . \quad (4)$$

τ is now a constant so that (4) can be integrated to give

$$\left(\beta-\frac{\alpha}{a}b\right)\tau^2 H+\left(\gamma-\frac{\alpha}{a}c\right)\tau^3 H+\ldots.<10^{-5}H$$

or

$$\left(\beta-\frac{\alpha}{a}b\right)\tau^2+\left(\gamma-\frac{\alpha}{a}c\right)\tau^3+\ldots.<10^{-5} \quad . \quad . \quad . \quad . \quad (5)$$

Here α is of the order [1])	-1.8×10^{-4}
β	$+2.4\times10^{-8}$
γ	1.0×10^{-10}
a	3.8×10^{-3}
b	0.6×10^{-6}
c	—

(These figures are correct for 0° and can therefore only be approximately applied for the mean temperature of the column).

Neglecting the terms in τ^3 on account of the small values of the coefficients γ and c expression (5) becomes

$$(2.4\times10^{-8}+3.0\times10^{-8})\tau^2<10^{-5} \quad \text{or} \quad \tau<14^\circ$$

[1]) These figures are taken from LANDOLT-BORNSTEIN: Physikalische Tabelle.

Hydrodynamics. — *Contribution to the theory of the vane anemometer.* By B. G. VAN DER HEGGE ZIJNEN. (Mededeeling N°. 24 uit het Laboratorium voor Aero- en Hydrodynamica der Technische Hoogeschool te Delft.) (Communicated by Prof. J. M. BURGERS.)

(Communicated at the meeting of September 24, 1932.)

Introduction.

In investigating as well as in constructing a vane anemometer two factors are of prime importance: the angle at which the vanes are to be set in order that the instrument commences to rotate at the lowest possible wind speed, and secondly the internal friction of the mechanism. So far as we know, only OWER [1]) published a method of calculating these quantities; however, his theory starts from a too much simplified field of velocity to arrive at reliable results, and applies only to a special case. Having regard to the present form of the theory of the screw propeller and the windmill, the treatment of the problem can be brought into a more exact and exhaustive form, as will be shown in the following lines.

Forces acting on the blades.

We suppose the internal friction of the mechanism to be small, though not negligible; consequently a certain amount of power is absorbed by the vane wheel, and this implies that the air passing the vane disc is retarded. In the same time a rotational component of the air speed appears in the slip stream behind the disc; hence the velocity diagram will be as sketched in fig. 1, in which most of the symbols introduced in the following formulae

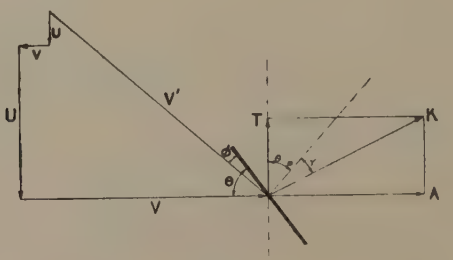

Fig. 1

have been indicated. The velocity V is the original wind speed, supposed to be uniform; the values of v, U and u relate to the centre of pressure of

[1]) E. OWER. A low-speed vane anemometer; Journ. Scient. Instruments, Vol. 3, N°. 4, 1926 The theory of the vane anemometer; Phil. Mag. 1926, p. 881. Measurement of Air Flow (CHAPMAN & HALL, London, 1927).

the vanes, the distance of which from the axis is denoted by r; ϱ is the density of the air, C a coefficient, such that the force K acting under the angle γ with the normal to the relative velocity V' is $\frac{1}{2}\varrho C F V'^2$, where F is the surface of a single vane. The number of vanes in the disc will be denoted by n. The area of the ring which is described by the vanes during their motion be F^*; in general it will differ from nF.

Both C and γ are functions of the effective angle of incidence ϕ. Experimental values have been obtained by EIFFEL [1]), who experimented with square, flat plates, and by OWER [2]), who investigated typical anemometer vanes. The measurements of EIFFEL have been repeated and extended recently by FLACHSBART [3]). However, for the present case the latter do not offer any particular advantage over EIFFEL's investigations: so in the following lines we shall accept the experimental $\gamma - \phi$ curve given by EIFFEL, and the relation between C and ϕ given by OWER (comp. fig. 2). A point of importance is that at a certain value of ϕ, γ attains a minimum value; if ϕ tends to 0, γ increases again to 90°, which is due to the thickness and to the surface friction of the plates. In the region $\phi < 5°$ no experimental results are available and we are restricted here to the dotted part of the curve; as will be shown later on this region is of great importance for the present research and the lacking of more accurate data is severely felt [4]).

Taking account of the axial velocity component v and of the component u in the plane of the vane, the forces acting on a single blade are (comp. fig. 1):

$$K = \tfrac{1}{2}\varrho\{(V-v)^2 + (U+u)^2\} C F \quad . \quad . \quad . \quad . \quad . \quad (1)$$

$$T = K \cos(\theta + \gamma - \varepsilon) \quad . \quad . \quad . \quad . \quad . \quad . \quad . \quad . \quad . \quad . \quad (2)$$

$$A = K \sin(\theta + \gamma - \varepsilon) \quad . \quad . \quad . \quad . \quad . \quad . \quad . \quad . \quad . \quad . \quad (3)$$

At the other hand A and T are also determined by the loss of linear momentum and the gain of angular momentum of the air passing through the vane disc. The total mass of air entering the disc in unit time is: $Q = \varrho F^* (V - v)$; as the velocity is slowed down from V far upstream to $V - 2v$ far downstream, the total axial force nA exerted will be:

$$nA = 2\varrho F^* (V - v) v \quad . \quad . \quad . \quad . \quad . \quad . \quad . \quad . \quad (4)$$

In the same way, considering the angular momentum supplied to the mass of air, which downstream obtains a tangential component approximately equal to $2u$, we find for the tangential force:

$$nT = 2\varrho F^* (V - v) u \quad . \quad . \quad . \quad . \quad . \quad . \quad . \quad . \quad (5)$$

---

[1]) G. EIFFEL, La résistance de l'air et l'aviation (H. DUNOD, Paris, 1911), p. 134.

[2]) E. OWER, Measurement of Air Flow p. 111.

[3]) O. FLACHSBART, Messungen an ebenen und gewölbten Platten; Ergebnisse der Aerodynamischen Versuchsanstalt zu Göttingen IV (Oldenbourg Verlag, München, 1932), p. 96.

[4]) As the blades are very small, and consequently work at rather low REYNOLDS' numbers, it may even be that C and γ to a certain extent will depend on V.

After some reductions the following relations are obtained (putting $\varkappa$ in stead of $n\,CF/4F^*$):

$$\tan(\theta-\varnothing)=\frac{U+u}{V-v} \quad . \quad . \quad . \quad . \quad . \quad . \quad . \quad . \quad (6)$$

$$\frac{u}{U+u}=\frac{\varkappa\cos(\theta+\gamma-\varnothing)}{\sin(\theta-\varnothing)\cos(\theta-\varnothing)} \quad . \quad . \quad . \quad . \quad . \quad . \quad . \quad (7)$$

$$\frac{v}{V-v}=\frac{\varkappa\sin(\theta+\gamma-\varnothing)}{\cos^2(\theta-\varnothing)} \quad . \quad . \quad . \quad . \quad . \quad . \quad . \quad . \quad (8)$$

$$\frac{v}{u}=\tan(\theta+\gamma-\varnothing) \quad . \quad . \quad . \quad . \quad . \quad . \quad . \quad . \quad (9)$$

Putting $N=\cos^2(\theta-\phi)+\varkappa\sin(\theta+\gamma-\phi)$, we have:

$$\frac{u}{V}=\frac{\varkappa\cos(\theta+\gamma-\varnothing)}{N} \quad . \quad . \quad . \quad . \quad . \quad . \quad . \quad (7^a)$$

$$\frac{v}{V}=\frac{\varkappa\sin(\theta+\gamma-\varnothing)}{N} \quad . \quad . \quad . \quad . \quad . \quad . \quad . \quad (8^a)$$

$$\frac{U}{V}=\frac{\sin(\theta-\varnothing)\cos(\theta-\varnothing)-\varkappa\cos(\theta+\gamma-\varnothing)}{N} \quad . \quad . \quad . \quad (10)$$

Inserting the values of u and v found in this way into (4) and (5), we obtain:

$$A^*=\frac{n\,A}{2\varrho\,F^*\,V^2}=\frac{\varkappa\sin(\theta+\gamma-\varnothing)\cos^2(\theta-\varnothing)}{N^2} \quad . \quad . \quad . \quad (4^a)$$

$$T^*=\frac{n\,T}{2\varrho\,F^*\,V^2}=\frac{\varkappa\cos(\theta+\gamma-\varnothing)\cos^2(\theta-\varnothing)}{N^2} \quad . \quad . \quad . \quad (5^a)$$

Now, as the driving torque $n\,T\,r$ just compensates the frictional torque, the magnitude of the tangential force T depends on the internal friction of the mechanism. The latter is partly due to the weight of the spindles, gearing, &c., which part can be taken as constant, at the other hand the internal friction increases with the axial load, therefore with A. In general the relation between the tangential and axial forces acting on the blades can be put into the form:

$$T=p+q\,A \quad . \quad . \quad . \quad . \quad . \quad . \quad . \quad . \quad . \quad (11)$$

where p and q may be assumed to be approximately constant, provided the vanes are rotating.

From this formula at once a conclusion can be drawn about the relation between U and V at very high velocities. Dividing both members of (11) by $2\varrho\,F^*\,V^2$ and neglecting $p/2\varrho\,F^*\,V^2$ in the limiting case, we have:

$$T^*\overset{\infty}{=}q\,A^* \quad . \quad . \quad . \quad . \quad . \quad . \quad . \quad . \quad (11^a)$$

from which, in consequence of (4a) and (5a):

$$\cot(\theta + \gamma - \varphi)_\infty = q \quad . \quad . \quad . \quad . \quad . \quad . \quad . \quad (12)$$

The absolute value of V now is eliminated from all relations and only proportions and angles are retained; the latter acquire a constant value.

If q be known (in general a direct determination of q in the case of an arbitrary instrument will not be an easy matter), then (12) gives the value of $(\theta + \gamma - \phi)_\infty$; as θ is known, this leads to $(\gamma - \phi)_\infty$, after which both angles γ_∞ and φ_∞ (in the case of extreme high velocities) can be found by means of fig. 2.

Inserting the values deduced in this way into (10), we have:

$$\left(\frac{U}{V}\right)_\infty = \frac{\sin(\theta - \varphi_\infty)\cos(\theta - \varphi_\infty) - \varkappa \cos(\theta + \gamma_\infty - \varphi_\infty)}{\cos^2(\theta - \varphi_\infty) + \varkappa \sin(\theta + \gamma_\infty - \varphi_\infty)} \quad . \quad (13)$$

It is apparent from (13) that $(U/V)_\infty$ is smaller than the tangent of the blade angle θ, also smaller than $(\theta - \phi_\infty)$, which fact is essentially due to the presence of the disturbing components u and v.

A more complete investigation of the equations deduced here, in which the amount $p/2\varrho F^* V^2$ is not neglected, may lead to the general relation between U and V, even at the smaller values of V. However, the deductions will be rather complicated and cannot be evaluated in an entirely explicit form; besides, as has been mentioned, eq. (11) is only an approximation. Hence we will not enter upon this question, but deduce below the internal friction for a particular instrument with an empirically determined calibration curve; in the same time the importance of v/V and u/U will be demonstrated.

Optimum blade angle.

The question concerning the blade angle for which a given instrument commences to rotate at the lowest possible wind speed can be answered in a general way from the formulae developed here.

In the initial stage of motion, when the vanes are on the point of commencing to rotate, but still are stationary, U will be zero, whereas the other velocity components will have values differing from zero. Then (7) reduces to:

$$\varkappa \cos(\theta + \gamma_0 - \varphi_0) = \sin(\theta - \varphi_0)\cos(\theta - \varphi_0) \quad . \quad . \quad . \quad (14)$$

The velocity components having vanished, for a certain value of $\varkappa$ (14) will give a relation between the angles, from which the initial incidence ϕ_0 can be found.

It is of importance to notice that in (14) the "density" nF/F^* of the vane circle plays a great part[1]); if the total area of the vanes approaches to the surface of the vane ring, that is, the denser the vane circle is, the

[1]) In the tables and in the diagrams the inverse ratio F^*/nF has been given.

smaller the incidence ϕ_0 appears to become. Conversily, if the vane ring is infinitely rarefied, which makes $\varkappa$ tend to zero, (14) immediately leads to the case of a single flat plate in an infinite field of flow with uniform velocity, for which $\theta = \phi_0$.

It is not possible to give an explicit solution of (14), if arbitrary values are assigned to the blade angle θ and to nF/F^* ; a solution can only be

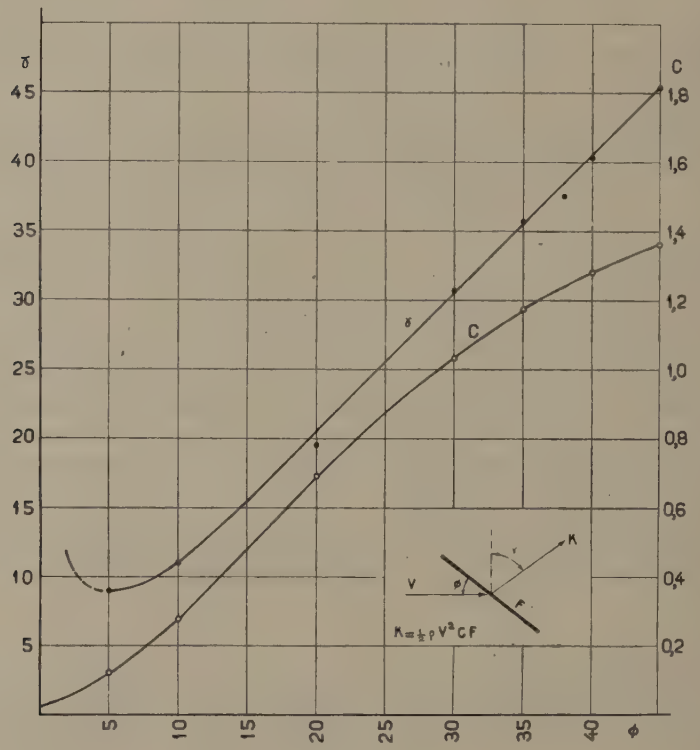

Fig. 2

found by trial (C and γ cannot be put as a mathematical function of ϕ and are to be derived from fig. 2). In this way the following values were determined :

Values of $\varnothing_0$

θ	30	35	40	45	50	55°
$F^*/nF = 1.0$	20.9	24.7	28.8	33.4	38.2	43.5°
$F^*/nF = 1.5$	23.3	27.5	31.9	36.8	41.9	47.4°
$F^*/nF = 2.0$	24.6	29.1	33.7	38.6	43.8	49.2°

Now in the commencement of the rotation T is entirely determined by the constructional details of the mechanism and can be treated as a given quantity; therefore the velocity at which the instrument starts will be minimum provided T^* (comp. (5a)) is maximum. A series of values of T^*, corresponding to the angle ϕ_0 found above, are collected in the accompanying table:

Values of T^*

θ	30	35	40	45	50	55°
$F^*/nF = 1.0$	0.133	0.141	0.144	0.140	0.134	0.123
$F^*/nF = 1.5$	0.103	0.110	0.113	0.110	0.105	0.093
$F^*/nF = 2.0$	0.085	0.090	0.092	0.091	0.085	0.077

In the case considered here the optimum blade angle appears to be 40°, independently of F^*/nF, as will be seen from fig. 3, where T^* is plotted

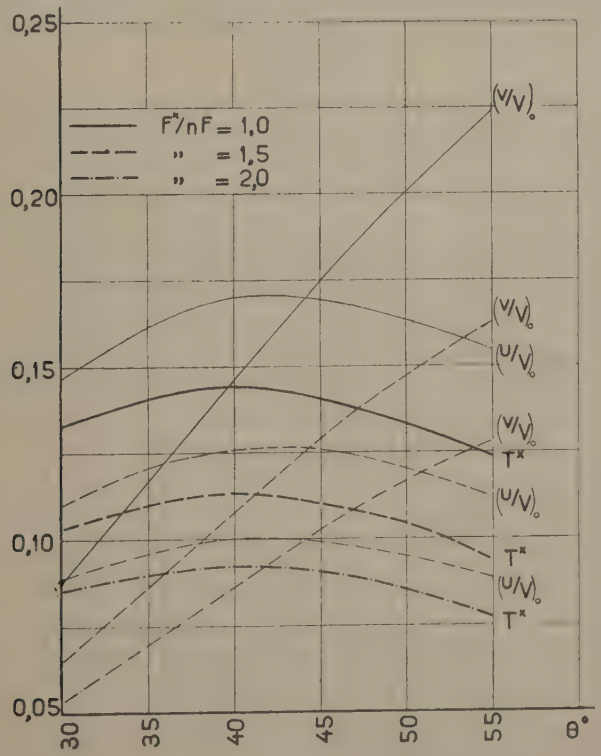

Fig. 3

against θ. It is easily verified that in the case of a single vane ($\varkappa = 0$) the optimum of the tangential force also occurs at about $\theta = 40°$. Therefore this value seems to hold in general for this type of vane; the result is confirmed by the experiments of OWER [1]).

Magnitude of the disturbing components u, v.

Finally the disturbing components u and v in the initial stage of motion, expressed in terms of V, were calculated from (7a) and (8a):

θ		30	35	40	45	50	55°
$F^*/nF = 1.0$	$(v/V)_0$	0.088	0.116	0.146	0.176	0.200	0.224
	$(u/V)_0$	0.147	0.161	0.170	0.169	0.164	0.154
$F^*/nF = 1.5$	$(v/V)_0$	0.065	0.086	0.107	0.129	0.147	0.163
	$(u/V)_0$	0.110	0.121	0.125	0.126	0.121	0.112
$F^*/nF = 2.0$	$(v/V)_0$	0.053	0.069	0.086	0.102	0.116	0.128
	$(u/V)_0$	0.089	0.096	0.100	0.100	0.095	0.088

These values are also represented in fig. 3. It is evident that the disturbing components in the case of the usual instruments (θ about 40 to 50°, F^*/nF between 1.0 and 1.5) are rather considerable and that it is not allowed — at least not in the initial stage of motion — to neglect them. What part they play at the higher velocities cannot be shown in the general case; it is possible, however, to calculate them for any given instrument as soon as the calibration curve is known.

To this end a common type of vane anemometer (constructed by FUESS. Berlin-Steglitz, number 1207) was calibrated in the Laboratory for Aero- and Hydrodynamics of the Technical University, Delft, after all vanes were set carefully at the same blade angle. The data of this instrument are the following:

Number of vanes . . . . . $n = 8$
Total surface of vanes . . . . . $nF = 19.2 \cdot 10^{-4}$ m²
Area of vane ring . . . . . $F^* = 25.4 \cdot 10^{-4}$ m²
Radius of centre of pressure . . . . $r = 0.0235$ m
Blade angle . . . . . $\theta = 53°15'$

The calibration curve (fig. 4) is linear from $V = 0.5$ m/sec upwards and satisfies in the region investigated the equation

$$U = 1.1360\, V - 0.230 \quad . \quad . \quad . \quad . \quad . \quad . \quad . \quad (15)$$

[1]) E. OWER, Measurement of Air Flow p. 123.

where U and V are expressed in m/sec (U being found from the number of revolutions).

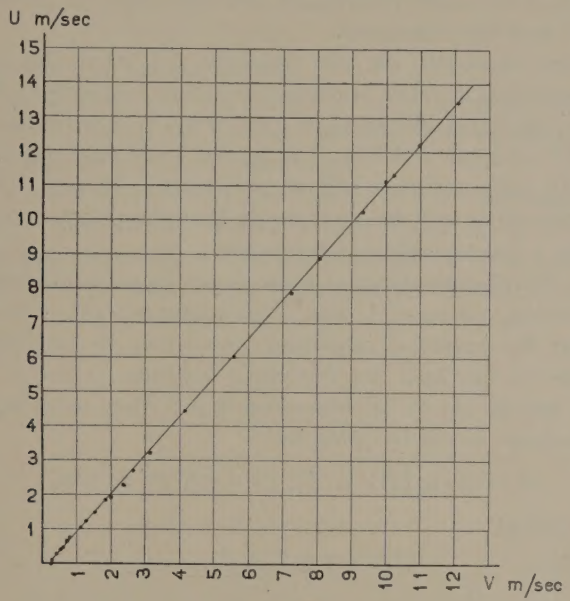

Fig. 4

ø	γ	C	v/V	u/U	U/V	V m/s	U m/s	$nA/2\varrho F^*$	$nT/2\varrho F^*$
42°12′	42°42′	1.320	0.172	—	0	(0.25)	0	—	—
10° 0′	11° 0′	0.278	0.0744	0.0656	0.8171	0.72	0.59	0.0358	0.0258
8° 0′	9°36′	0.210	0.0614	0.0479	0.9036	0.99	0.89	0.0564	0.0397
6° 0′	9° 6′	0.148	0.0480	0.0321	0.9979	1.66	1.66	0.1261	0.0841
5° 0′	9° 0′	0.122	0.0419	0.0258	1.0464	2.57	2.68	0.264	0.170
4° 0′	9° 9′	0.098	0.0357	0.0200	1.0972	5.93	6.50	1.210	0.744
3°50′	9°12′	0.094	0.0346	0.0191	1.1059	7.64	8.45	1.950	1.191
3°45′	9°13′	0.092	0.0340	0.0186	1.1105	9.02	10.02	2.67	1.62
3°40′	9°14′	0.090	0.0334	0.0182	1.1148	10.8	12.1	3.80	2.31
3°35′	9°15′	0.088	0.0328	0.0177	1.1194	13.9	15.5	6.08	3.67
3°30′	9°16′	0.086	0.0323	0.0173	1.1238	18.9	21.2	11.11	6.69
3°25′	9°17′	0.084	0.0318	0.0168	1.1283	29.9	33.7	27.5	16.4
3°20′	9°18′	0.082	0.0311	0.0163	1.1333	85.2	96.5	219	130
3°17′	9°19′	0.081	0.0308	0.0161	1.1377	∞	∞	∞	∞

For a number of values of the angle of incidence the corresponding values of C and γ were read off from fig. 2, then with the aid of (10) the ratio U/V could be found. Introducing this ratio into (15), absolute values of U and V have been deduced.

As has been remarked, the determination of C and γ for small values of ϕ (corresponding to high velocities) is rather inaccurate; however, as the factor $\varkappa$ appears to be small, the influence of this inaccuracy on the value of U/V is much reduced. The results have been tabulated in the accompanying table, together with the values of v/V, u/U, $nA/2\varrho F^*$ and $nT/2\varrho F^*$, though it will be understood that these latter quantities are affected with a greater relative uncertainty.

It will be seen that the limiting value of the angle of incidence is 3°17′, the corresponding values of V and U becoming infinite — at least if it is assumed that the empirical calibration curve may be extrapolated indefinitely. That in this case the disturbing velocities u and v still are of importance, can be shown by observing that if they were neglected, the angle of incidence would be given by:

$$\theta = \text{arc tg } U/V = 53°15' - 48°39' = 4°36'.$$

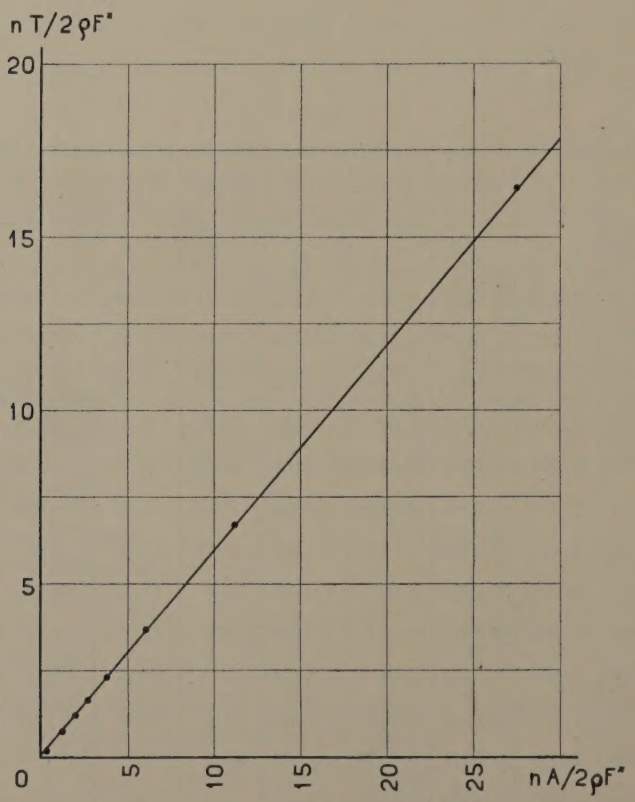

Fig. 5

The value of C corresponding to $\phi = 4°36'$ is 0.112; hence neglecting u and v the value of the force components would become about 38 % too high.

Determination of internal friction.

From the limiting case we deduce $(T/A)_\infty = cot\ (\theta + \gamma - \phi)_\infty = cot\ 59°17' = 0.594$. Hence this must be the value of q (at least for the higher velocities) for this particular instrument.

In order to check the relations expressed by (11) the values of $nA/2\varrho F^*$ and $nT/2\varrho F^*$ given in the table have been plotted in fig. 5. It will be seen that the points approximately arrange themselves on a straight line. The value of p in (11) is too small to be read off directly from the diagram fig. 5.

ERRATUM.

Proc. Royal Acad. Amsterdam, Vol. **35**, N°. 6, 1932 (p. 750).

Chemistry. — *Oxidation of phenol with peracetic acid. (Contribution to the knowledge of the substitution of benzene).* By Prof. J. BÖESEKEN and R. ENGELBERTS.
